A role for SDF-1α in overcoming myelin-induced neurite outgrowth inhibition

Inaugural Dissertation

zur

Erlangung des Doktorgrades der

Mathematisch-Naturwissenschaftlichen Fakultät

der Heinrich-Heine-Universität Düsseldorf

vorgelegt von

Jessica Verena Opatz

aus Emsdetten

Mai 2007

Aus dem Institut für Molekulare Neurobiologie
der Heinrich-Heine-Universität Düsseldorf

Gedruckt mit Genehmigung der Mathematisch-Naturwissenschaftlichen Fakultät
der Heinrich-Heine-Universität Düsseldorf

Referent: Prof. Dr. Hans Werner Müller

Koreferent: Prof. Dr. Heinz Mehlhorn

Tag der mündlichen Prüfung: 5. Juli 2007

To my family

and

In loving memory of Sally

Table of contents

1. Summary

Since lately, the fields of neurobiological and immunological research have shared interests. Evidence exists that chemokines and their receptors, formerly primarily characterized for their role in development and maintenance of the immune system, also excert crucial functions in the nervous system, where they are suggestedly involved in the maintenance of central nervous system, CNS, homeostasis, in neuronal patterning during ontogenesis, and further act as mediators in pathophysiological events.

A major aim of neurobiological research is the propagation of axonal outgrowth following injury of the adult mammalian CNS. Here, regeneration is severely impaired due to a plethora of factors, and CNS myelin-associated proteins were reported to mainly inhibit the regenerative growth of lesioned axons.

Recently, the α-chemokine SDF-1 was demonstrated to abrogate embryonic neurite outgrowth inhibition as induced by potent chemorepellent molecules with a role in early nervous system development. In this thesis, it was investigated whether SDF-1 is further able to overcome myelin-associated outgrowth inhibition of postnatal mammalian PNS neurons. It was found that postnatal dorsal root ganglion neurons, DRG neurons, displayed a significantly reduced outgrowth performance on a surface coated with adult CNS myelin, and that this effect could be reverted and growth was restored following application of SDF-1α. Moreover, SDF-1α-mediated effects were significantly enhanced if cells were “primed” by pretreatment with this chemokine prior to plating on myelin. Furthermore, experimental findings pointed to a role for the cognate receptor to SDF-1, CXCR4, and elevation of intracellular cAMP levels in SDF-1α-induced neurite outgrowth promotion. While SDF-1 recently was demonstrated to interact with an alternative receptor, RDC1, this study reveals a region-specific distribution of CXCR4, but not RDC1, in myelin-sensitive DRG neurons at early stages of cultivation. Thus, these findings further suggested a role for SDF-1α-/CXCR4-signalling in (postnatal) neurite outgrowth and branching. Interaction of SDF-1 and CXCR4 thus might constitute, if not a possible therapeutic tool, a key element in cell growth-regulatory processes.

Albeit SDF-1 exists in several isoforms which are generated from a common mRNA-precursor molecule through alternative splicing, only splice products SDF-1α and β

have been analyzed thoroughly to date. In this thesis, Ca^{2+}-elevating properties of a novel isoform, SDF-1γ, were investigated and compared to the Ca^{2+}-regulatory activity of the α-transcript.

2. Introduction

2.1 Chemokines and chemokine receptors

2.1.1 Chemokine versatility

In the course of the recent decades, the field of action of chemokines and chemokine receptors has undergone an enormous evolution and currently displays an almost stunning complexity. First characterized as key modulators in lymphopoiesis, chemokines and their cognate receptors were initially described to mainly control development, differentiation and trafficking of leukocytes, thus excerting crucial functions in the regulation of the innate and adaptive immune response (Horuk and Peiper, 1996; Murphy et al., 2000; Rossi et al., 2000; Zlotnik and Yoshie, 2000). During the recent years, a large number of highly divergent functions in a broad range of biological processes could be additionally attributed to the chemokine system (Horuk, 1998). Today, a role for various members of this superfamily has been confirmed in the healthy and in the diseased organism, respectively, and chemokines are involved in multiple developmental processes as well as in the propagation of infectious and autoimmune diseases and cancer. In accordance to their role in the chemotaxis of hematopoietic cells, they direct the migration of germ cells and stem cells (Doitsidou et al., 2002; Claps et al., 2005). Chemokines reportedly function in tumour growth and metastasis formation, and their expression often is differentially regulated either in malignant cells or in tissues which represent targets for metastasis, where these molecules were described to act on angiogenesis and migration (Strieter et al., 1995; Rempel et al., 2000; Müller et al., 2001). Due to their role in development and maintenance of the immune system, chemokines are involved in acute and chronic inflammatory events, directing the action of immune cells in diseases such as atherosclerosis or allergic responses (Murdoch and Finn, 2000). The importance of chemokine systems in viral pathogenesis is documented by coreceptor functions of the chemokine receptors CCR5 and CXCR4 for various HIV- as well as SIV strains (Feng et al., 1996; Zhang et al., 1996). As a singularity, DARC, the Duffy antigen receptor for chemokines, is a chemokine receptor which lacks any apparent signalling function, and is solely known for its role in cell entry of the

malaria-causing protozoon *Plasmodium vivax* (Horuk et al., 1993; Horuk, 1994; Neote et al., 1994; Horuk and Ng, 2000).

To date, the chemokine system comprises at least 50 structurally related peptide agonists and 20 cognate receptors. Due to their structural homology, chemokines proved to be ideal molecules to be discovered through bioinformatics, a method which further facilitated and accelerated the identification and characterization of new members of this group (Rossi and Zlotnik, 2000).

2.1.2. Structure and classification of chemokines

The term “chemokines” is short hand for “chemotactic cytokines” and was first coined in the year 1993 (Lindley et al., 1993). Chemokines are small (8–14 kDa), mostly basic, molecules sharing a number of characteristic features due to which they display a common fold even in the case of only a low sequence identity (Fernandez and Lolis, 2002). Generally, chemokines can be structurally subdivided into three different parts: They consist of a highly disordered N-terminus, a core protein comprising three β–sheet strands arranged in the shape of a Greek key with the single strands separated by short loops, and an α–helical C-terminus (Murdoch and Finn, 2000; Murphy et al., 2000). All members of the chemokine superfamily exhibit a characteristic cysteine motif located in their N-terminal amino acid sequence, commonly comprising four cysteine residues which form disulphide bonds between the first and third and second and fourth cysteine, respectively. The chemokines known to date are classified into four subfamilies according to the number and sequential relationship of these structurally relevant cysteines (Baggiolini et al., 1997). Two main subfamilies comprise the majority of all chemokine members hitherto identified. The cysteine residues of the α– or CXC-chemokines are separated by one additional amino acid, whereas in the β- or CC-chemokine group the cysteines are immediately adjacent. Of two other subfamilies, only prototypic members have been characterized to date. The CX_3C-chemokine fractalkine is a membrane-bound glycoprotein, with three amino acid residues interspersed between the cysteines, whereas the C-chemokine member lymphotactin comprises only two of the four relevant cysteine residues (Kelner et al., 1994; Imai et al., 1997).

2.1.3 Chemokine encoding genes

The genes coding for members of the different chemokine subfamilies are currently designated *small secreted cytokines*, *scy* (Murphy et al., 2000). According to this nomenclature, CC-chemokines are encoded by *scya*-genes, whereas CXC-chemokines are encoded by *scyb*-genes. The majority of those genes are clustered in distinct chromosomal locations, probably due to a common origin from a single ancestral gene by duplication. Spatial distance of a chemokine-encoding gene to other members of the same subfamily seems to be closely linked to a distinctive role of the encoded protein (Zlotnik and Yoshie, 2000). The unique function of the constitutively expressed α–chemokine SDF-1 is emphasized by the fact that the encoding gene is located on human chromosome 10 (murine chromosome 6), whereas the other members of this group are mapped to human chromosome 4 (murine chromosome 5).

2.1.4 Structure and classification of chemokine receptors

Chemokines excert their functions mainly as secreted proteins, but are further able to use glycosaminoglycans to tether to the plasma membrane and thus form a stable gradient (Murphy et al., 2000; Onuffer and Horuk, 2002). While they mainly act as monomers, in high concentrations or in crystallographic studies they have been described to exist in higher orders, as dimers or even as multimers (Fernandez and Lolis, 2002). Two major sites of receptor interaction have been identified to date in the flexible N-terminal portion of the chemokine ligand and on the rigid loop following the second cysteine, respectively (Crump et al., 1997; Murphy et al., 2000; Fernandez and Lolis, 2002).

Signalling by chemokines occurs upon binding to and activation of chemokine receptors, members of the rhodopsin family of heptahelical $G_{i/q}$ protein-coupled receptors, GPCRs. GPCRs constitute a large family consisting of more than 100 receptor molecules which are activated upon interaction with chemoattractants, peptide hormones or light. Up to now, at least 20 G protein-coupled chemokine receptors have been identified, mainly on the basis of structural homology.

Chemokine receptors are generally defined by their ability to induce directional migration of receptor-expressing cells towards a gradient of a certain chemotactic cytokine (Horuk and Peiper 1996; Murphy et al., 2000; Bajetto et al., 2002). According to the classification of their chemokine ligands, the group of chemokine receptors is subdivided into four different subfamilies or classes. The receptor nomenclature is based on their preference for a certain chemokine subfamily, replacing “L” (for ligand) in the chemokine nomenclature with “R” (for receptor), followed by the number of the encoding gene in the order of identification (Zlotnik and Yoshie, 2000). Details on the officially approved nomenclature of chemokines and chemokine receptors can not be comprehensively presented here and are provided in a review published by the International Union of Pharmacology (Murphy et al., 2000).

Chemokine receptors display an intrafamily structural homology comparable to that of their ligands. Their genes are, similar to the chemokine-encoding genes, mostly grouped together in clusters mapped to the human chromosomes 2 and 3 (murine chromosomes 1 and 9). Common features of the chemokine receptors described to date are a conserved structure with an amino acid sequence identity of 25–80%, a molecular weight of approximately 40 kDa, and a common length of 340–370 amino acid residues. Chemokine receptors display a tertiary structure characteristic for all members of the rhodopsin receptor family, including an extracellular N-terminus and intracellular C-terminus and seven transmembrane domains, and they mainly couple to various members of the $G_{i/q}$ class of heterotrimeric G proteins (Horuk and Peiper, 1996; Bajetto et al., 2002). Binding and activation of a chemokine receptor by its ligand occurs through both the N-terminus and extracellularly located, loop-like domains, whereas intracellular signalling is triggered upon interaction of the cytosolic domains and the C-terminal tail of the receptor with various effector molecules. Signalling through chemokine receptors is often highly promiscuous, as an individual receptor may bind one or more chemokines of the same subfamily, and vice versa, but does usually not occur between members of different subfamilies.

2.1.5 A two-step model of chemokine/chemokine receptor interaction

The current two-step binding and activation model seems to generally hold true for the interaction of chemokine receptors and their ligands (Yancey et al., 1989; Siciliano et al., 1994; Kolakowski et al., 1995). In this model, interaction of the chemokine with an initial binding site leads to a conformational change of the receptor which effects exposition of binding site 2. The overall conformational change induced by ligand binding is then transmitted to the intracellular domains and triggers downstream signalling through a plethora of effector molecules (Murdoch and Finn, 2000). In detail, this model will be exemplarily described for SDF-1 and CXCR4 in the following.

The majority of chemokine receptors seem to be preferentially coupled to G_i proteins, since chemokine-triggered signalling events can be mostly abrogated by application of pertussis toxin, PTX (Murdoch and Finn, 2000). Recent studies hint to the fact that chemokine receptors convey their functionality not only by signalling through G proteins, but further directly interact with other downstream effectors as well. This theory is based on the observation that diverse signalling events are triggered, depending on the ligand and receptor, and the cell type and developmental stage, respectively (El-Shazly et al., 1999; Barlic et al., 2000). Apart from an interaction with chemokine receptors, binding of chemokines to glycosaminoglycans, GAGs, such as heparin has been shown to either potentiate or inhibit chemokine activities *in vitro* (Maione et al., 1991; Webb et al., 1993). The sites for ligand-receptor interaction are primarily located in the N-terminal region, while the C-terminal α–helix provides interaction sites for GAGs (Cai et al., 2004).

2.1.6 Chemokines in the nervous system

Since lately, the fields of neurobiological and immunological research have shared interests. Evidence exists that chemokines, formerly primarily characterized for their role in development and maintenance of the immune system, also excert crucial functions in the nervous system (Horuk et al., 1997; Horuk et al., 1998; Mennicken et al., 1999). Recent data hint to the fact that chemokines and their cognate receptors

are involved in the maintenance of CNS homeostasis, in neuronal patterning during ontogenesis, and further act as mediators in pathophysiological events in the nervous system. Both chemokines and chemokine receptors are expressed at low levels in several structures of the brain, and could be demonstrated to be rapidly upregulated by neuroinflammatory stimuli. In the CNS, expression of chemokines and chemokine receptors such as IL-8, MIP-1α, CCR5 and CX_3CR1 could be mapped to various cell types. Amongst others, expression was detected in astrocytes, microglia, and neurons as well as in fibroblasts and endothelial cells (Lacy et al., 1995; He et al., 1997; Harrison et al., 1998; McManus et al., 1998). IL-8 reportedly mediates survival of neurons and leads to proliferation of glial cells in rat hippocampal cultures (Araujo and Cotman, 1993). Moreover, RANTES could recently be demonstrated to trigger migration and differentiation in mouse embryonic DRG cells *in vitro* (Bolin et al., 1998).

Chemokines are involved in numerous pathophysiological events in the CNS. First, infiltration of immune cells is indispensable to respond to challenges such as trauma, stroke, infection or autoimmune disorders. After focal or global ischemia, GRO-α and MCP-1 are rapidly upregulated in the vicinity of damaged tissue and in infiltrating immune cells (Liu et al., 1993; Wang et al., 1995; Gourmala et al., 1997). Furthermore, chemokines and chemokine receptors are involved in the growth and propagation of tumours and suggestedly act in neurodegenerative diseases as diverse as Alzheimer´s disease and HIV-associated dementia (Schall, 1994; Strieter et al., 1995; Horuk et al., 1997; Hesselgesser et al., 1998).

To date, the chemokine system most prominently expressed in the central nervous system is the α–chemokine SDF-1 and its cognate receptor, CXCR4. The finding that neurobiology and immunology are closely linked was namely based on the notion that SDF-1 and CXCR4 direct migration events not only of hematopoietic cells, but also of neurons during early embryonic development of the CNS, as will be outlined in the following. The abundant and constitutive expression patterns of both this chemokine and chemokine receptor suggest that these molecules obtain fundamental roles in neurophysiology and neuroimmunology.

However, lately it has emerged that neurotactin and its cognate receptor, CX_3CR1, suggestedly excert important functions in the nervous system, as neurotactin is the only chemokine which was found to be expressed at higher levels in the CNS than in the periphery including structures of the immune system (Bazan et al., 1997).

2.1.7 SDF-1/CXCL12: general structure and particularities

The chemokine stromal cell-derived factor-1, SDF-1, also designated CXC chemokine ligand 12, CXCL12, was originally identified applying the signal sequence trap cloning strategy (Tashiro, 1993). Unlike the genes for the majority of the CXC chemokines, which can be mapped to human chromosome 4 (murine chromosome 10), the gene coding for SDF-1 is located on human chromosome 10 (murine chromosome 6), underlining its singularity among the members of this family (Shirozu et al., 1995; Baggiolini et al., 1997; Dealwis et al., 1998). Human as well as murine SDF-1 exists in six isoforms (α, β, γ, δ, ε, θ), whereas in rat three isoforms (α, β, γ) have been described to date (Fig. 2.1), all of which derive from one common mRNA precursor molecule by means of alternative splicing (Gleichmann et al., 2000; Yu et al., 2006).

For SDF-1α, the most extensively studied variant, the tertiary structure has been determined by NMR-spectroscopy and displays both structural homologies to other chemokine members as well as considerable differences (Crump et al., 1997). SDF-1 exhibits a fold characteristic for chemokines, comprising a highly disorganized, mobile N-terminal region, three antiparallel β–sheet strands and an α–helical C-terminus. All isoforms share both a common N-terminus and core region, but differ considerably with regard to the length of their C-terminal domain, which in the instance of SDF-1β and SDF-1γ comprises 4 and 30 additional amino acid residues, respectively (Fig. 2.1). Moreover, the SDF-1β and SDF-1γ transcripts display several putative proteolytic cleavage sites which could give rise to secreted peptides (Gleichmann e al., 2000). The SDF-1-isoforms identified to date display characteristic expression patterns, as could be confirmed by quantitative RT-PCR and *in situ*-hybridization applying isoform-specific probes. According to recent observations, human and murine α- and β-variants are expressed in a similar manner and are highest in liver, pancreas and spleen, whereas SDF-1γ could be solely detected in the heart. The δ-transcript of SDF-1 is present in several adult tissues but shows highest expression levels in the fetal liver (Yu et al., 2006). Conversely, earlier analysis revealed that SDF-1γ mRNA, apart from a prominent expression in heart, is the major variant in the adult CNS and PNS in rat *in vivo* (Gleichmann et al., 2000). Both SDF-1- and SDF-1γ-specific hybridization signals document spatio-temporal

alterations which indicate a post-transcriptional regulation of SDF-1-expression during rat nervous system development. SDF-1γ-transcripts, and possibly also SDF-1β-transcripts, are detected in structures such as neocortex, cerebellum and hippocampus. Transcripts are prominent in neurons, oligodendroglia and Schwann cells of the nervous system (Gleichmann et al., 2000).

According to its N-terminally located cysteine motif, SDF-1 belongs to the CXC-family of chemokines, but differs considerably from other members of this group in the average sequence identity, packing of the hydrophobic core and surface charge distribution (Crump et al., 1997). While sequential and structural resemblance to other chemokines is only low, SDF-1α is highly conserved (99%) between human and mouse except for a single conservative change at position 18, whereby this interspecies identity suggests a fundamental role of SDF-1 in various biological processes (Dealwis et al., 1998; Lapidot et al., 2002). SDF-1 is a highly basic protein with 21% of the total residues provided by arginine, lysine and histidine. While clusters of positive surface charges can be mapped to the first and second β–strand of the core protein, the C-terminal α–helix predominantly comprises negatively charged amino acid residues. The C-terminal domain thus provides optimal binding sites for heparin or other cell surface bound GAGs and enables SDF-1 to interact with the extracellular matrix, ECM, or cell membranes (Avigdor et al., 2004).

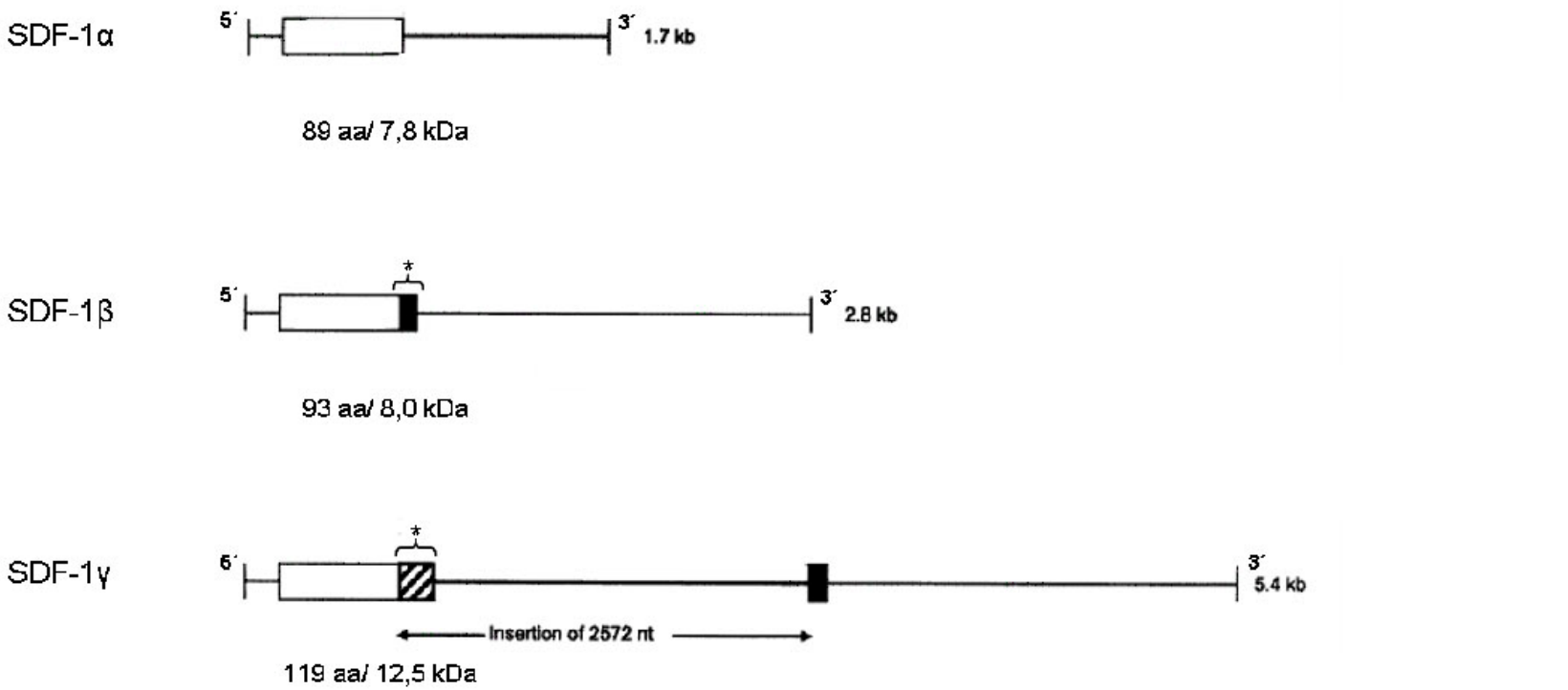

Fig. 2.1. (see also next page)

(see also previous page)

Fig. 2.1. Schematic representation of rat SDF-1-isoforms α, β, and γ. Identical graphic elements indicate identical or homologous sequences. Protein-coding regions are represented by rectangles, 5´- and 3´- UTRs are represented by lines. Isoform-specific C-terminal extensions including putative proteolytic cleavage sites are marked by asterisks. The last four codons of the coding region constituting the C-terminal extension of SDF-1β are depicted in black. The C-terminal extension of the SDF-1γ-coding region comprising 30 codons is represented as a hatched box. The SDF-1γ-specific insertion of 2572 nucleotides, nt, is marked by arrows. UTR, untranslated terminal repeat; kb, kilo base; kDa, kilo Dalton; aa, amino acids.

2.1.7.1 Binding of SDF-1 to CXCR4 as a paradigm for chemokine receptor activation

SDF-1 binds and signals through the CXC chemokine receptor 4, CXCR4. The two site model for SDF-1 binding to CXCR4 is compatible with the current knowledge of other chemokines and their cognate receptors, and suggestedly represents a general model for this family of chemoattractants. Structural elements crucial for receptor binding and activation are contained in the amino acid residues 1–17 of SDF-1, with the sequence KPVSLSYR-CPC-RFFESH, as well as in the proximal N-terminal region and second extracellular loop, ECL2, of CXCR4 (Crump et al., 1997; Elisseeva et al., 2000). While approaching the receptor, SDF-1 presumably transmits an electrostatic signal which facilitates the initial contact of the RFFESH binding motif with the N-terminus of CXCR4 (Crump et al., 1997). According to the model, the RFFESH site is required for optimal binding, but is not sufficient for receptor activation. The first docking step is followed by a conformational change of extracellular and transmembrane receptor domains, leading to the formation of a binding groove among the receptor helices. In the course of these events, the N-terminal region of SDF-1, which is disordered in solution, becomes structured and establishes contact with the receptor groove, whereby the first two N-terminal amino acid residues of SDF-1, Lys-1 and Pro-2, trigger receptor activation by interacting with the ECL2 of CXCR4 (Crump et al., 1997; Doranz et al., 1999). As SDF-1 is highly basic, interaction with the receptor is presumably dependent on a stretch of

negatively charged amino acid residues in ECL2. The third extracellular domain of CXCR4, ECL3, might additionally contribute to receptor activation, although data are inconclusive in this regard.

Cytoplasmic domains of CXCR4 crucial for SDF-1 mediated signalling were identified by studies performed with CXCR4 chimeras and mutants (Roland et al., 2003, Ahr et al., 2005). The DRY box (Asp-Arg-Tyr) is located in the second intracellular loop, ICL2, and represents a highly conserved motif among GPCRs which demonstratedly is indispensable for G protein-activation. Mutation of this motif was shown to frequently result in abrogation of chemokine signal transduction, as could be demonstrated for the α- and β-adrenergic receptors and CCR5, respectively (Fraser et al., 1988; Gosling et al, 1997). Conversely, this motif, even though present in CXCR4, is apparently not required for the majority of SDF-1-dependent signalling events. It could be demonstrated that ICL3 is the only intracellular receptor domain which is indispensable for at least the transduction of G protein-dependent signalling upon SDF-1 binding (Roland et al., 2003). Conversely, while ICL1 is essential in CXCR4 conformation and stability, this domain is not mandatory for CXCR4 activation. Chemotaxis mediated by SDF-1 and CXCR4 requires multiple signal transduction pathways, including ICL3-dependent activation of Janus kinase (Jak)/signal transduction and activation of transcription, STAT, and G_i protein-signalling, ICL2, and the C-terminal part of CXCR4. Except for a role in chemotaxis, the C-terminal tail of CXCR4 was reported to solely contribute to receptor desensitization and internalization (Roland et al., 2003). However, recent studies hint to additional signalling functions of this domain (Lefkowitz and Shenoy, 2005).

Signalling is terminated upon receptor protein phosphorylation at serine/threonine residues in the C-terminal domain, followed by β–arrestin-dependent receptor internalization (Roland et al., 2003). Thereby, phosphorylation facilitates the process of internalization considerably, but is obviously not a prerequisite (Haribabu et al., 1997). In accordance with this model, the two N-terminal residues of MCP-1, MCP-3 and RANTES, represent the major activation sites for their cognate receptors. As the activation sites of chemokine receptors are generally located in the N-terminal region, the model presented here suggestedly might generally apply for chemokine/chemokine receptor interactions.

2.1.7.2 Downstream effectors and biological functions of SDF-1/CXCR4 signalling

Biological functions conveyed by SDF-1 and CXCR4 are multifold (Fig. 1.2) and can, in the context given here, be introduced only briefly (Nagasawa et al., 1994; Lazarini et al., 2003; Kucia et al., 2004). The signalling events involved include phosphorylation of components of the focal adhesion complex such as proline-rich tyrosine kinase-2, Pyk2, p130Cas, focal adhesion kinase, FAK, paxillin, Crk and Crk-L (Wang et al., 2000; Lee at al., 2004). SDF-1-dependent signalling involves the activation of extracellular-signal regulated kinases 1 and 2, ERK1/2, protein kinase C, PKC, phospholipase C-γ, PLC-γ, phosphatidylinositol 3-kinase, PI3K, as well as of regulators of transcription such as nuclear factor κ–B, NFκ-B, and the Jak/STAT pathway. One of the main characteristic features of SDF-1-dependent signalling is a rapid elevation of intracellular Ca^{2+} levels in a PTX-sensitive manner, mainly by depletion of intracellular stores.

2.1.7.3 The SDF-1/CXCR4 axis as a key regulator of mammalian development and maintenance

Expression of SDF-1 and CXCR4 was described to be abundant and constitutive in a plethora of different cell and tissue types and is mirrored by the impressing versatility of mediated functions (Fig. 2.2). SDF-1 and CXCR4 are, amongst others, indispensable for the establishment and maintenance of a functional immune system. Initial studies on recombinant SDF-1 characterized this chemokine as a pre-B-cell growth stimulating factor, PBSF, which supports proliferation of stromal cell-dependent B-cell lines *in vitro* (Nagasawa et al., 1994). SDF-1 is abundantly expressed by stromal cells of the bone marrow, where it effects the retention of CXCR4-expressing hematopoietic cells during maturation. SDF-1 promotes chemotaxis of immune cells and directs them to sites of inflammation, and it further is a potent regulator for homing, development and maintenance of hematopoietic stem cells (Kucia et al., 2004). Engraftment and repopulation of non-obese diabetic/severe combined immunodeficient (NOD/SCID) mice with CD34+ enriched cord blood cells

demonstratedly depends on the presence of SDF-1 and CXCR4, as application of CXCR4-blocking antibodies prior to the transplantation of stem cells was shown to result in a marked reduction of engraftment (Peled et al., 1999).

Lately, it has become obvious that SDF-1 generally acts as a key player in the developing and mature organism, where it directs organogenesis, vascularization, and angiogenesis as well as pathophysiological processes (Lazarini et al., 2003; Kucia et al., 2004; Lieberam et al., 2005). Various publications could demonstrate that SDF-1, in addition to its effects on hematopoietic progenitors, promotes either survival or growth of a number of normal or malignant receptor-expressing cell types, as for example neuronal progenitors and germ cells (Zou et al., 1998; Bagri et al., 2002; Belmadani et al., 2005): During embryonic nervous system development, a functional SDF-1/CXCR4 axis is a prerequisite for proper formation of the cerebellum and the dentate gyrus, as SDF-1 expression in the *pia mater* reportedly prevents premature inward migration of CXCR4 positive cerebellar granule cells. Moreover, this chemokine was demonstrated to concomitantly regulate the mitogenic response of these cells to Sonic hedgehog, SHH, by downregulation of cAMP and protein kinase A activity (Klein et al., 2001). A crucial role of the SDF-1/CXCR4 axis in embryonic development initially was suggested by knock out studies in mice. The notion that deletion of either the CXCR4 or SDF-1 encoding gene results in almost identical, perinatally lethal, phenotypes, indicated for the first time that receptor and ligand presumably interact in a monogamous manner. The phenotype of mutant mice is characterized by a deficient B-cell lymphopoiesis and myelopoiesis as well as by an abnormal neuronal and cardiovascular development (Tachibana et al., 1998; Zou et al., 1998; Peng et al., 2004).

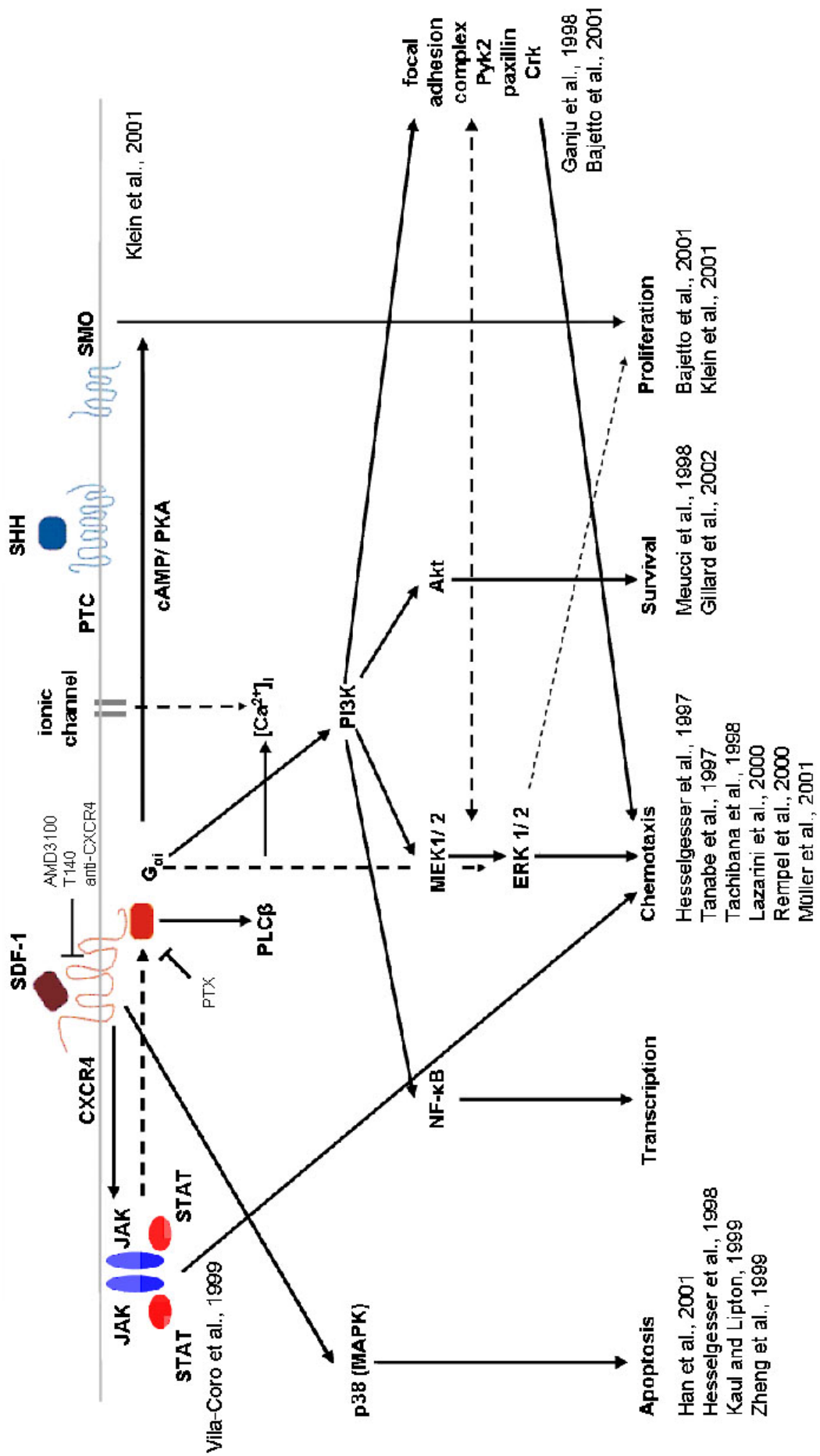

Lazarini et al., 2003 (mod.)

Fig. 2.2 (see also next page).

(see also previous page)

Fig. 2.2. Schematic representation of SDF-1-mediated biological processes. Interaction of SDF-1 and its cognate receptor, CXCR4, mediate various biological functions through activation of diverse signal transduction events. See text for details.

2.1.7.4 SDF-1/CXCR4: pathophysiological implications

Both SDF-1 and CXCR4 are highly expressed in glioma, glioblastoma and astrocytoma cells, and display a marked upregulation in breast and prostate cancer (Muller et al., 2001; Zhou et al., 2002; Rubin et al., 2003; Mochizuki et al., 2004; Wang et al., 2005). Survival and growth of neoplastic cells are stimulated in a paracrine fashion, and tumour angiogenesis is promoted by the attraction of endothelial cells to the tumour microenvironment (Barbero et al., 2003; Smith et al., 2004; Orimo et al., 2005; Burger et al., 2006). Moreover, SDF-1 acts as a molecular beacon for tumour cells, promoting metastasis formation by directing CXCR4-positive malignant cells to the sites of SDF-1 expression (Geminder et al., 2001; Muller et al., 2001; Peled et al., 2002; Allinen et al., 2004). Expression of SDF-1 and CXCR4 is upregulated during inflammatory processes in several brain diseases (Lazarini et al., 2003). Exemplarily, SDF-1-overexpression was noted in pontine neurons of human brains with spinocerebellar ataxia type 3, and CXCR4 expression was demonstrated to be increased in HIV and SIV encephalitis as well as experimental allergic encephalitis, EAE. Similar to chemokine receptor CCR5, CXCR4 was early identified to act as a coreceptor for HIV-1 strains, providing a binding site for HIV-1 glycoprotein gp120 (Zou et al., 1998). The site of interaction with gp120 shows an overlap with that for SDF-1 binding and activation, thus rendering SDF-1 an inhibitor to HIV-1 infection. Approaches employing SDF-1 agonists as potential therapeutic targets are currently being investigated. Interaction of gp120 with CXCR4 has been reported to be causative for severe neuronal loss in the course of HIV-1 pathogenesis through direct and indirect mechanisms (Hesselgesser et al., 1998). Whether interaction of SDF-1 and its cognate receptor is also able to mediate survival or demise of neuronal cells *in vitro* is highly controversial and presumably depends on the amount of microglial and astroglial cells present in the cultures. It has been demonstrated that CXCR4 signalling by SDF-1 as well as HIV glycoprotein

gp120 can lead to an astrocytic release of tumor necrosis factor α, TNFα, and glutamate, causing neuronal damage and apoptosis (Kaul and Lipton, 1999). Contradictory, SDF-1 has been reported to excert neuroprotective functions such as to increase survival of Purkinje neurons deprived of their trophic support and promote survival and proliferation of neuronal progenitors (Peng et al., 2004). Furthermore, SDF-1 was shown to excert crucial functions in tissue repair and regeneration, as it attracts circulating stem and progenitor cells to areas of tissue damage (Imitola et al., 2004). According to recent studies, expression of SDF-1β mRNA is transiently upregulated after peripheral nerve lesion, thus suggesting a role in nerve regeneration (Gleichmann et al., 2000).

2.1.7.5 Structural heterogeneity of CXCR4 and its functional relevance

The cognate receptor to SDF-1, chemokine receptor CXCR4, displays a remarkable degree of structural heterogeneity which perfectly mirrors its multifunctional reaction to SDF-1 exposure and its ability to promote proliferative as well as differentiative or chemotactic responses in a variety of cell or tissue types (Gupta and Pillarisetti, 1999; Baribaud et al., 2001; Sloane et al., 2005).
The molecular masses of CXCR4 isoforms as characterized by isoform-specific RT-PCR, Northern blot and SDS-PAGE analysis to date, are highly divergent, comprising 45–47 kDa in MoltT4 cells, or 59–62 kDa and 90 kDa in monocytes, respectively (Endres et al., 1996; Feng et al., 1996; Lapham et al., 1996; Lapham et al., 1999). Other as for the human splice variant CXCR4-Lo, which differs from the normal splice variant only with regard to an N-terminal extension of 9 amino acids, these considerable variations in the molecular weight of recently identified CXCR4 isoforms can not be attributed to either gene splicing or genetic polymorphism alone (Heesen et al., 1997; Gupta and Pillarisetti, 1999; Sloane et al., 2005). Numerous posttranslational modifications such as N-glycosylation, disulfide formation, tyrosine sulfation and serine chondroitin sulfation might be partially responsible for certain variations (Chabot et al., 1999; Farzan et al., 1999; Chabot et al., 2000; Farzan et al., 2002). However, as CXCR4 heterogeneity is reportedly observed in cells which express receptor variants lacking the respective targets for posttranslational modification, receptor diversity does not seem to be solely dependent on the

presence of structural motifs required for glycosylation, sulfation or G protein-coupling. Further structural functional CXCR4-isoforms might arise from oligomerization of receptor molecules in a non-covalent manner, as was described to occur in the course of CXCR4-dependent Jak/STAT signalling (Ahr et al., 2005).

According to recent studies, cells can be roughly grouped into two categories based on their respective CXCR4 SDS-PAGE profiles (Sloane et al., 2005). Members of the first group express a predominant CXCR4 isoform, which nonetheless differs in a cell-type dependent manner. Nalm-6 cells and Jurkat cells express a 75 kDa isoform of CXCR4, whereas primary HUVEC cells demonstratedly express a variant of approximately 110 kDa. Members of the second group display multiple isoforms; this group includes CEMT4 cells, transfected cells overexpressing CXCR4 such as HeLa cells, and primary lymphocytes. In accordance with the structural differences described, CXCR4 isoforms differ strongly in their function (Amara et al., 1997; Doranz et al., 1999; Lazarini et al., 2000). Reportedly, T-lymphoid CEMT4 cells are able to bind SDF-1 as well as to mediate HIV-1 binding and infection, but do neither display ligand-mediated chemotaxis nor calcium influx (Sloane et al., 2005). Jurkat cells also fail to elicit a calcium flux response, but migrate towards a gradient of SDF-1. Thereby, chemotaxis in Jurkat cells is presumably mediated by a 75 kDa variant of CXCR4, which is absent in CEMT4 cells. Thus, a cell or tissue specific isoform expression might underlie the many cell or tissue specific CXCR4 functions described to date. The structural heterogeneity described in various studies further accounts for the cell and tissue type-dependent ability of antibodies directed against CXCR4 to reliably detect receptor expression, block interaction with SDF-1, and inhibit HIV-1 infection. The antibody most commonly used, mouse monoclonal antibody 12G5 clone, which binds two epitopes in ECL1 and ECL2 of CXCR4 in a conformation-dependent manner, recognizes only a subpopulation of CXCR4 and thus was noted to frequently effect a miscalculation of CXCR4 expression (Sloane et al., 2005).

2.1.7.6 RDC1 as an alternative receptor to SDF-1

Recently, an orphan receptor, RDC1, was demonstrated to act as a novel receptor for SDF-1 as well as a coreceptor to genetically diverse HIV-1, HIV-2 and SIV strains (Shimizu et al., 2000; Balabanian et al., 2005).

In the course of its varied history, RDC1, originally cloned from a canine thyroid library on basis of its homology with conserved domains of G protein-coupled receptors, was initially reported to act as a G_s protein-coupled receptor for vasoactive intestinal peptide, VIP (Sreedharan et al., 1991). Later, it was defined as the receptor for calcium gene-related peptide or adrenomedullin, respectively (Sreedharan et al., 1991). These observations were finally dismissed, rendering RDC1 orphan until only recently, when, based on combined phylogenetic and chromosomal location studies, RDC1 was claimed to excert CXC-chemokine receptor function (Cook et al., 1992; Nagata et al., 1992; Balabanian et al., 2005).

SDF-1, the only known natural ligand for CXCR4, was demonstrated to bind to and signal through RDC1 (Balabanian et al., 2005). Thereby, binding of this chemokine to RDC1 reportedly elicits chemotaxis in T lymphocytes and generally triggers receptor desensitization and internalization in RDC1 expressing cells. SDF-1 mediated receptor functions of CXCR4 and RDC1, respectively, seem to complement one another, as the concomitant blockade of both receptors by application of specific antibodies leads to additive inhibitory effects in T cell migration. Interaction of SDF-1 with RDC1 was described to occur in a specific and dose-dependent manner, and with an affinity higher than that estimated for CXCR4, as defined by binding studies with biotinylated ligand molecules. As for CXCR4, binding of SDF-1 to RDC1 involves the N-terminus of this receptor, as it displaces binding of anti-RDC1 antibody directed against the N-terminal receptor domain (Balabanian et al., 2005). These observations are supported by amino acid similarities displayed by sequence alignments of the N-termini of CXCR4 and RDC1, whereby both receptors exhibit acidic and aromatic residues known to mediate binding of HIV gp120 and SDF-1 (Balabanian et al., 2005).

Due to its abundance and to the evolutionary conservation revealed by antibody-based studies of the human homolog of canine RDC1, this receptor was early predicted to convey crucial physiological functions in various cell and tissue types

(Law and Rosenzweig, 1994). A hydropathicity plot for RDC1 shows typical features of a G protein-coupled receptor, such as an extracellular N-terminus, seven transmembrane-spanning regions and an intracellular C-terminus. RDC1 possesses high sequence similarity with known chemokine receptors and contains typical chemokine receptor signatures such as the DRY motif at the boundary of the third transmembrane helix and the second intracellular loop, a CxNPxxY sequence in the seventh transmembrane domain, and four conserved cysteine residues in its extracellular segments. Moreover, the C-terminus of RDC1 comprises several conserved serine and threonine residues which might act as targets for receptor phosphorylation during receptor desensitization. Similar to CXCR4, it could be demonstrated that endocytosis of RDC1 requires the integrity of the C-terminal domain of the receptor, whereas this domain is not necessarily required to excert general receptor functions (Haribabu et al, 1997; Balabanian et al., 2005). The gene encoding murine RDC1 is located on chromosome 1 in close proximity to the genes coding for the chemokine receptors CXCR1, CXCR2 and CXCR4. In humans, a similar arrangement was found on chromosome 2. The predicted 362 amino acid sequence of murine RDC1 displays 92% and 91% similarity to human and dog orphan receptor RDC1, respectively, with two long trenches of complete amino acid conservation, and shares 43% amino acid similarity to rabbit and mouse CXCR2. Underscoring its kinship with members of the chemokine receptor superfamily, RDC1 acts as a coreceptor for various HIV-1, HIV-2 and SIV strains, and in particular for the CXCR4-tropic HIV-2 ROD strain (Shimizu et al., 2000).

Taken together, these evidences support the hypothesis that RDC1 is a potential chemokine receptor, although until now there is only limited knowledge on cellular and tissue distribution of RDC1 gene expression, and reports on RDC1 as a receptor for SDF-1 are contradictory. (Balabanian et al., 2005; Infantino et al., 2005). Similar to CXCR4, RDC1 is ubiquitously expressed in hematopoietic as well as in non-hematopoietic tissues, and its mRNA can be detected in brain, heart, spleen, kidney, and in PBLs as well as in tumours from brain and peripheral vasculature endothelium. RDC1 appears to be tightly regulated during the development of B cells, and expression of RDC1 correlates with their capacity to differentiate into plasma cells upon polyclonal activation (Infantino at al., 2005). The orphan receptor RDC1 thus presumably acts as a high affinity receptor for SDF-1, whereby interaction depends on the intact N-terminus of this chemokine. As six CXC-receptors have

been characterized to date, it has been supposed that RDC1 should, in accordance with chemokine nomenclature, be renamed CXCR7 (Balabanian et al., 2005). The reported expression of RDC1 in malignant cells might implicate a function of the SDF-1/RDC1 axis in pathological processes, as could repeatedly be shown for interaction of SDF-1 and CXCR4. As mice mutant for either SDF-1 or CXCR4 display a similar defective phenotype suggestive of a monogamous relationship of receptor and ligand, the role of RDC1 is not understood yet. Nonetheless, the highly conserved sequences of RDC1 and SDF-1 among the species suggest that SDF-1/RDC1 interactions might have conserved functional significance.

2.2 Nervous system regeneration

As axons and neurites are undistinguishable to the spectator until specification of the former at a certain time point in development, both will in the following be referred to as neurites.

2.2.1 Mechanisms of neurite outgrowth and elongation

Neurite outgrowth and branching during developmental and regenerative processes is based on the dynamic rearrangements of the cytoskeletal apparatus (Dickson, 2002; Dent et al., 2003). External guidance cues influencing neurite outgrowth, whether they be attractive or repellent forces, are sensed by the growth cone, a highly motile structure at the distal end of the neurite, in a mechanism not fully understood yet. Information received and processed in the neuritic tip is then translated by means of highly complex protein-protein interactions into a coordinated assembly of cytoskeletal components comprising microtubules and actin filaments.

2.2.2 Structure and function of the nervous system

The vertebrate nervous system can be roughly subdivided into the CNS, comprising the brain and spinal cord, and the PNS, formed by the cranial and spinal nerves

including their branches and the autonomic glia. The nervous tissue of the spinal cord integrates sensory information received from the body and sends it to the brain, while at the same time coordinating body movements by propagating motor commands caudally along the spinal cord, transmitting them to local spinal motor circuits and peripheral nerves. The underlying processes are executed by two groups of highly specialized cells, neurons and glia.

2.2.3 CNS injury

The origin of a CNS lesion can either be a progressive neurological disease or a traumatic lesion which affects the brain or spinal cord. Although both brain and spinal cord tissue are protected to some extent by cranial bones or the vertebrae of the spinal column, respectively, damage does easily occur.

The origin of a spinal cord lesion is most frequently effected by a mechanical insult such as the contusion and compression of nervous tissue by a displacement of bones or vertebrae of the spine (Baptiste and Fehlings, 2006). Damage to the CNS is often accompanied by severe neuronal loss and a disruption of axonal and neuritic connections in brain and spinal cord circuitry, which finally results in a marked impairment of physical and mental abilities (Blight, 2002). Depending on the site and severity of the lesion, this event leads to an abrogation of communication between muscles and brain and a partial or complete paralysis (Schwab et al., 2002). Generally, the initial insult to the nervous system which is characterized by the mechanical destruction of tissue, is followed by a second phase in which cell loss is elicited by the disruption of blood supply, or the formation of toxic compounds leading to apoptosis (Schwab and Bartholdi, 1996; Fawcett and Asher, 1999; Dumont et al., 2001; Baptiste and Fehlings, 2006).

While in the embryonic central nervous system, as well as in the adult peripheral nervous system, regeneration of injured nerve fibre tracts occurs spontaneously, regrowth in the adult mammalian central nervous system is often markedly limited. Soon after injury, the compromised axons undergo a process termed “Wallerian degeneration”, during which they are irretrievably lost, and newly formed growth cones collapse soon after outgrowth. On a cellular level, this degenerative process is characterized by four phases: After the initial insult, the compromised axon loses its

myelin sheath, this loss being accompanied by a decrease in conductivity (1). Subsequently, the lesioned axon retracts, and synaptic connections are lost (2). This phase is ensued by a reactive cellular response, involving the activation and attraction of astrocytes and microglia (3). In a terminal stage aberrant sprouting can occur, which is finally terminated by neuronal cell death, if the level of growth-promoting factors is too low (4).

2.2.4 CNS regeneration failure: inhibitors and mechanisms

Limitation of CNS regeneration can be ascribed to various factors: First, at the site of injury a fibrous and glial scar is formed by invading fibroblasts and glial cells, constituting a physical barrier to regrowth (Fawcett and Asher, 1999; Klapka and Müller, 2006; Yiu et al., 2006). Second, upon contact with the cell body or axons, inhibitors associated with the extracellular matrix or released by myelin-producing cells, trigger intracellular events which then lead to a growth arrest and a collapse of the newly formed growth cone (Tang et al., 2001; Filbin, 2003; Schwab et al., 2005). Moreover, there is growing evidence that the intrinsic state of the compromised neuronal cell might be of importance for the regenerative ability of the axon, directing the cellular response to inhibitory environmental cues according to intracellular second messengers and effector molecules (Blackmore and Letourneau, 2005). Of the inhibitors to central nervous system regeneration, various have been identified to date (Filbin, 2003). Although they are abundantly present in the intact spinal cord, and at least some are thought to have a role in the control of aberrant sprouting and the stabilization of mature connections, their normal and developmental functions have not been clarified as yet. (Benson et al., 2005).

Myelin, which largely contributes to the formation of white matter in the nervous system, is formed by highly specialized cells in the CNS as well as the PNS, oligodendrocytes and Schwann cells, respectively, and acts as an insulating multilayered membrane to axons, maintaining the rapid and efficient transmission of electrical signals by allowing saltatory excitation. Unlike other membranes, myelin consists of lipid and protein in a ratio of 70:30%, and contains high amounts of galactoplipids. In accordance with other membranes, the remaining major lipids of

both PNS and CNS myelin are cholesterol and phospholipids. Despite various similarities, quantitative and compositional differences exist concerning the basic lipid classes and proteins present in PNS and CNS.

In the adult mammalian CNS, white matter areas constitute, amongst others, a major obstacle to the regenerative growth of lesioned axons. This effect can, before all, be ascribed to the presence of growth inhibitory molecules associated with myelin or released by the latter after a traumatic injury (Tang et al., 2001; Schwab et al., 2005). CNS myelin first was postulated as a major source of inhibition when immobilized CNS myelin, but not PNS myelin, was found to inhibit axon outgrowth in various experiments. Proteins associated with CNS myelin and released upon injury were first demonstrated to negatively regulate neuronal regeneration as early as in 1928, when Ramón y Cajal pointed to white matter growth adversary effects in the adult mammalian CNS (Ramón y Cajal, 1928). In the following, these observations were supported by Schwab and colleagues who in the late 1980s were the first to characterize molecular mechanisms underlying myelin-induced growth inhibition (Caroni and Schwab, 1988; Caroni and Schwab, 1988b). Only few of the myelin-associated inhibitors, MAIs, have been characterized to date, of which three have been extensively studied.

2.2.4.1 Nogo

Nogo, a major inhibitor to CNS axon regeneration, was originally characterized as an antigen to the IN-1 antibody which was demonstrated to abrogate oligodendrocyte-mediated neurite outgrowth inhibition *in vitro* (Caroni et al., 1988; Spillmann et al., 1998)

Nogo is a glycosylated transmembrane protein with a molecular weight of approximately 220 kDa which contains a leucin-rich repeat, LRR, domain crucial for receptor interaction. Members of the LRR protein family have a role in protein-protein interactions that are of importance, amongst others, in neural development (Kobe et al., 2001). The MAI Nogo exists in three different isoforms, Nogo-A, Nogo-B, Nogo-C, which are all dedrived from one common gene template by alternative splicing and promoter usage. The splice variants comprise a common C-terminus of 188 amino acids which is also termed the reticulon-homology domain, RHD. Nogo proteins

constitute members of the reticulon, RTN, family of proteins and are accordingly named RTN4 (Chen et al., 2000). In evolutionary terms, reticulons are ancient proteins, and members of this family are found in all eukaryotes.

Of the three different isoforms, Nogo-A in particular has been demonstrated to act as an inhibitor to regeneration of adult CNS axons, whereby inhibitory effects are conveyed through at least two different domains (Chen et al., 2000; GrandPrè et al., 2000; Brittis and Flanagan, 2001). The first inhibitory region is a loop-like domain comprising 66 amino acids which is located in the RHD between two hydrophobic stretches, named Nogo-66 (GrandPre et al., 2000). The second inhibitory domain, even though not thoroughly characterized yet, was termed amino-Nogo, central inhibitory domain or NiG and can presumably be mapped to a region specific to Nogo-A (Prinjha et al., 2000). While Nogo-66 is exposed to neuronal contact sites on the extracellular side of the oligodendrocyte plasma membrane, the method of interaction for amino-Nogo is not fully understood yet. As this domain is generally located on the cytosolic site of the membrane, interaction with the neuronal surface would either require a spatial rearrangement of the whole Nogo molecule or a release of amino-Nogo from damaged oligodendrocytes in the course of CNS injury. Nogo has been described to act through a GPI receptor accordingly named Nogo66 receptor, NgR, as part of a tripartite inhibitory complex, by a mechanism that will be elucidated in the following (Domeniconi and Filbin, 2005; Domeniconi et al., 2005).

2.2.4.2 OMgp

First identified in 1988 in human CNS white matter, the highly glycosylated oligodendrocyte-myelin glycoprotein, OMgp, has been demonstrated to act as an inhibitor to post-injury regeneration of CNS neurons *in vitro* (Wang et al., 2002; Vourc´h and Andres, 2004).

OMgp comprises approximately 110 kDa, and excerts its inhibitory function presumably through NgR and its associated receptor complex, as cleavage of NgR from the cell surface leads to insensitivity of neurons to the inhibitory protein. The mature form of OMgp comprises 401 amino acid residues which can be subdivided into four different domains. Binding of OMgp to the tripartite inhibitory receptor complex, namely NgR, reportedly requires the evolutionary highly conserved LRR

domain characteristic for GPI-linked proteins, and the C-terminal domain containing serine-threonine repeats.

OMgp, which is linked to the cell membrane by a glycosylphosphatidylinositol, GPI, anchor, is abundantly expressed in the CNS, where it is present on the cell surface of neurons and mature oligodendrocytes positive for myelin basic protein, MBP, and is enriched in myelin layers adjacent to axons (Mikol et al., 1988; Mikol et al., 1990; Habib et al., 1998). Northern Blot analysis of rodent CNS showed an increase in murine OMgp mRNA levels from postnatal day P0 to P21 with a maximum in the late stages of myelination, before expression of this molecule decreases and reaches a stable level of expression at P24. Besides promoting growth cone collapse and regeneration failure in the lesioned adult mammalian CNS, OMgp is suggestedly involved in the formation and maintenance of myelin sheaths during development (Vourc´h and Andres, 2004). Moreover, the LRR domain further seems to be involved in the inhibition of cell proliferation, and mutations in the OMgp gene locus lead to a heterozygous genotype characteristic for Neurofibromatosis type I (Habib et al., 1998).

2.2.4.3 MAG

Another well-studied inhibitor present in CNS myelin is the myelin-associated glycoprotein, MAG (McKerracher et al., 1994; Tang et al., 2001).

MAG, which can be grouped into the superfamily of sialic acid binding, Ig like lectins, Siglecs, according to five Ig domains in the extracellular region, shares 45–50% amino acid sequence identity with CD22 and sialoadhesin, two other members of this superfamily (Kelm et al., 1994). A proteolytic fragment, comprising the complete extracellular domain of MAG, is released from purified or damaged myelin in the nervous system, resulting in an enrichment of inhibitory protein at the site of injury (Tang et al., 2001). Neurite outgrowth inhibition by MAG is dependent on the complete extracellular domain, as fusion proteins comprising only the first three Ig domains fail to elicit neuronal growth arrest (Tang et al., 1997). MAG abrogates neurite outgrowth of neuronal cells *in vitro*, and regeneration can be promoted by targeting this MAI with specific antibodies. Similar to various axonal guidance cues with a role in nervous system development, MAG acts in a bifunctional way

(Hasegawa et al., 2004). Depending on type and developmental stage of the neurons, MAG either promotes or inhibits axonal growth (Johnson et al., 1989; McKerracher et al, 1994; Mukhopadhyay et al., 1994; DeBellard et al., 1996). Interestingly, the switch from growth promotion to inhibition thereby occurs at birth for all types of neurons studied to date. Exceptionally, for DRG neurons this switch was reported to take place at postnatal day P3 to P4 (DeBellard et al., 1996). The inhibitory effect of MAG on neuronal cells is further confirmed by studies performed with MAG-deficient mice, where extensive axonal regeneration could be observed following CNS injury. As stated by early studies on this protein, MAG presumably accounts for 60% of the total inhibitory properties of CNS myelin in regeneration (McKerracher at al., 1994).

Surprisingly, axon outgrowth inhibition by Nogo, OMgp, and MAG is, despite of the structural diversity of these proteins, demonstratedly conveyed by a common tripartite receptor complex (Domeniconi et al., 2005). The intricate intracellular signalling machinery downstream of this complex, leading to growth cone collapse and growth arrest, has not been completely unravelled to date. Initial binding of myelin-associated inhibitors occurs via the Nogo66 receptor, NgR. As NgR represents a GPI-linked receptor which lacks a transmembrane as well as a cytosolic domain, transmission of the inhibitory signal to the intracellular side has to be conveyed by at least one coreceptor. The neurotrophin receptor $p75^{NTR}$ and the transmembrane protein LINGO-1 were reported to act together with NgR to trigger axon growth inhibition upon ligand binding. At least for MAG, the interplay of the components of receptor complex and intracellular signalling machinery has been largely elucidated (Fig. 2.3). Signalling thereby involves a process of regulated intramembrane proteolysis, RIP, which constitutes a novel mechanism in receptor signalling typified by processing of highly divergent proteins (Brown et al., 2000). Upon interaction of the ligand with the tripartite receptor complex, cleavage and shedding of the extracellular domain, ECD, of $p75^{NTR}$ is initiated by activation of a membrane-bound α–secretase complex (Hooper et al., 1997). This step is obligatory for a second proteolytic event within the transmembrane domain of $p75^{NTR}$. The second cleavage step requires activation of PKC and is performed by a γ–secretase complex, thus finally releasing the $p75^{NTR}$ intracellular domain, ICD. Release of this fragment into the neuronal cytosol seems, at least in the instance of MAG, to be a

prerequisite for activation of the small GTPase Rho and subsequent outgrowth inhibition. In a number of recent publications, Rho was identified as a key intracellular effector for growth inhibitory signalling by myelin inhibitors (Wang et al., 2002; Yamashita et al., 2002; Mi et al., 2004). In its active GTP-bound state, Rho rigidifies the actin cytoskeleton, a mechanism which under certain conditions could lead to a complete inhibition of axon elongation and thus mediate growth cone collapse. The ICD fragment presumably displaces Rho-GDI from the Rho complex, rendering Rho in an activated state. According to experimental observations published only recently, a subsequent activation of both Rho and ROCK could lead to phosphorylation of LIM kinase 1, LIMK1. LIMK1 was described to phosphorylate and deactivate cofilin, a major regulatory protein of the actin depolymerising factor/cofilin family (Hsieh et al., 2006). As Nogo-66 and OMgp have also been described to convey their inhibitory effects through NgR, it can be assumed that their mode of action might be similar to the one described for MAG. Action of myelin-inhibitory proteins thus suggestedly triggers deregulation of actin dynamics and stability, which then leads to a collapse of the axonal growth cone, growth arrest, and regenerative failure.

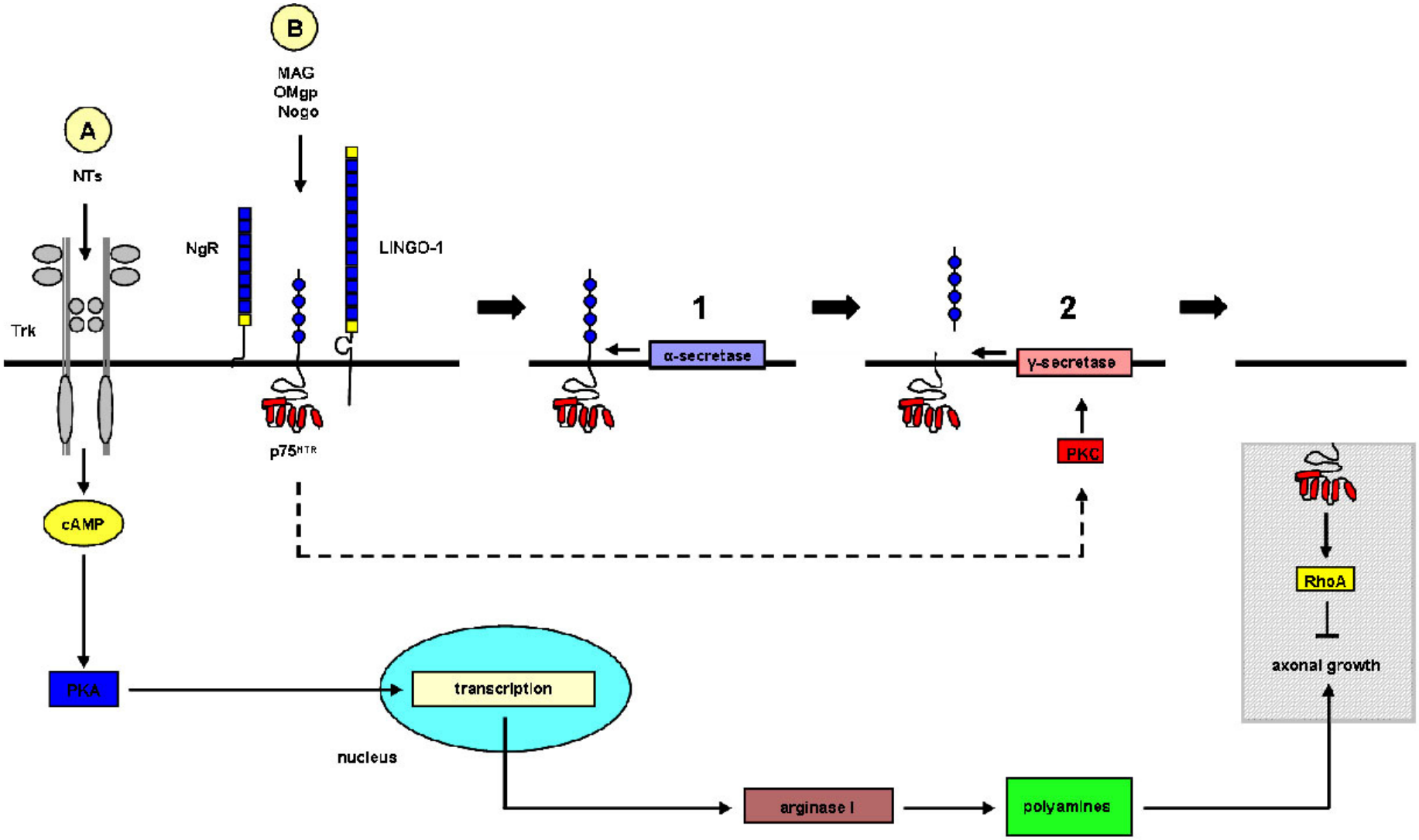

Fig. 2.3. (see also next page)

(see also previous page)

Fig. 2.3. Proposed model of promotion and inhibition of axonal outgrowth. Elevation of intracellular cAMP levels through neurotrophin-mediated activation of Trk receptor increases neuronal outgrowth in a transcription-dependent manner (A). Axonal growth inhibition is induced by myelin proteins MAG, OMgp and Nogo-66 (B). Upon interaction of inhibitors with the tripartite NgR/$p75^{NTR}$/LINGO-1 receptor complex, $p75^{NTR}$ is cleaved through consecutive action of α-secretase (1) and γ-secretase (2). The cytosolic fraction of $p75^{NTR}$ activates RhoA and abrogates axonal growth (shaded box). Growth inhibition by myelin proteins is partially regulated in an autocrine fashion by p75NTR-dependent activation of PKC (dashed arrow).

2.2.4.4 Slits, netrins, semaphorins and ephrins

The direction of axons to their proper targets affords the finely tuned cooperation of attractive and repulsive guidance molecules. Slits, netrins, semaphorins and ephrins act as signposts to outgrowing neurons during the formation of central and peripheral nervous system circuitry (Goshima et al., 2000; Dickson, 2002; Goldshmit et al., 2006). While netrins, slits and the majority of semaphorins are secreted molecules that tether to the extracellular matrix or cell membranes, ephrins as well as few semaphorins are cell surface-expressed. Generally, slits, semaphorins and ephrins act as repellents, whereas netrins can be attractive as well as repulsive. Frequently, action of these guidance molecules is regulated in a context-dependent manner. For each of the families, specific receptors have been identified: Netrins bind to and signal through UNC-40/DCC and UNC-5 receptors, slit proteins interact with Roundabout, Robo, receptors, signalling of semaphorins is mediated by neuropilin and plexin receptors, and ephrins constitute ligands to Eph receptors (Dickson, 2002). The modes of action of members of the four families to direct axonal outgrowth differ and are not fully understood yet. As cytoskeletal rearrangements represent a key event in the attraction and repulsion of the growth cone, the Rho familiy of GTPases, which direct the formation of a wide range of cytoskeletal structures, is presumably implicated in axon guidance (Dent et al., 2003).

While the number of guidance molecules is comparably low, the corresponding pathways by which axonal direction occurs show a remarkable versatility. According to recent studies, this can be ascribed to a number of mechanisms by which slit,

netrin, semaphorin and ephrin functionality is amplified, such as the developmental regulation of guidance cues, the alternation of cellular responses due to specific intrinsic or additional extrinsic factors, or the assembly of complexes triggering new signalling pathways.
In the adult, these guidance molecules presumably take over an inhibitory role upon contact with regrowing axons after CNS injury. For instance, Ephrin-B3 and Sema4D/CD100, which excert a role in axonal pathfinding and are expressed in postnatal myelinating oligodendrocytes, demonstratedly inhibit neurite outgrowth of postnatal CNS neurons (Moreau-Fauvarque et al., 2003; Benson et al., 2005).

2.2.4.5 CSPGs

In addition to myelin-inhibitory proteins as well as developmentally active guidance molecules, molecular properties of astrocytes, fibroblasts and microglia contribute to the formation of a non-permissive environment for lesioned axons. In the wake of a CNS injury, astrocytes in the affected area often become hypertrophic and attain a reactive phenotype. Release of inhibitory extracellular matrix molecules such as aggrecan, phosphacan, and NG2 – chondroitin sulphate proteoglycans, CSPGs – demonstratedly leads to an outgrowth inhibition of lesioned axons at the site of injury (Monnier et al., 2003; Yiu and He, 2006). Whether growth-adversary effects are attributable to the glycosaminoglycan, GAG, side chains, or the core protein, has not been clearly stated yet, as studies on an overcoming of growth inhibition after chondroitinase-mediated side chain digestion remain inconclusive or even contradictory up to now. CSPGs are present in both the glial scar and in myelin and mediate inhibition of neurite outgrowth of various neuronal cell types in a manner at least partly different from the aforementioned inhibitory agents. Nonetheless, as blocking of the Rho/ROCK pathway abrogates the inhibitory activity of CSPGs, it might be suggested that different inhibitory to neurite growth share at least some components of the signalling pathways involved (Monnier et al., 2003; Yiu and He, 2006).

2.2.5 Strategies for CNS regeneration

With an estimated annual number of approximately 10 000 new cases in North America alone, spinal cord injury, SCI, resulting in partial or complete paralysis, mainly contributes to the number of disabled patients requiring life-time intensive care (Sekhon and Fehlings, 2001; The National SCI Statistic Center, 1999). While medical means of intervention still are limited, novel therapeutic approaches to increase CNS regeneration and overcome functional impairment are permanently under investigation.

The pathobiology of SCI is generally adressed as a “two-staged” process (Sekhon and Fehlings, 2001; Jacobs and Fehlings; 2003; Stys, 2004). In acute traumatic SCI, a primary mechanical insult to the spinal cord initially results in a severe loss of neurological function below the level of injury. While immediate damage is due to compression, shear, laceration or contusion of the affected nervous tissue, it is later followed by the activation of a delayed secondary cascade of harmful events, which finally results in the progressive degeneration of the spinal cord (Baptiste and Fehlings, 2006). Those events include, amongst others, glutamate excitotoxicity, disturbance in ionic homeostasis, oxidative cell injury and a robust inflammatory response. Thereby, the complexity of SCI both allows and requires therapeutical interventions at different levels.

Several strategies are applied to repair the injured spinal cord, all of which are currently tested in animal models based on the artificial infliction of CNS injury, or are already applied in human clinical trials (Schwab, 2002; Baptiste and Fehlings, 2006).

2.2.5.1 Pharmacological approaches

Numerous pharmacological approaches have been undertaken to prevent neurological deficits following SCI, of which the most extensively investigated is application of the glucocorticoid methylprednisolone sodium succinate, MPSS (Bracken et al., 1984; Bracken et al., 1990; Bracken et al., 1992; Otani et al., 1994; Bracken et al., 1997). Research on the neuroprotective properties observed for MPSS demonstrated that the agent acts as an antioxidant and further mediates the

downregulation of inflammatory response by reduction of TNFα protein synthesis and NF-κB activity.

Besides of MPSS, several other pharmacological interventions have been tested, as for example 21-Aminosteroids, gangliosides, or sodium channel blockers to counteract the deleterious accumulation of intracellular sodium following the injury (Hall, 1993; Bracken et al., 1994; Rosenberg et al., 1999; Geisler et al., 2001; Stys, 2004). Unfortunately, one of the main drawbacks of these pharmacological approaches is the fact that treatment has to be administered in a narrow time frame of hours to days to be efficient. Thus, alternative strategies are tested which are based on profound knowledge of molecular and cellular events during CNS development and regeneration provided by developmental neurobiology to allow for increased flexibility in therapeutic interventions (Horner and Gage, 2000; Blight, 2002; Hulsebosch, 2002; Schwab, 2002).

2.2.5.2 Nerve grafts and abrogation of inhibitory molecules

Peripheral nerve grafts, embryonic tissue grafts or artificially engineered scaffolds such as polymer channels containing growth-supportive cells or neurotrophins, are implanted to bridge the lesion and offer a growth-permissive environment to regenerating axons (Cheng et al., 1996; Ramon-Cueto et al., 1998; Bunge, 2001). With this, axons are able to avoid contact with MAIs as well as the extracellular matrix while crossing the lesion site through the graft. Conversely, even though the implantation of growth-permissive grafts proved to be beneficial for bridging CNS lesion sites, regenerating axons often cross the borders to the normal CNS environment only reluctantly.

Following an alternate strategy, inhibitory molecules present in the spinal cord after injury are targeted either by blocking antibodies or by enzymatic cleavage. Axonal outgrowth inhibition by Nogo, MAG or OMgp, can demonstratedly be abrogated by application of specific antibodies or preimmunizing lesioned animals with CNS myelin (Savio and Schwab, 1990; Schnell and Schwab, 1990; Schwab and Bartholdi, 1996; Huang et al., 1999). Moreover, enzymatical treatment of growth-adversary CSPGs by application of chondroitinase ABC was demonstrated to result in growth promotion of regenerating axons. Besides the various inhibitory molecules, components of the

ensuing signalling events can be targeted to induce outgrowth promotion. To this end, effector molecules implicated in growth inhibition, such as Rho and ROCK, are targeted by specific inhibitors, resulting in improved axonal regeneration (Brösamle et al., 2000; Brittis and Flanagan, 2001; Moon et al., 2001; McKerracher and Higuchi, 2006).

2.2.5.3 Application of neurotrophic factors

Parallel to the strategies enlisted above, application of neurotrophic factors could presumably contribute to axonal regeneration in the adult mammalian CNS. Expression of neurotrophins such as NGF, BDNF or NT-3 is abundant in the developing nervous system, but decreases in the adult. It was demonstrated that the delivery of neurotrophic factors into the immediate vicinity of the lesion site by means of osmotic pumps or genetically engineered cells can, at least partially, re-establish an environment similar to the one in embryonic development and thus restore the growth-promoting properties of the CNS environment (Bregman et al., 1998; Horner and Gage, 2000; Lacroix and Tuszynski, 2000).

2.2.5.4 Cellular replacement strategies

As damage to the spinal cord is often accompanied by a severe loss of both glial and neuronal cells, of late, cellular replacement strategies employing stem cell grafts have been considered to represent a promising therapeutic approach for CNS regeneration (Gage et al., 1995; Flax et al., 1998; Liu et al., 1999). Multipotent stem cells are engrafted at the lesion site, where they might adapt to the region by differentiating into the appropriate neuronal and glial subpopulations. Alternately, engrafted stem cells could obtain a supportive role after transplantation and thus excert survival promoting effects, as was recently described for Purkinje neurons (Li et al., 2006).

2.2.5.5 Altering the intrinsic neuronal state: a role for cAMP in regeneration

As there exists increasing evidence that axonal regeneration in the lesioned adult mammalian CNS is at least partially dependent on the intrinsic state of the neuronal cells, approaches are under investigation to manipulate intracellular signalling events and restore early developmental outgrowth properties at least partially to the effect that inhibitors to regeneration are ignored and axonal regrowth is performed despite the presence of an growth-adversary surrounding, as for example during embryogenesis. Thereby, main targets are cAMP or components of cAMP-dependent signal transduction cascades, as will be further outlined in the following (Cai et al., 2001; Gao et al., 2003; Gao et al., 2004).

During the recent decades of research in the field of nervous system regeneration, the cyclic adenosine monophosphate, cAMP, has increasingly gained attention as a putative modulator of axonal regeneration after spinal cord injury (Cai et al., 1999). A role for cyclic nucleotides in neurite outgrowth and regeneration was proposed early, when a conditioning lesion of the peripheral branch proved to promote central axon regeneration of dorsal root ganglia, DRGs, and was concomitant with an increase of intracellular cAMP levels (Qiu et al., 2002). Further, in various studies elevation of cAMP by injection into the cell body or by application of external stimuli demonstratedly increased the regenerative capacity of adult neuronal cells (McQuarrie et al., 1978; Qiu et al., 2002). The second messenger molecule cAMP is synthesized from ATP mainly by GPCR-dependent, membrane-bound adenylyl cyclases, and is rapidly degraded by phosphodiesterases. It regulates cellular processes through a variety of signalling pathways, and an increase of intracellular cAMP levels triggers, amongst others, the activation of PKA. While this effector molecule has been reported to promote outgrowth in its active form despite the presence of CNS inhibitory molecules *in vivo* as well as *in vitro*, the mode of action has not been unravelled to date. PKA could directly act on cytoskeletal behaviour, or promote neurite outgrowth by altering gene expression (Cai et al., 2002). One of the genes constituting a putative target for cAMP/PKA action is the Arginase, Arg, encoding gene, an enzyme to which neuroprotective effects have been ascribed (Esch et al., 1998). Arginase exists in two isoforms, cytosolic ArgI and mitochondrial ArgII, both of which catalyze the hydrolysis of arginine to ornithine and urea

(Nakamura et al., 1990; Seiler, 2000). Recently, it has been suggested that the growth-promoting properties of intracellular cAMP might be attributable to the ArgI-dependent synthesis of polyamines (Cai et al., 2002). Polyamines are polycations which are ubiquitously present in all prokaryotic and eukaryotic organisms analyzed to date. The three polyamines identified as yet are the diamine putrescine, the triamine spermidine, and the tetraamine spermine, which are all synthesized from ornithine in an ArgI-dependent manner. Initially, polyamines were described to excert a role in the control of nuclear protooncogene expression, activation of protein kinases and transcription factors. Moreover, effects of polyamines on growth, developmental and regenerative processes of the nervous system have been suggested by various studies (Ingoglia et al., 1982; Gilad and Gilad, 1988; Gilad et al., 1996). As polyamines are known to be regulators of cytoskeletal rearrangement processes, they could act upon axonal outgrowth by increasing the stability of components of the cytoskeleton or rearrange them according to external guidance cues.

2.3 Aim of this thesis

The aforementioned limited capacity of adult mammalian CNS neurons to recover has placed neuronal regeneration in the focus of neurobiological investigations. Although several strategies have been reported to ameliorate shortcomings of neuronal regeneration following injury, recovery is too often only transient and its mechanisms are poorly understood. In recent work, SDF-1 and its cognate receptor, CXCR4, were described to efficiently redirect axonal outgrowth behaviour and neuronal responses to embryonic inhibitory guidance cues. In this study, it was intended to apply the findings of latter investigations, which describe a role for SDF-1 in embryonic nervous system development, on an *in vitro* model of postnatal neuronal regeneration in the complex inhibitory environment of adult CNS myelin. Combined with the immunocytochemical analysis of a) neuronal signalling mechanism as triggered by SDF-1 in postnatal neurons as well as b) expression and cellular distribution of SDF-1 and its receptors, CXCR4 and RDC1, the investigative approach intended to answer

whether SDF-1 has a role in overcoming myelin-induced neurite outgrowth inhibition in postnatal neurons.

which signalling events mediate a possible growth promoting function of SDF-1.

whether expression and cellular distribution of either or both receptor(s) to SDF-1 are indicative of a specific role in a presumed SDF-1-induced neurite outgrowth promotion.

In a second part of this thesis, a recently characterized isoform of SDF-1, SDF-1γ, should be analyzed in its function in cellular Ca^{2+} homeostasis. While various transcripts of this chemokine have been characterized to date with regard to molecular and structural particularities, no isoform-specific biological functions could be identified. By comparing SDF-1γ- and SDF-1α-mediated Ca^{2+} signalling, it was intended to investigate a putative role of the C-terminal extension of the γ-transcript, and to identify components of the signal transduction pathway for either isoform.

3. Materials and methods

3.1 Materials

3.1.1 Animals, primary cells and cell lines

Embryonic and postnatal Wistar rats were subjects for preparation of primary cells used in the following experiments. Pregnant Wistar rats were subjects for preparation of adult mammalian CNS myelin. Animals were bred within the animal facility (Tierversuchsanlage, TVA) of the Heinrich-Heine-Universität, Düsseldorf, under pathogen-free conditions. They were maintained in temperature- (21°C) and humidity- (50 +/- 5%) controlled animal housing, on a 12 h light/dark cycle. All interventions and animal handling procedures described in this thesis were conducted in compliance with the German Animal Protection Law.

3.1.2 Media and supplementary reagents

3.1.2.1 Media

name/ catalogue number	supplier
Dulbecco´s modified Eagle medium (DMEM) Cat. No. 31885-023	GIBCO (Invitrogen) Eggenstein, Germany
HAM´s F12 (nutrient mixture) Cat. No. 21765-029	GIBCO (Invitrogen) Eggenstein, Germany

3.1.2.2 Reagents

name/ catalogue number	supplier
trypsin/EDTA (1x), 0.05% Cat. No. 25300-054	GIBCO (Invitrogen) Eggenstein, Germany
recombinant human SDF-1α Cat. No. 350-NS	R&D Systems Wiesbaden-Nordenstadt, Germany
poly-D-lysine (PDL) hydrobromide Cat. No. P7889	Sigma-Aldrich Munich, Germany
collagenase type I Cat. No. C-0130	Sigma-Aldrich Munich, Germany
Dulbecco´s phosphate buffered saline (PBS) Cat. No. H15-002	PAA Cölbe, Germany
Fluoromount-G Cat. No. 0100-01	SouthernBiotech (Biozol Diagnostica) Eching, Germany
foetal bovine serum (FBS) Gold Cat. No. A15-151	PAA Cölbe, Germany
Forene (Isofluran) Cat. No. B506	Abbott Wiesbaden, Germany
Fura 2-AM Cat. No. F-0888	Sigma-Aldrich Munich, Germany

laminin (mouse) Cat. No. L-2020	Sigma-Aldrich Munich, Germany
nerve growth factor (NGF) -2.5S Cat. No. N 6009	Sigma-Aldrich Munich, Germany
penicillin-streptomycine (penicillin G sodium/ streptomycine-sulfate), 5000 units/ml Cat. No. 15070-063	GIBCO (Invitrogen) Eggenstein, Germany
Pluronic F-127 Cat. No. P-2443	Sigma-Aldrich Munich, Germany
5´dFUrd Cat. No. F-8791	Sigma-Aldrich Munich, Germany
Aprotinin Cat. No. A-1153	Sigma-Aldrich Munich, Germany
Pepstatin Cat. No. P-5318	Sigma-Aldrich Munich, Germany
Leupeptin Cat. No. L-2884	Sigma-Aldrich Munich, Germany

3.1.2.3 Antibodies

name/ catalogue number	antigen	host	dilution	fixation	supplier
anti-CD184 (fusin) Cat. No. 555972	CXCR4, ECL	mouse	1:100	4% PFA	BD Pharmingen Heidelberg, Germany
anti-CD184 (fusin) Cat. No. BP2211	CXCR4, ECL	rabbit	1:100	4% PFA	Acris Hiddenhausen, Germany
anti-human CXCR4 (fusin), clone 12G5 Cat. No. MAB170	CXCR4, ECL	mouse	1:100 (5 µg/ml)	4% PFA	R&D Systems Wiesbaden-Nordenstadt, Germany
anti-RDC1 Cat. No. IMG-71142	RDC1, ECL	rabbit	1:100	4% PFA	Imgenex (Biomol GmbH) Hamburg, Germany
antiserum cocktail to neurofilaments Cat. No. NA 1297	neurofilament (NF-L, NF-M, NF-H)	rabbit	1:2000	4% PFA	Affinity (Biotrend) Cologne, Germany
anti-phospho-CREB Cat. No. 9191	phospho-CREB (Ser-133)	rabbit	1:1000	4% PFA	Cell Signaling Technology (New England Biolabs) Frankfurt, Germany
anti-SDF-1 Cat. No. MAB350	SDF-1 (N-terminus)	mouse	1:100	4% PFA	R&D Systems Wiesbaden-Norderstadt, Germany
alexa Fluor® 488 Cat. No. A11001	mouse	goat	1:500	4% PFA	Molecular Probes (Invitrogen)

					Karlsruhe, Germany
alexa Fluor® 488 Cat. No. A11008	rabbit	goat	1:500	4% PFA	Molecular Probes (Invitrogen) Karlsruhe, Germany
alexa Fluor® 594 Cat. No. A11005	mouse	goat	1:500	4% PFA	Molecular Probes (Invitrogen) Karlsruhe, Germany s
alexa Fluor® 594 Cat. No. A11012	rabbit	goat	1:500	4% PFA	Molecular Probes (Invitrogen) Karlsruhe, Germany
biotinylated IgG Cat. No. BA-1000	rabbit	goat	1:500	4% PFA	Vector Laboratories (Alexis) Grunberg, Germany
isotype control $IgG_{2A,\kappa}$ Cat. No. MAB003	---	goat	1:100 (5 µg/ml)	4% PFA	R&D Systems Wiesbaden-Norderstadt, Germany
isotype control $IgG_{2A,\kappa}$ Cat. No. 550339	---	mouse	1:50 (5 µg/ml)	4% PFA	BD Pharmingen Heidelberg, Germany

3.1.3 Technical devices and software

Centrifugation steps described for the preparation and maintenance of cells (3.2.1) were performed using a Hettich Rotana/R centrifuge (Hettich; Tuttlingen, Germany).

Centrifugation steps described for the preparation of myelin (3.2.2) were performed using a Beckman L8-70 M Ultracentrifuge (Beckman Coulter; Krefeld, Germany).

Determination of total protein concentrations following the preparation of myelin (3.2.2) was performed using an ELISA Reader MRX (Dynex Technologies; Worthing UK).

Fluorescence microscopy and data analysis (3.2.3; 3.2.4; 3.2.5) was performed using the Nikon Eclipse TE200 and Lucia 4.1 software (Nikon GmbH; Düsseldorf, Germany).

Ca^{2+} imaging and data analysis (3.2.6) was performed using an Olympus IX50 microscope (Olympus; Hamburg, Germany) and Merlin 2.0 software (Chromaphor; Ascheberg, Germany).

3.2 Methods

3.2.1 Preparation and maintenance of cells

3.2.1.1 Dissociated DRGs

P6 Wistar rat pups were anaesthetized for up to 3 minutes with the inhalative Forene (Abbott). After decapitation and evisceration, the body was disinfected with 70% ethanol and fixed on a styrofoam board with the ventral side facing upwards. The muscle tissue surrounding the backbone was carefully removed, and nerve fibre bundles emanating from the spine were excavated by seizing the individual nerve fibre bundles at their junction with the spine with tweezers. Nerve fibre bundles were uprooted by working the tweezers in a combination of pulling and revolving movements. Alternatively, DRGs of the upper body were prepared by consecutively discerping corresponding vertebrae with tweezers. DRGs attached to nerve fibre bundles were dissected from the fibres and transferred into 0.6% glucose solution. For tissue dissociation, DRGs were transferred to DMEM, dissected, and incubated in DMEM, 0.3% collagenase type I, and 0.025% trypsin/EDTA, for 30 min at 37°C and 10% CO_2. Pre-digested tissue fragments were triturated with a constricted glass Pasteur pipette and centrifuged in DMEM/FBS at 1500 rpm for 10 min. After centrifugation, the supernatant was removed, and the pellet was resuspended in 1 ml of DRG medium. The cell density was determined using a Thoma chamber**.** Dissociated DRGs were cultivated at 37°C and 10% CO_2 as described for the corresponding assays (3.2.3; 3.2.4; 3.2.5)

Glucose solution

	%	g/50 ml
in PBS		
glucose	6.0	3.0

DMEM/FBS

	ml/500 ml
DMEM (low glucose, 1000 mg/ ml)	500,0
FBS	50,0
L-glutamine (200 mM)	5,0
penicillin-streptomycin (5000 units/ ml)	5,0

DRG medium

	µl/ml
in DMEM/ FBS	
NGF (10 µg/ ml)	1,0
5´dFUrd (100 nM)	10,0

3.2.1.2 Astrocytes (generation of ACM)

P0-1 Wistar rat pups were anaesthetized for up to 3 min with the inhalative Forene. After decapitation, the head was placed in an upright position on a sterile gauze compress. The skin was removed and the head incised along the dorsal midline of the skull. The skullcap was removed and the brain was taken out. After removal of the dura mater, the neocortex was dissected for each brain hemisphere sparing the hippocampi. Brain slices were freed from the meninges and the tissue was crudely fragmented. Tissue fragments were resuspended in DMEM and subsequently centrifuged at 1500 rpm for 1 min. Cell separation was achieved by triturating the cell suspension using a constricted glass Pasteur pipette. Cells were resuspended in an additional volume of 9 ml DMEM and filtrated through sterile nylon gauze (pore size: 60 µm). Finally, the cell suspension was topped up with DMEM/FBS and was centrifuged at 1500 rpm for 5 min. The supernatant was discarded and the pellet was resuspended in 5 ml DMEM/FBS. Astrocytes were cultivated in T75 cell culture flasks in presence of DMEM/FBS at 37°C and 10% $C0_2$. One flask was prepared for each brain hemisphere. DMEM/FBS was freshly supplemented every 2-4 days until the cultures reached confluency. To remove non-astroglial contaminations, confluent astrocyte cultures were incubated on a shaker at 37°C and 200 rpm over night. Then, astrocyte cultures were rinsed three times with PBS and supplemented with N2. To generate serum-free astrocyte-conditioned medium (ACM), confluent and purified astrocyte cultures were rinsed with PBS and cultivated in presence of N2 medium (20-30 ml/T75 cell culture flask) for at least 24 h. The conditioned medium then was harvested and filtrated using a sterile filter. Astrocyte cultures were used up to four times for the generation of ACM.

DMEM/FBS medium

	ml/ 500 ml
DMEM (low glucose, 1000 mg/ ml)	500,0
FBS	50,0
L-glutamine (200 mM)	5,0

N2

	ml/ 500 ml
DMEM (low glucose, 1000 mg/ ml)	375
HAM´s F12	125
insuline (5 µg/ml)*	1
transferrine (100 µg/ml)	1
hormone mix	0.6
L-glutamine (200 mM)	5

* freshly prepared

Hormone mix

	µM
progesterone (in EtOH)*	0.02
putrescine (in EtOH)*	100
sodium selenite*	0.03

Each solution has a final volume of 2 ml. Individual solutions are stored as aliquots at -20°C.

3.2.1.3 Cortical neurons

A pregnant Wistar rat was anaesthetized with the inhalative Forene and killed by dislocation of the cervical vertebrae. The peritoneum was opened and the uterus containing the embryos was taken out. Embryos were decapitated one at a time, and each head was placed in an upright position onto a sterile petri dish. The skin was removed and the head incised along the dorsal midline of the skull. The skullcap was removed and the brain was taken out. After removal of the dura mater, the brain hemispheres were folded apart and the neocortex was dissected for each brain hemisphere sparing the hippocampi. Brain slices were freed from the meninges and the tissue was crudely fragmented. Tissue fragments were resuspended in DMEM and subsequently centrifuged at 2000 rpm for 30 sec. After centrifugation, the supernatant was removed and the tissue was incubated for 8 min in 10 ml trypsin/EDTA at 37°C and 10% CO_2. The reaction was stopped by adding 10 ml DMEM/FBS, and the tissue suspension was again centrifuged at 1500 rpm for 1 min. The supernatant was discarded and the pellet was resuspended in 1 ml DMEM. Cell separation was achieved by triturating the cell suspension using a constricted glass Pasteur pipette. Cells were resuspended in an additional volume of 9 ml DMEM and filtrated through sterile nylon gauze (pore size: 30 µm). Finally, the cell suspension was topped up with DMEM/FBS and was centrifuged at 1500 rpm for 5 min. The supernatant was discarded and the pellet was resuspended in 1 ml astrocyte-conditioned medium (ACM). Cell density was determined using a Thoma chamber, and the suspension was diluted in ACM to a final density of $2x10^6$ cells/ml. Cortical neurons were seeded at a density of $1x10^5$ cells/cm^2 and cultivated at 37°C and 10% CO_2. For generation of ACM, see 3.2.1.2.

3.2.1.4 Leptomeningeal fibroblasts

Leptomeningeal fibroblasts were prepared from meninges of P0-1 Wistar rat pups. Briefly, P0-1 Wistar rat pups were sacrificed as described before (3.2.1.2) and the brain was harvested. Meninges were prepared from both brain hemispheres, crudely fragmented and centrifuged in DMEM at 2000 rpm for 30 sec. The tissue was then incubated in 0.025% trypsin/EDTA for 10 min at 37°C and 10% CO_2. The reaction was stopped by adding 10 ml DMEM/FBS and the tissue was triturated using a constricted glass Pasteur pipette. Subsequentially, the cell suspension was centrifuged at 1500 rpm for 5 min. The supernatant was discarded and the pellet resuspended in 5 ml DMEM/FBS. Leptomeningeal fibroblasts were cultivated in T75 cell culture flasks in presence of DMEM/FBS at 37°C and 10% $C0_2$. One flask was prepared for each brain hemisphere. DMEM/FBS was freshly supplemented every 2-4 days. Upon reaching confluency, leptomeningeal fibroblasts were propagated by passage in a ratio of 1:5.

3.2.1.5 HeLa cells

HeLa cells were cultivated in DMEM/FBS up to 70% confluency in T75 cell culture flasks and propagated by continuous passage in a ratio of 1:10.

3.2.2 Preparation of adult rat CNS myelin

A pregnant Wistar rat was anaesthetized with the inhalative Forene, killed by dislocation of the upper cervical vertebrae, and was decapitated. The whole brain was taken out and shock-frozen at -20°C. The frozen brain was thawed on ice directly before preparation of myelin. Medulla and brain stem were harvested, transferred into 2 ml of buffer A, and tissue fragments were minced with a Polytron (Kinematica; Luzern, Switzerland). After adding 2 ml of buffer A, the tissue suspension was thoroughly homogenized in a 5 ml-douncer (B. Braun Biotech International; Melsungen, Germany). Subsequently, 4 ml of buffer B were added and carefully mixed with a pipette. To build a gradient, 2 ml of buffer D were filled into a 12 ml-Beckman tube (Beckman Coulter; Krefeld, Germany. The tissue suspension was carefully placed onto buffer D while avoiding bubble formation Finally, 1 ml of buffer C and 1 ml of buffer A were subsequently put on top of the tissue suspension. Buckets of a precooled SW 41 Ti ultracentrifugation rotor were put in balance and fitted into the rotor. The tissue suspension was centrifuged for ≥ 14 h at 40 000 rpm and 4°C. The Beckman tube containing the brain homogenate was taken out, and the myelin protein-containing phase forming a lutescent layer was isolated using a glass Pasteur pipette. Extracted myelin protein was transferred to a 5 ml-douncer, topped up with ice cold *Aqua bidest.* and homogenized in a 5 ml-douncer. The homogenate was transferred to a 12 ml-Beckman tube and centrifuged for ≥ 14 h at 40 000 rpm at 4°C. The Beckman tube containing the myelin protein-pellet was taken out, and the supernatant was discarded. The pellet was resuspended in an appropriate volume of 10 mM HEPES buffer, and the amount of total protein was determined using a Lowry-based colorimetric assay (Bio-Rad; Munich, Germany). Myelin was diluted to a final protein concentration of 10 µg/ml in 10 mM HEPES buffer containing inhibitors to protease activity. Aliquots were stored at -20°C.

Buffers

	mM	g/100 ml

Buffer A

sucrose	250,0	8,56
HEPES pH 7.15	25,0	0,65
KCl	500,0	3,72
$MgCl_2 * 6 H_2O$	5,0	0,10
DTT	3,0	0,05

Buffer B

sucrose	2550,0	87,28
HEPES pH 7.15	25,0	0,65
KCl	500,0	3,72
$MgCl_2 * 6 H_2O$	5,0	0,10
DTT	3,0	0,05

Buffer C

sucrose	850,0	29,10
HEPES pH 7.15	25,0	0,65
KCl	500,0	3,72
$MgCl_2 * 6 H_2O$	5,0	0,10
DTT	3,0	0,05

	mM	g/100 ml

Buffer D

sucrose	1900,0	65,00
HEPES pH 7,15	25,0	0,65
KCl	500,0	3,72
$MgCl_2$ * 6 H_2O	5,0	0,10
DTT	3,0	0,05

HEPES buffer

	mM
HEPES pH 7.15	10

Protease inhibitors

	mg/ml
Aprotinin[1,3]	1
Pepstatin[2,3]	1
Leupeptin[2,3]	1

[1] in *Aqua dest.*

[2] in ethanol

[3] diluted to a final concentration of 1 µg/ml in HEPES buffer

3.2.3 Neurite outgrowth assay

The neurite outgrowth assay was performed on 8-well Permanox labtek chamber slides (Nalge Nunc; Erkerode, Germany) coated with PDL (1 h/room temperature) and subsequently laminin (37°C/1 h) at a concentration of 1 mg/ml or 1 µg/ml, respectively. Myelin was left to dry under a laminar flow (room temperature/over night) at a final concentration of 2 µg of total protein/well. As a control, slides coated with PDL and laminin alone were stored at 4°C over night. Prior to plating of cells, the slides were washed once with PBS. Dissociated P6 DRGs were plated at a final density of $5x10^4$ cells/well and incubated at 37°C and 10% CO_2 for 24 h, if not noted otherwise. For pharmacological treatment, cells were cultivated with or without application of SDF-1α at a final concentration of 50, 200, or 500 ng/ml, respectively. SDF-1α was applied either directly to the cells or in a preincubation step at 37°C and 10% CO_2 for 1 h prior to plating. For preincubation experiments, dissociated DRGs were incubated in DRG medium and SDF-1α for at 37°C and 10% CO_2 for 1 h prior to plating on myelin. After pretreatment, SDF-1α either stayed in the medium during the whole incubation period, or cells were substituted with SDF-1α free medium after preincubation. Blocking experiments were performed with the bicyclam antagonist AMD3100 at a final concentration of 1 µg/ml or 5 µg/ml, respectively. For blocking experiments, cells were pretreated with AMD3100 for 15-20 min prior to application of SDF-1α. Pretreated cells were incubated at 37°C and 10% CO_2 for additional 23 h. To abort the experiment, samples were fixed in 4% paraformaldehyde, PFA, at room temperature for 10 min and subsequently stained for neurofilaments. Optionally, cells were counterstained for the Schwann cell marker protein S-100. Samples were viewed with a Nikon Eclipse TE 200 microscope. Picture acquisition and data analysis were performed using the Lucia software (Nikon GmbH; Düsseldorf, Germany). For quantitative analysis, nine pictures were taken randomly per well at 4x magnification, and the number of neurons showing neurite outgrowth as well as the total number of neurons in the microscopic fields were determined. Outgrowing neurons were defined as neurofilament-positive cells showing three or more neurites each with a length of at least the cell body diameter (Ng and Lozano, 1999; Qiu et al., 2005).

3.2.4 Assay for CREB phosphorylation and translocation into nuclei

The assay for phosphorylated CREB was performed on glass coverslips (Ø 13 mm) coated with PDL (4°C/over night) and subsequently laminin (4°C/over night) at a concentration of 1 mg/ml or 13 µg/ml, respectively. Dissociated DRGs were plated at a density of $1x10^5$ cells/ well and incubated in DRG medium at 37°C and 10% CO_2 for 24 h. Cells were then stimulated by application of SDF-1α at a final concentration of 200 ng/ml, or forskolin at a final concentration of 6 µM, respectively, at 37°C and 10% CO_2 for 1–120 min. Samples were fixed with 4% PFA at room temperature for 10 min, permeabilized in PBS containing 0.2% Triton-X-100 and stained for pCREB with the rabbit polyclonal antibody 9191 directed against the phosphorylated form of Ser-133 of pCREB according to the manufacturer´s protocol. Finally, samples were incubated in DAPI at room temperature for 30 sec to visualize nuclei and mounted in Fluoromount-G. For staining of neurofilaments, Triton-X-100 was applied at a final concentration of 0.1% in PBS. Picture acquisition and data analysis were performed as described before (3.2.3). For analysis of pCREB immunoreactivity, 30 pictures per coverslip were taken randomly at 20x magnification, and the number of pCREB-positive neurons as well as the total number of neurons was determined. Thereby, pCREB-positive neurons were defined as cells displaying an intensely labelled nucleus.

3.2.5 Immunocytochemistry

For immunocytochemical analysis of receptor expression and distribution, and chemokine expression and distribution, respectively, cells were seeded on glass coverslips (Ø 13 mm) coated with PDL (4°C/over night) and subsequently laminin (4°C/over night) according to cell-specific requirements. Briefly, for cultivation of primary neurons glass coverslips were coated with PDL and laminin at a concentration of 1 mg/ml or 13 µg/ml, respectively. For cultivation of leptomeningeal fibroblasts and HeLa cells, glass coverslips were coated with PDL and laminin at a concentration of 1 mg/ml or 4 µg/ml, respectively. Dissociated DRGs were plated at a cell density of 1.25-2.5x10^4 cells/well. Cortical neurons were plated at a cell density of 1x10^5 cells/cm^2. Leptomeningeal fibroblasts and HeLa cells were plated at a cell density of 2.5-5x10^4 cells/well. After 24-144 h, cultured cells were fixed in 4% PFA at room temperature for 10 min and preincubated in normal goat serum, NGS, at a final concentration of 3% in PBS. Samples were stained with primary antibodies at 4°C over night. For detection of primary antibodies, samples were stained with secondary antibodies at room temperature for 2 h. For dilution of primary and secondary antibodies, please refer to chapter 2.1.2.3. Finally, samples were incubated in DAPI at room temperature for 30 sec to visualize nuclei and were mounted in Fluoromount-G. For staining of neurofilaments, Triton-X-100 was applied at a final concentration of 0.1% in PBS. Picture acquisition and data analysis were performed as described before (3.2.3). For immunocytochemical protocols as applied in the neurite outgrowth assay (3.2.3) or the assay for CREB phosphorylation and translocation into nuclei (3.2.4), please refer to the corresponding chapters.

3.2.6 Ca^{2+}-imaging

3.2.6.1 Experimental setup

For Ca^{2+}-imaging experiments (Takahashi et al., 1999), Hela cells were cultivated on UV-permeant glass coverslips (Ø 15 mm) which were coated according to cell-specific requirements. Briefly, for cultivation of HeLa cells glass coverslips were coated with PDL (4°C/over night) and subsequently laminin (4°C/over night) at a concentration of 1 mg/ml or 4 µg/ml, respectively. HeLa cells were plated at a density of 2.5-5x10^4 cells/well and grown up to 70% confluency before conducting Ca^{2+} measurements. Prior to recording, the glass coverslips were transferred into a petri dish containing 2 ml bath solution supplemented with 10 µl Fura 2-AM dye solution and 3 µl Pluronic F-127 detergent solution. Cells were incubated at 37°C and 10% CO_2 for 30–45 min and were then transferred into dye-free bath solution for 10–15 min. For recording, a single glass coverslip was tightly fitted into an experiment-adapted petri dish with a volumetric capacity of 1 ml and topped with dye-free bath solution. To assess for non-specific elevation of intracellular Ca^{2+}, cells were first recorded following application of chemokine-free bath solution prior to starting the key experiments. To assess for elevation of intracellular Ca^{2+} mediated by either SDF-1α or SDF-1γ, respectively, 1 ml of bath solution supplemented with either isoform at a final concentration of 50–300 nM was applied. Blocking experiments were performed with either an anti-CXCR4 antibody (12G5 clone; R&D Systems; Wiesbaden-Nordenstadt, Germany) or *Bordetella pertussis* toxin, PTX. Cells were preincubated in supplemented bath solution in presence of either the antibody (500 ng/µl) or PTX (100 ng/ml) for 15-30 min prior to starting the experiments. As a control, an isotype control antibody to IgG_{2A} (500 ng/µl) was applied. To assess for the general ability of the recorded cells to perform elevation of intracellular Ca^{2+}, cells were finally treated with 1 ml of bath solution supplemented with ATP. For each experiment, cells were recorded for a time span of 120 sec with pictures taken in alternation each second at an excitation wavelength of 340 nm or 380 nm, respectively. For experimental analysis, regions of interest, ROIs, were marked according to cell borders and the background was substracted prior to calculating the

alteration of Ca^{2+}-dependent fluorescence. Alterations of ROI-specific Ca^{2+}-levels/fluorescence intensities were given as ratio units (see 3.2.6.2). Ca^{2+}-dependent alterations in fluorescence intensity were plotted in a graph with ratio units presented on the Y-axis and time presented on the X-axis.

Bath solution

	mM	g/500 ml
NaCl	150,0	4,38
KCl	2,0	0,07
$MgCl_2$ * 6 H_2O	1,0	0,10
$CaCl_2$ * 2 H_2O	2,8	0,21
sucrose (anhydrous)	20,0	9,45
HEPES	10,0	1,19

Glutamate solution

	mM	g/50 ml
glutamate	2,0	0,0185

ATP solution

	mM	g/50 ml
ATP	2.0	0,0551

Loading dye

	mM	mg/ml
Fura 2-AM*	2,0	1,0

* in DMSO (anhydrous)

3.2.6.2 Qualitative calculation of Ca^{2+} changes

Alterations of intracellular Ca^{2+} were calculated from fluorescence intensities at the two different excitation wavelengths (F_{nm}) over time. The detected fluorescence intensities depended on three parameters: (1) Concentration of fluorescent dye in the cell (c), (2) thickness of the cell or sample (d), and (3) optical properties of the measurement units (K). Furthermore, fluorescence intensities were considered a function of intracellular Ca^{2+}-concentrations.

$$F_{nm} = c \times d \times K \times f([Ca^{2+}]_i)$$

Relative alterations of intracellular Ca^{2+} could be calculated without further knowledge of c, d, and K, as an elevation of intracellular Ca^{2+} levels resulted in an increase of F_{340} and a decrease of F_{380}, respectively, for Fura 2-AM.

$$\frac{F_{340} = c \times d \times K \times f([Ca^{2+}]_i)}{F_{380} = c \times d \times K \times f([Ca^{2+}]_i)}$$

As parameters c, d, and K underwent only minor changes in the course of a single measurement, they could be eliminated to this effect that only the quotient of fluorescence intensities remained. Information on fluorescence intensities alone thus allowed the calculation of respective ratio values, R-values, which were given as ratio units, R-units, for certain time points of measurement.

$$R = F_{340}/ F_{380} = f''([Ca^{2+}]_i)$$

The basis for calculation of a single R-value was the information of fluorescence intensities of both wavelengths at a certain time point in measurement, contained in a single frame. In this study, a single frame consisted of two seconds in which one picture was taken for each wavelength. One experiment thus entailed 60 frames or 120 seconds, respectively. Experiments were performed and presented in pseudocolour to allow for an exact representation of intracellular dye concentration. Prior to starting the experiment, a reference picture was taken for each sample in greyscale. According to this picture, cell borders were defined and ROIs were chosen during experimental analysis. To calculate the percentage of responsive cells for individual experiments, raw data were analyzed using the customized EXCEL programm Ca^{2+}LCULATE (Fabian Kruse, Düsseldorf, Germany). Briefly, cells were considered to be responsive to an external stimulus if they displayed an elevation of intracellular Ca^{2+} that was at least 20% above the basal level. Cell-specific Ca^{2+} increase was taken into account if peak length duration was between 2-55 frames, as a permanent elevation is indicative of an impaired regulation of cellular Ca^{2+} homeostasis. For cells which displayed an oscillatory elevation of intracellular Ca^{2+} levels, only the first peak was included in calculation of the overall number of responsive cells.

4 Results

4.1 SDF-1α effects overcoming of myelin-induced neurite outgrowth inhibition

Myelin was demonstrated to represent one of the major obstacles to regenerative growth of postnatal CNS neurons. To test for growth promoting properties of SDF-1α, this chemokine was applied in an *in vitro* model of regeneration of cultured P6 DRG neurons on a crude fraction of CNS myelin.

4.1.1 Neurite outgrowth of P6 DRG neurons is impaired on CNS myelin

During development, DRG neurons undergo a conversion in their sensitivity towards adult CNS myelin at P3/P4. Neurite outgrowth of cultured P6 DRG neurons was significantly impaired on surfaces coated with laminin and myelin, compared to control cells on laminin alone (Fig. 4.1,A; Fig. 4.2,A,B). In presence of myelin, the mean number of neurons displaying three or more neurites with a length of at least the cell body diameter was significantly reduced to 21.37% (± 3.38% SEM) of laminin-only controls (Fig. 4.1,A; Fig. 4.2,A,B, arrowheads). Outgrowing neurons on laminin and myelin displayed an altered patterning characterized by reduction of both neurite length and number of branching events as well as marked fasciculation, compared to laminin-only controls (Fig. 4.1,C,D). Reduced numbers of outgrowing neurons on myelin were not due to an impaired adherence on myelin, as a comparison of total cell numbers revealed that latter were even slightly elevated on myelin-coated surfaces, compared to laminin controls (data not shown).

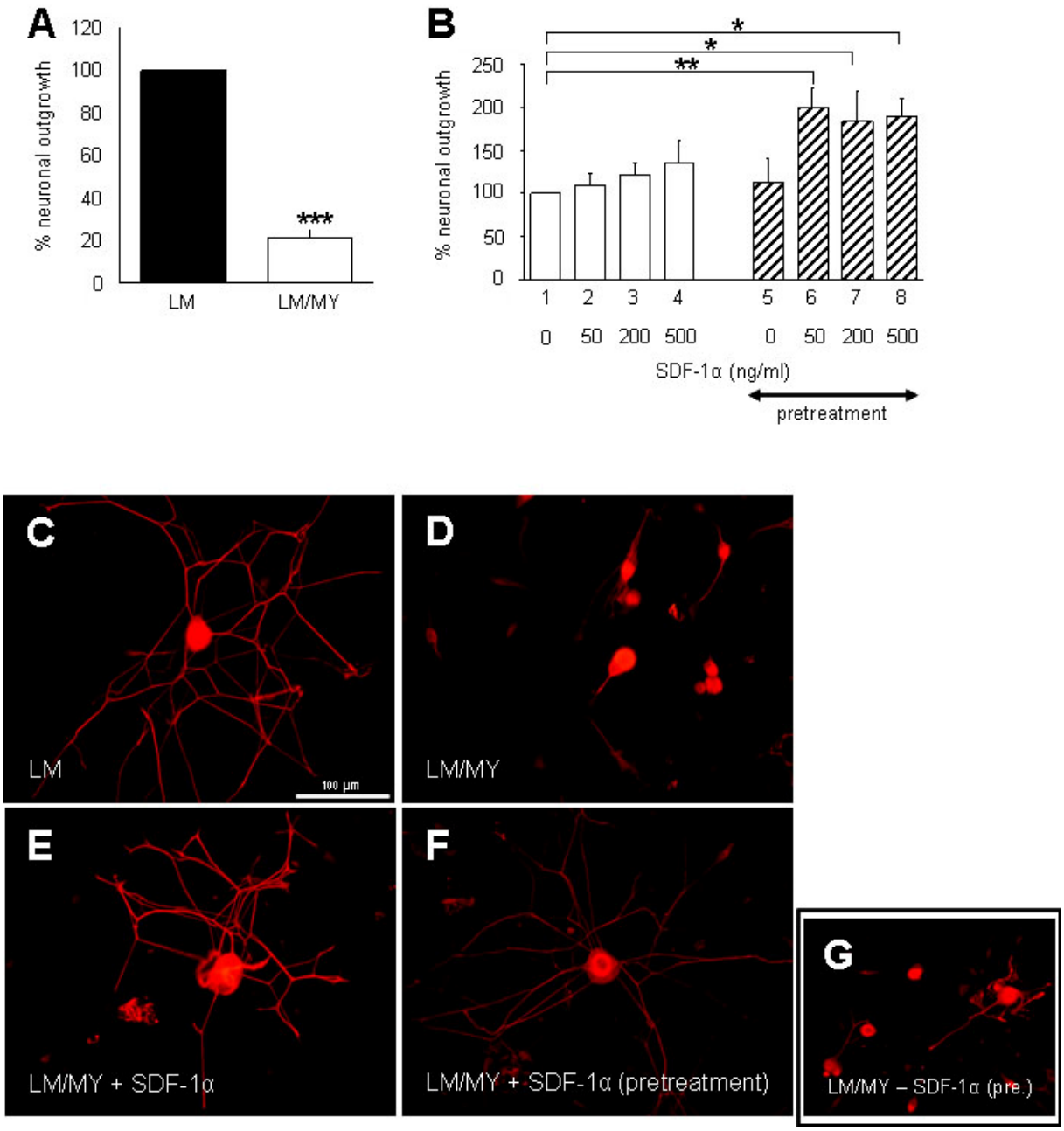

Fig. 4.1. SDF-1α mediates overcoming of myelin-induced neurite outgrowth inhibition (I). Outgrowth of P6 DRG neurons is restricted on myelin substrate. Compared to laminin-controls, the number of outgrowing neurons is significantly reduced on myelin (A), and neurite patterning is severely impaired (C,D). Application of SDF-1α (B, bars 2-4) markedly increases neurite outgrowth and improves neurite patterning on myelin (B,E). Pretreatment with SDF-1α (B, bars 6-8) prior to cell plating on myelin increases outgrowth promoting effects and significantly enhances the number of outgrowing neurons, while neurite patterning displays further improvement (B,F). Neurons preincubated in medium (G) alone show weak outgrowth promotion on myelin. Results (mean ± SEM) are from eight (A,B) independent experiments and are expressed as percentage of neurons displaying three or more neurites with a length of at least the cell body diameter. Values are normalized for

numbers of untreated cells growing out on laminin (A) or myelin (B), arbitrarily set at 100%. *p<0.05, **p<0.01, ***p<0.001 (student´s t-test), compared to control cells. Pictures chosen for presentation (D-G) are representative of eight independent experiments (n = 8).

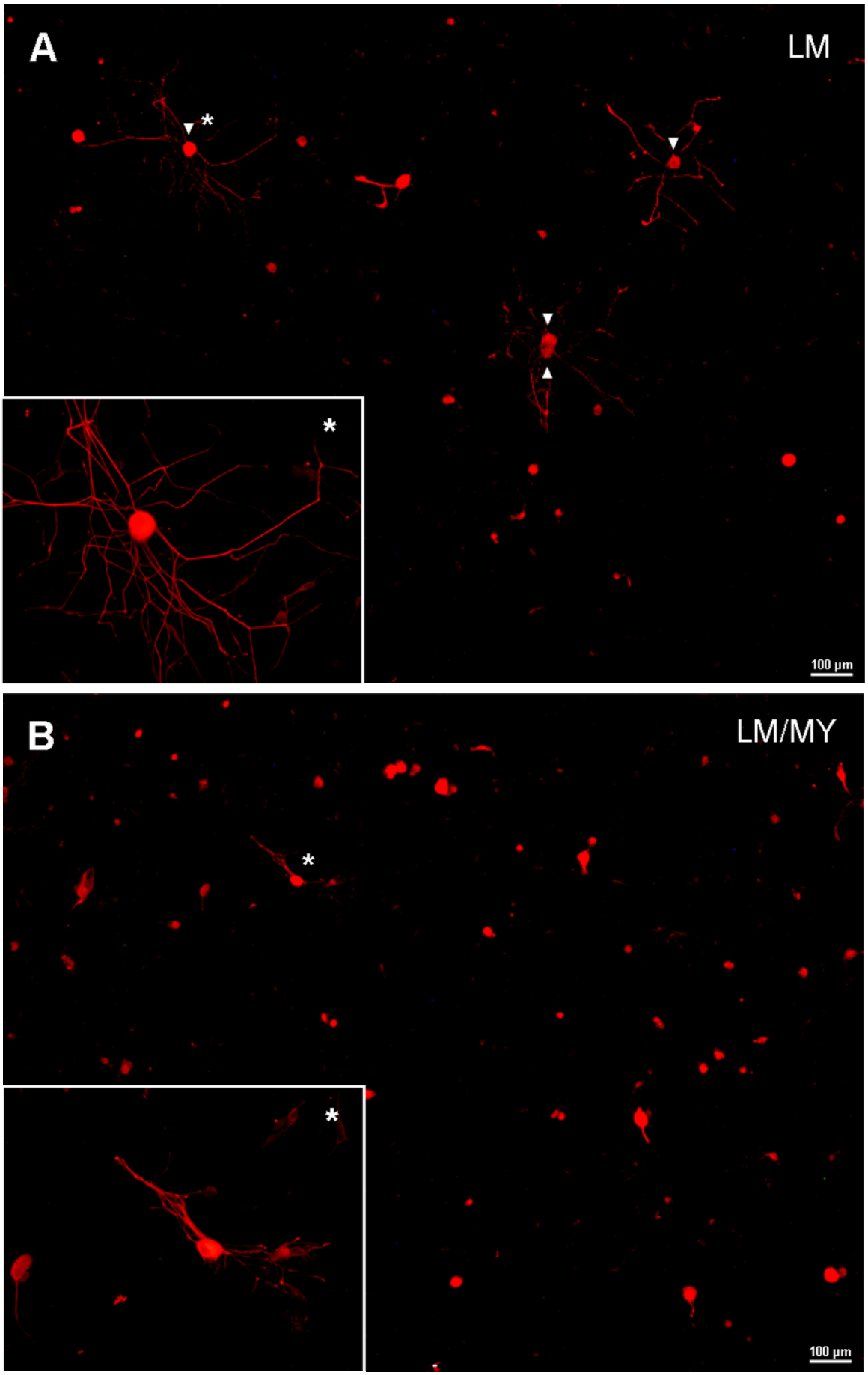

Fig. 4.2. (I, see also next page)

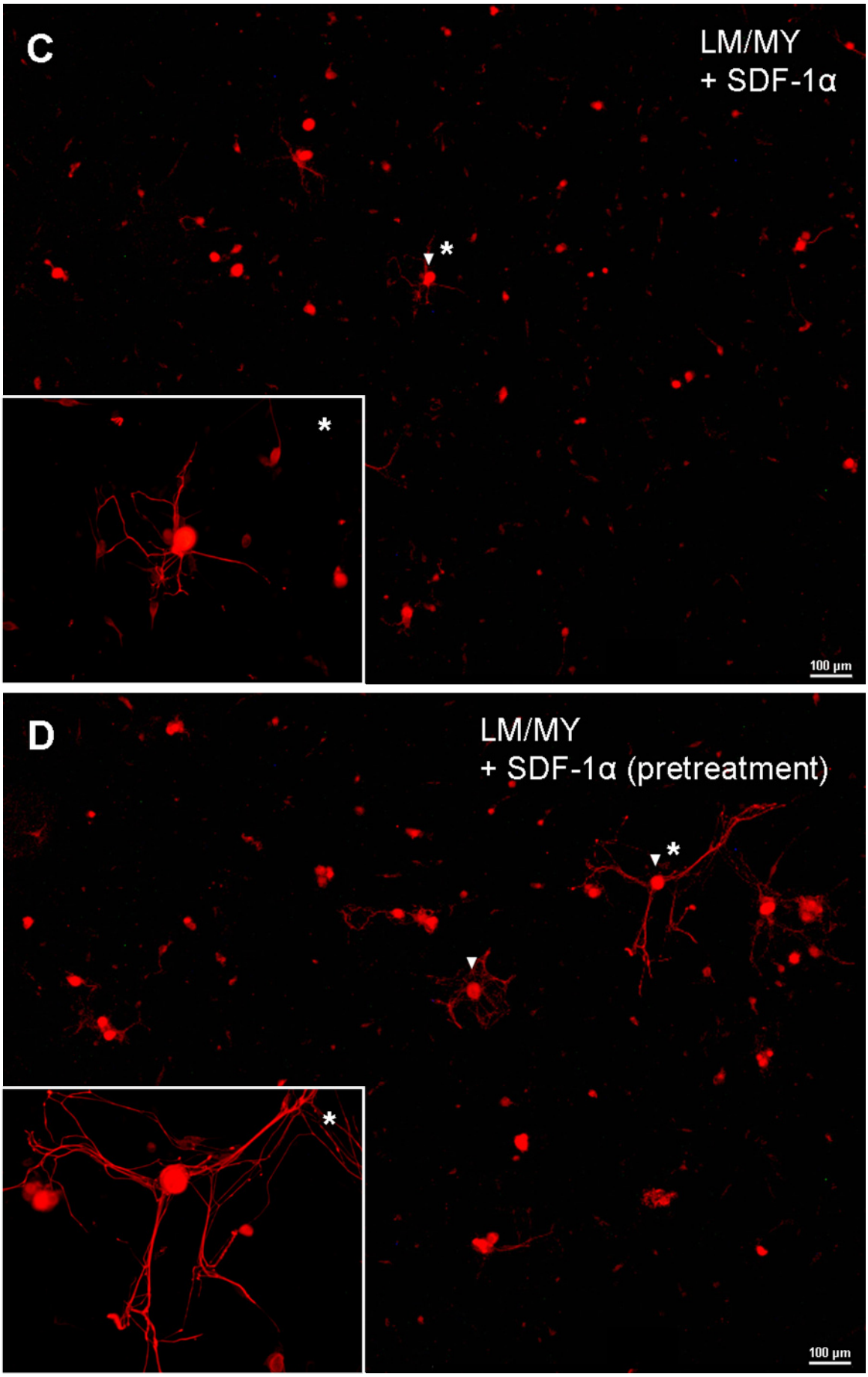

Fig. 4.2. (II, see also next page)

(see also previous page)

Fig. 4.2. SDF-1α mediates overcoming of myelin-induced neurite outgrowth inhibition (II). Compared to laminin-only controls (A), the number of outgrowing neurons is markedly reduced on myelin (B). Application of SDF-1α without (C) or with (D) pretreatment leads to an increase in the number of outgrowing neurons of myelin. Outgrowing neurons are indicated by arrowheads, selected neurons depicted in both low and high resolution are indicated by asterisks. Pictures chosen for presentation (A-D) are representative of eight independent experiments (n = 8).

4.1.2 SDF-1α mediates overcoming of myelin-induced outgrowth inhibition

Myelin-induced neurite outgrowth inhibition was abrogated by application of SDF-1α in a dose-dependent manner at a concentration of 50–500 nM (Fig. 4.1,B, bars 2-4). Application of SDF-1α led to an increase in both number and length of neuronal processes growing out in presence of myelin as well as to improved neurite patterning (Fig. 4.1,E; Fig. 4.2,C). After 24 h *in vitro*, the number of DRG neurons with three or more neurites was markedly, albeit not significantly, increased in SDF-1α-treated myelin cultures, compared to control cells cultivated without SDF-1α (Fig. 4.1,B, bars 1-4; Fig. 4.2,B,C, arrowheads). SDF-1α-mediated effects were strongest at a concentration of 500 nM with an increase in the mean number of outgrowing neurons of 35.27% (± 26.29% SEM), compared to medium alone (Fig. 4.1,B, compare bar 1 to 4).

4.1.3 Preincubation with SDF-1α increases outgrowth promoting effects

Neurite outgrowth promoting effects of SDF-1α were increased by preincubation of cells with this chemokine for 1 h prior to plating the neurons on surfaces coated with laminin and myelin (Fig. 4.1,B, bars 6-8; Fig. 4.2,D). P6 DRG neurons which were pretreated with SDF-1α displayed a significant increase in the mean number of outgrowing neurons of 99.74% (± 22.30% SEM) at a concentration of 50 nM, compared to cells treated with medium alone (Fig. 4.1,B, compare bar 1 to 6; Fig. 4.2,B,D, arrowheads). SDF-1α-pretreated DRG neurons showed a marked

improvement of both number and length of neuronal processes growing out in presence of myelin, compared to cells growing without SDF-1α or cells growing in the presence of SDF-1α that did not receive pretreatment (Fig. 4.1,D-F; Fig. 4.2,B-D). Neurite patterning of SDF-1α-pretreated DRG neurons on myelin was similar to outgrowth of laminin-only controls (Fig. 4.1,C,F; Fig. 4.2,A,D). Preincubation alone had a weak outgrowth promoting effect, as DRG neurons preincubated with medium displayed slightly improved outgrowth on myelin (Fig. 4.1,G). However, pretreatment of myelin-cultivated neurons with SDF-1α was necessary, but not sufficient, to significantly elevate neurite outgrowth, as withdrawal of SDF-1α following pretreatment mainly abrogated neurite outgrowth promotion (data not shown).

4.1.4 SDF-1α-mediated growth promotion on myelin is CXCR4-dependent

To assess whether the cognate receptor to SDF-1, CXCR4, is involved in SDF-1α-mediated growth promotion, anti-CXCR4 antagonist AMD3100 was applied to P6 DRG neurons prior to pretreatment with SDF-1α and plating on myelin (Fig. 4.3, bars 5-12). At low concentrations of AMD3100 (1 µg/ml), SDF-1α-mediated growth promotion was significant at 50 ng/ml of applied chemokine with an increase of 88.15% (± 25.55% SEM) in the mean number of outgrowing neurons, compared to significant outgrowth promotion at concentrations of 50-500 ng/ml in controls preincubated with SDF-1α alone (Fig. 4.3, compare bars 1-4 to bar 6). Conversely, cells on myelin which were preincubated with high doses of AMD3100 (5 µg/ml) displayed no significant neurite outgrowth promotion following pretreatment with SDF-1α, compared to SDF-1α-only controls (Fig. 4.3, compare bars 2-4 to 10-12). However, overall outgrowth promotion following AMD3100-treatment was observed in cultures with or without application of SDF-1α. This growth promotion on myelin was marked, albeit not significant, at a concentration of 1-5 µg/ml, where neurons treated with this antagonist alone displayed an increased mean number of outgrowing neurons of 54.00% (± 28.04% SEM) or 86.27% (± 19.42% SEM), respectively, compared to neurons without AMD3100 and SDF-1α (Fig. 4.3, compare bar 1 to 5,9).

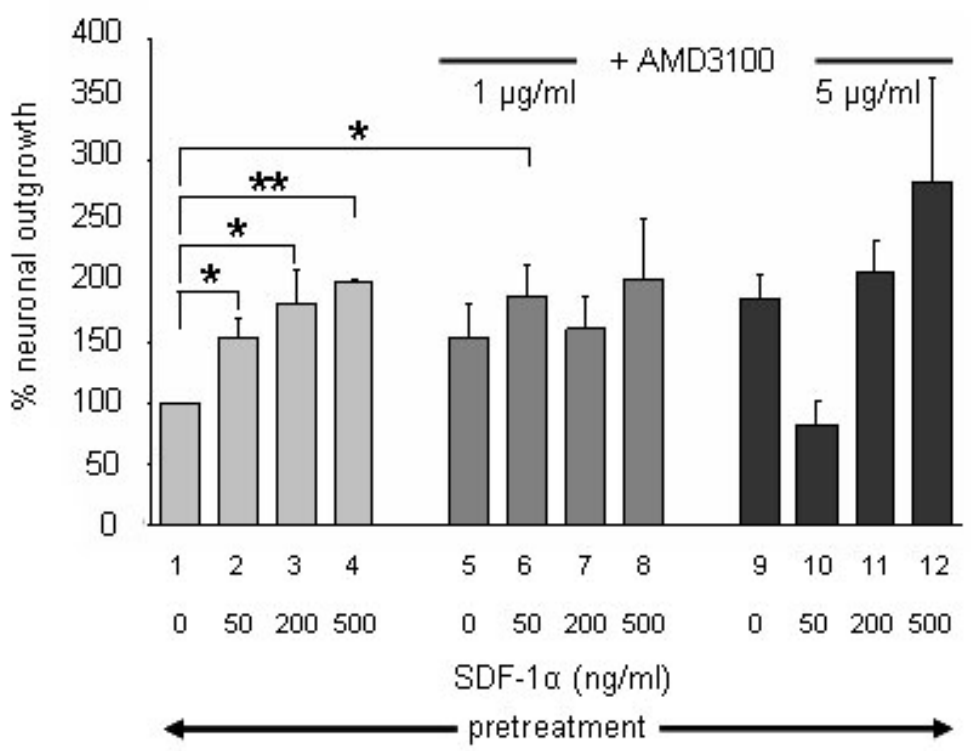

Fig. 4.3. SDF-1α-induced neurite outgrowth promotion is presumably CXCR4-dependent. Pretreatment with low doses of AMD3100 without (bar 5) or with (bars 6-8) subsequent application of SDF-1α does not abrogate SDF-1α-mediated neurite outgrowth promotion, but effects an increase in the number of outgrowing neurons. Application of high doses of AMD3100 either alone (bar 9) or together with SDF-1α (bars 10-12) results in further increased neurite outgrowth promotion on myelin. Results (mean ± SEM) are from three independent experiments (n = 3) and are expressed as percentage of neurons displaying three or more neurites with a length of at least the cell body diameter. Values are normalized for numbers of untreated cells growing out on myelin, arbitrarily set at 100%. *p<0.05, **p<0.01 (student´s t-test), compared to control cells.

4.2 SDF-1α mediates alterations of intrinsic neuronal settings through cAMP/pCREB

To elucidate the signalling events which are involved in SDF-1α-mediated neurite outgrowth promotion, DRG neurons were assessed for cAMP-dependent CREB phosphorylation and translocation into nuclei. P6 DRG neurons were treated with a short pulse of SDF-1α at a concentration of 200 ng/ml prior to staining for phosphorylated CREB and for neurofilaments.

4.2.1 Application of SDF-1α leads to CREB phosphorylation and translocation into neuronal nuclei

SDF-1α-treated cells displayed a significant upregulation in the mean number of pCREB-positive nuclei 20 min after application of this chemokine (Fig. 4.4,A, arrow). DRG neurons in which CREB was both phosphorylated and translocated in response to SDF-1α-treatment displayed intensely labelled nuclei (Fig. 4.5,C,D, arrows). In non-responsive or untreated cells, cytoplasm was diffusely stained, while nuclei remained unlabelled (Fig. 4.5,A,B, dashed arrows). Thereby, the mean number of pCREB-positive nuclei showed a maximum increase of 90.0% (± 32.4% SEM) following application of SDF-1α, compared to untreated cells. The time which was required for maximum elevation of pCREB differed in a preparation-dependent manner (Fig. 4.4,C,D, arrows). Generally, single experiments displayed considerable variations with respect to SDF-1α-induced CREB phosphorylation and translocation into neuronal nuclei. An initial downregulation in the number of pCREB-positive nuclei following application of SDF-1α was repeatedly observed (Fig. 4.4,C,D, dashed arrows). As experiment-specific variations hampered an evaluation of the maximum increase in SDF-1α-induced pCREB-immunoreactivity, the time-independent mean from the maximum values of all experiments was calculated. It revealed a significant mean maximum increase of 134.3% (± 26.3% SEM) in the number of pCREB-positive nuclei, compared to control conditions, 1-60 min after application of SDF-1α (Fig. 4.4,B). Furthermore, the mean number of pCREB-positive nuclei was significantly increased (1300.4 ± 330.7% SEM) by forskolin at a

concentration of 6 µM 5 min after application (Fig. 4.4,A, arrowhead; Fig. 4.5,E,F, arrows).

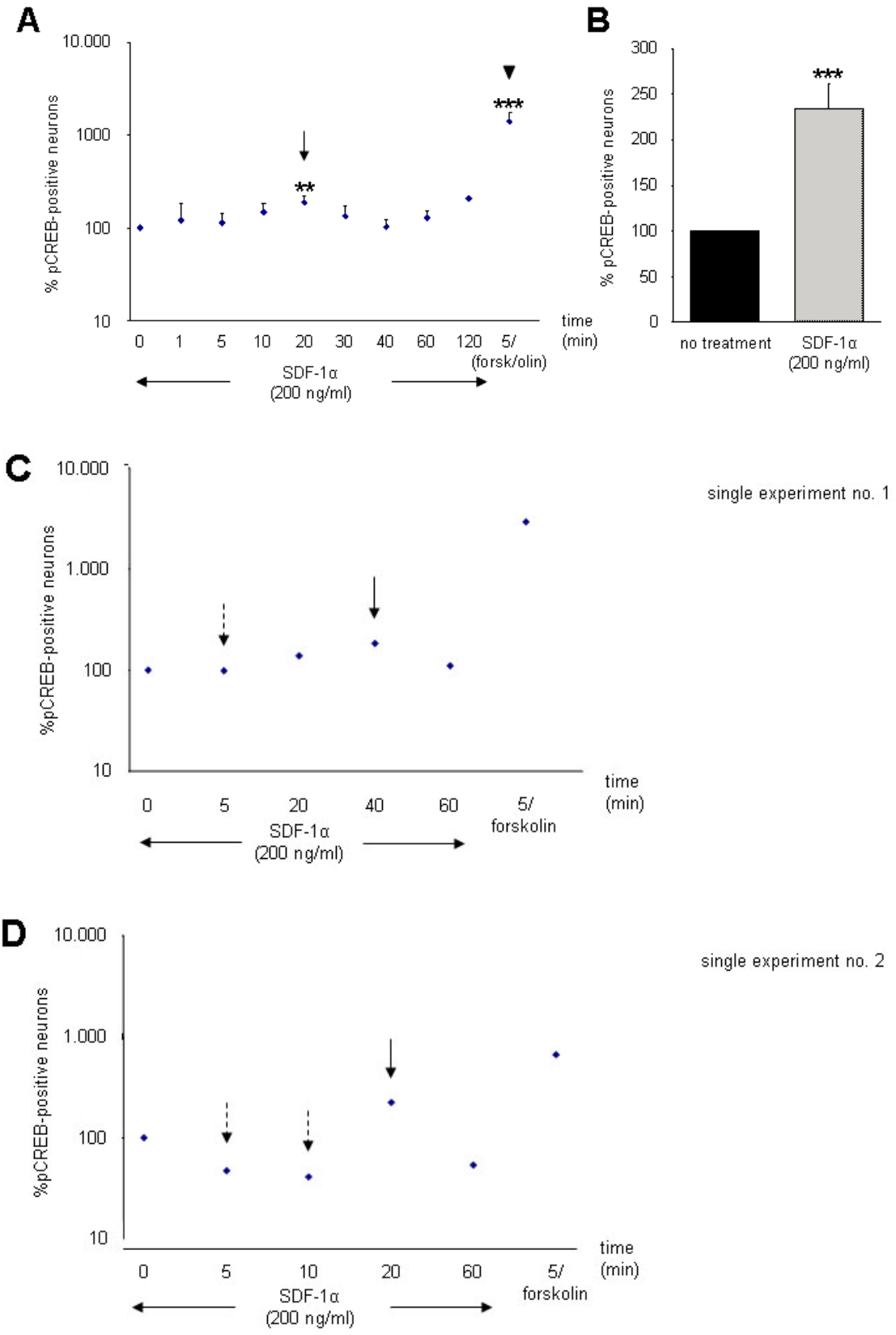

Fig. 4.4. (see also next page)

(see also previous page)

Fig. 4.4. Application of SDF-1α mediates CREB phosphorylation and translocation into nuclei of DRG neurons (I). CREB phosphorylation and translocation into nuclei is significantly increased in SDF-1α-treated P6 DRG neurons, but not in untreated controls (A, arrow, B). The mean maximum increase in pCREB-immunoreactivity is significant following application of SDF-1α at a concentration of 200 ng/ml (B). Forskolin induces a significant upregulation in the number of pCREB-positive nuclei directly after application (A, arrowhead). Upregulation of the number of pCREB-positive nuclei following application of SDF-1α is highly variable, and time required for a maximum increase in CREB phosphorylation and translocation to neuronal nuclei differs in an experiment-dependent manner (C,D, arrows). Following application of SDF-1α, an initial decrease in the amount of pCREB-positive nuclei is repeatedly observed (C,D, dashed arrows). Results (mean $\pm$ SEM) are from nine (A,B) independent experiments (n = 9) and are expressed as percentage of neurons displaying intense labelling of nuclei following staining for pCREB. Values are normalized for numbers of untreated cells. *$p<0.05$, **$p<0.01$, ***$p<0.001$ (student´s t-test).

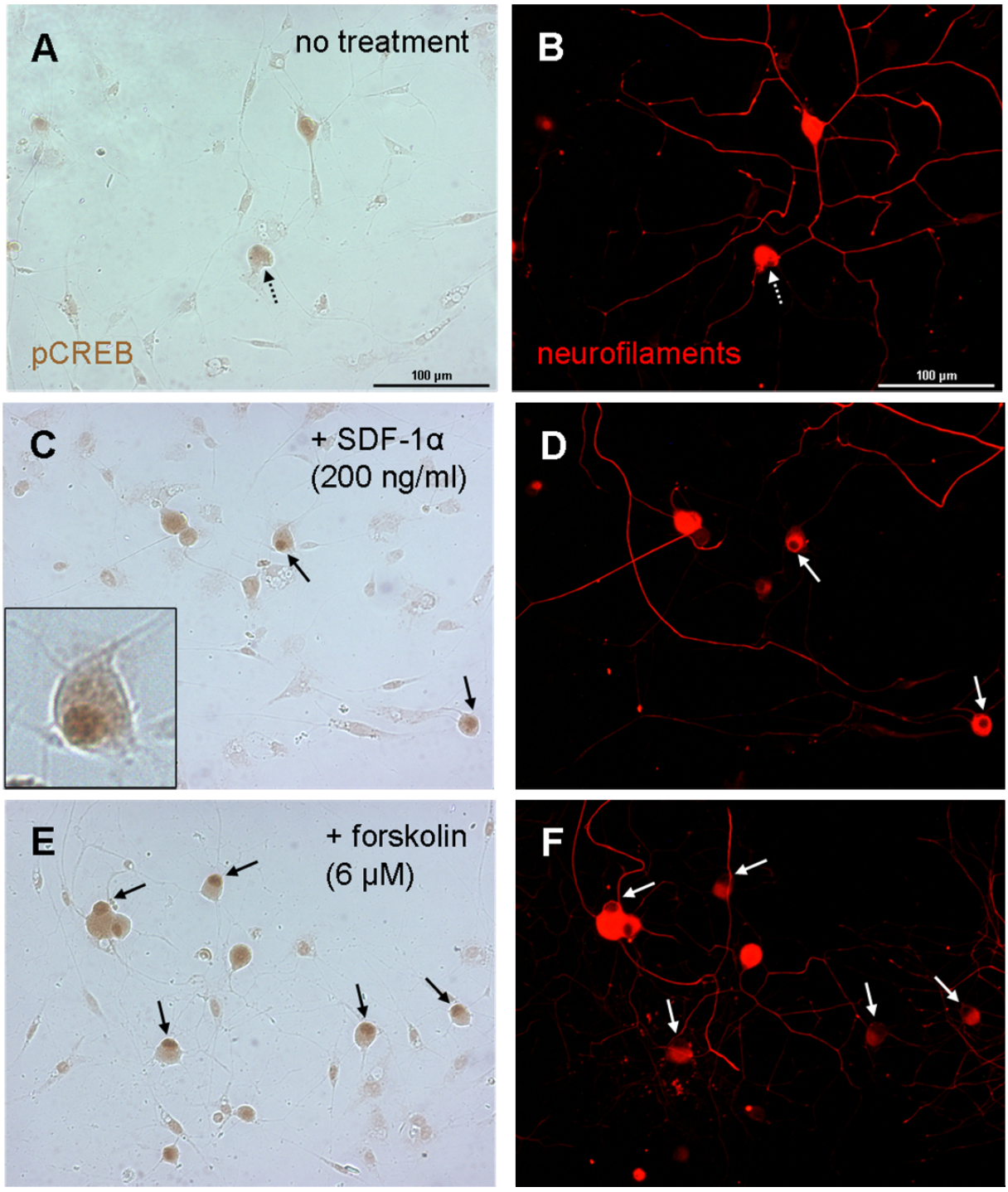

Fig. 4.5. Application of SDF-1α mediates CREB phosphorylation and translocation into nuclei of DRG neurons (II). The number of pCREB-positive nuclei is low in untreated P6 DRG neurons counterstained for neurofilaments (A,B, dashed arrows). Following application of SDF-1α, pCREB-immunoreactivity is significantly upregulated in neuronal nuclei (C,D, arrows). Treatment of cells with the adenylate cyclase activator forskolin results in a significant increase in the proportion of pCREB-positive nuclei (E,F, arrows). Pictures chosen for presentation (A,C,E) are representative of nine independent experiments (n = 9).

4.2.2 SDF-1α-mediated CREB phosphorylation and translocation into neuronal nuclei is presumably CXCR4-independent

To assess whether SDF-1α-mediated CREB phosphorylation and translocation into neuronal nuclei is CXCR4-dependent, DRG neurons were pretreated with anti-CXCR4 antagonist AMD3100 prior to application of this chemokine. Following an initial delay in response and a downregulation of pCREB in antagonist-treated cells, AMD3100-preincubated neurons displayed a significant upregulation (151.7% ± 25.9 SEM) in the mean number of pCREB-positive nuclei subsequent to SDF-1α-treatement, compared to control conditions (Fig. 4.6,B, arrow,C). Application of SDF-1α alone resulted in an increase of 117.9% (± 60.6 SEM), compared to untreated cells, which had no statistical significance (Fig. 4.6,A, arrow,C). Calculation of the time-independent maximum increase following application of both antagonist and SDF-1α to P6 DRG neurons resulted in a marked, albeit not significant, upregulation (215.5% ± 89.7 SEM) in the mean number of pCREB-positive nuclei in DRG neurons, compared to untreated cells, while the mean number was significantly increased (125.9% ± 8.0 SEM) following treatment with SDF-1α alone (data not shown). Both the overall mean numbers (Fig. 4.6,A,B) as well as the mean maximum values (Fig. 4.6,C,D) showed a stronger increase following concomitant application of AMD3100 and SDF-1α than following application of SDF-1α alone. The effect of forskolin (Fig. 4.6,A,B,D) was slightly abrogated following pretreatment with AMD3100 (1063.6% ± 106.5 SEM), as compared to forskolin-only controls (1253.0% ± 194.8 SEM).

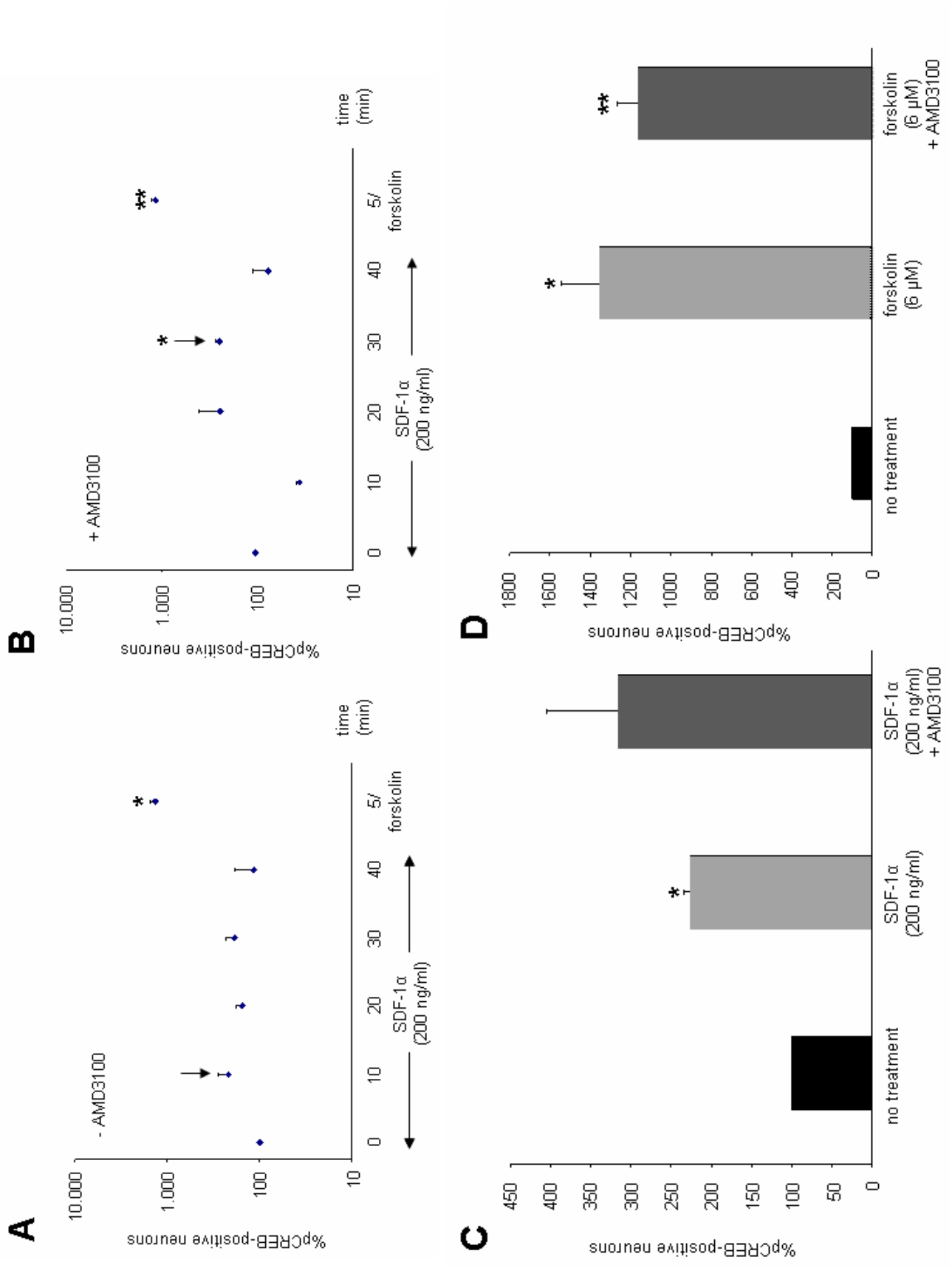

Fig. 4.6. (see also next page)

(see also previous page)

Fig. 4.6. SDF-1α-mediated increase in CREB phosphorylation and translocation into neuronal nuclei is CXCR4-independent. Unlike cells treated with SDF-1α alone (A), pretreatment of P6 DRG neurons with AMD3100 prior to application of SDF-1α results in a significant increase (B) in the mean numbers of pCREB-positive nuclei. Mean maximum increase in pCREB-immunoreactivity is prominent following application of both antagonist and SDF-1α, compared to cells treated with SDF-1α alone (C,D). Mean maximum increase of pCREB-positive nuclei following application of forskolin is slightly decreased, but statistically significant, after pretreatment with AMD3100 (C,D). Results (mean ± SEM) are from two (A-D) independent experiments (n = 2) and are expressed as percentage of neurons displaying intense labelling of nuclei following staining for pCREB. Values are normalized for numbers of untreated cells. *$p<0.05$, **$p<0.01$ (student´s t-test).

4.2.3 SDF-1α-mediated CREB phosphorylation and translocation into neuronal nuclei is presumably PKA-dependent

To assess whether SDF-1α-mediated upregulation of pCREB involved cAMP-dependent activation of PKA, P6 DRG neurons were pretreated with the PKA inhibitor KT5720 prior to application of this chemokine. Pretreatment with KT5720 resulted in a slight downregulation in the mean increase of pCREB-positive nuclei following application of SDF-1α, compared to cells treated with this chemokine alone (Fig. 4.7,A,B, arrows). While SDF-1α-treated cells displayed a marked, albeit not significant, increase in the number of pCREB-positive nuclei of 96.6% (± 96.4 SEM), as compared to untreated cells, application of both the inhibitor and SDF-1α effected a slighter increase of 86.2%. Calculation of the maximum increase resulted in a marked, albeit not significant, upregulation (137.05% ± 76.0 SEM) of pCREB-immunoreactivity in SDF-1α-treated cells, and a lower, but significant, increase (93.0% ± 25.6 SEM) in cells following application of both KT5720 and SDF-1α (data not shown). Both the overall mean numbers as well as the mean maximum values displayed a decreased upregulation of pCREB as mediated by SDF-1α, following application of the inhibitor. Prominent upregulation (1636.3% ± 586.5 SEM) of pCREB-immunoreactivity following application of forskolin was further increased

(2330.4% ± 637.4 SEM) if forskolin was applied after pretreatment with KT5720 (Fig. 4.7,A,B).

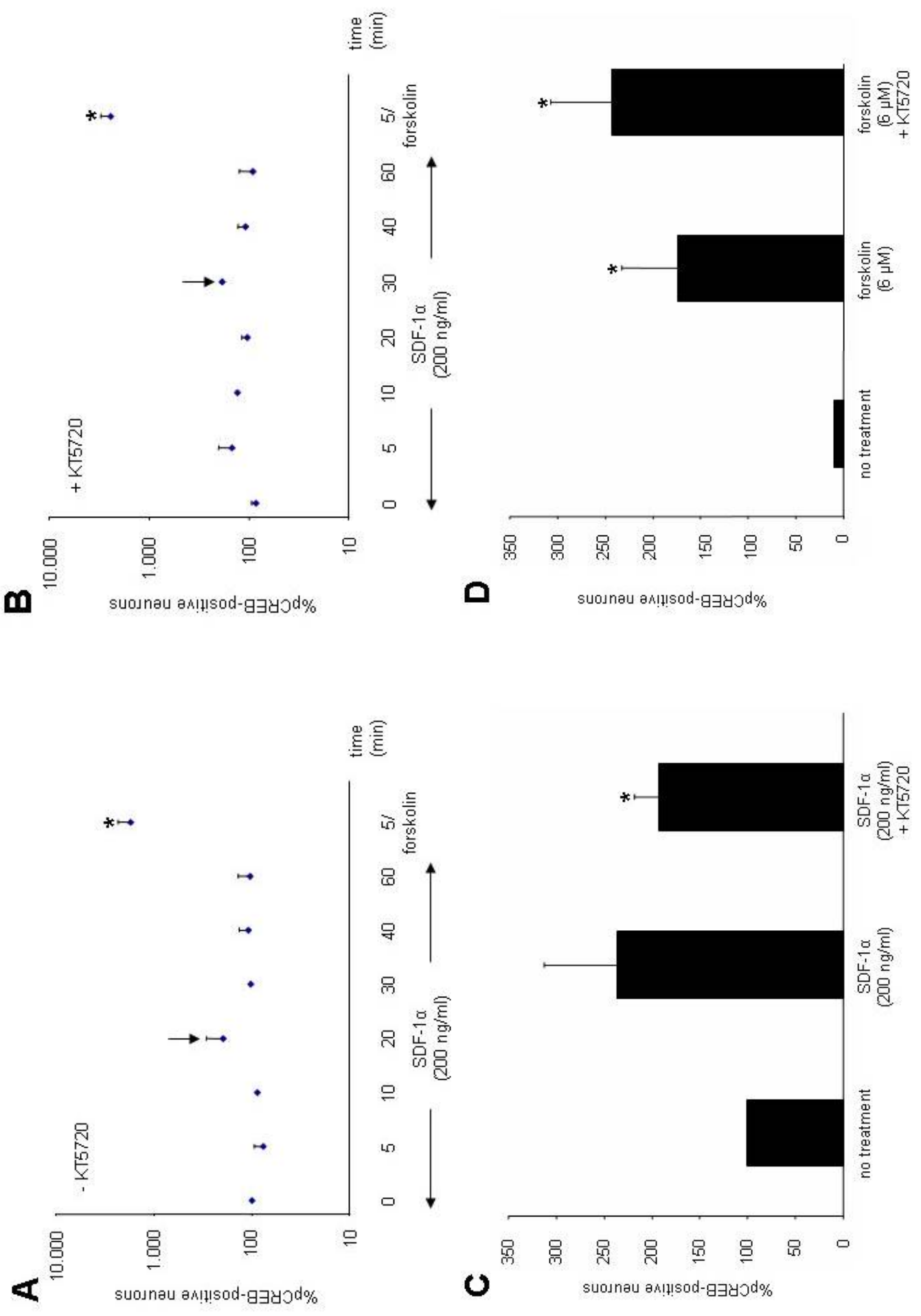

Fig. 4.7. (see also next page)

(see also previous page)

Fig. 4.7. SDF-1α-mediated increase in CREB phosphorylation and translocation into neuronal nuclei is PKA-dependent. SDF-1α-mediated increase in the mean number of pCREB-positive nuclei is slightly downregulated following pretreatment of P6 DRG neurons with KT5720, compared to cells treated with SDF-1α alone (A,B). Mean maximum increase in pCREB-immunoreactivity is significant following application of both inhibitor and SDF-1α, but is decreased as compared to cells treated with SDF-1α alone (C,D). Forskolin-induced upregulation of pCREB-immunoreactivity is markedly increased after pretreatment of neurons with KT5720, compared to untreated cells or cells treated with SDF-1α alone (C,D). Results (mean ± SEM) are from three (A-D) independent experiments (n = 3) and are expressed as percentage of neurons displaying intense labelling of nuclei following staining for pCREB. Values are normalized for numbers of untreated cells. *p<0.05, (student´s t-test).

4.3 *In vitro* expression and distribution of CXCR4 and RDC1

To assess expression and distribution of both cognate receptors to SDF-1, CXCR4 and RDC1, in various cell types, P6 DRG neurons, Schwann cells, cortical neurons HeLa cells, and leptomeningeal fibroblasts, were immunocytochemically analyzed.

4.3.1 DRG neurons

CXCR4-immunoreactivity was detected in 95.92% (± 2.19 SEM) of cultured P6 DRG neurons, where it was distributed in a characteristic pattern on neuronal cell bodies and along neurites counterstained for neurofilaments after 24 h *in vitro* (Fig. 4.8,A-C, Fig. 4.9,A,C,D). On neurites, CXCR4 displayed an evenly spaced distribution, and was predominantly located adjacent to growth cones (Fig. 4.8,D-I, dashed arrows) and near branching points (Fig. 4.8,G-I, asterisks). Thereby, these regions were further characterized by a splayed configuration of neurofilaments (Fig. 4.8,D-I). Spatial distribution of CXCR4-immunoreactivity on cellular processes of cultured DRG neurons was time-dependent (Fig. 4.10,A-F). Expression of CXCR4 was equally prominent on both neurofilament-positive neurites and cell bodies after 24 h (Fig. 4.10,A,D). CXCR4-immunoreactivity on neurites decreased in the course of *in*

vitro incubation, while it remained strong on neuronal cell bodies after 48-72 h (Fig. 4.10,B,C). Conversely, staining for neurofilament remained unaltered after 24-72 h *in vitro* (Fig. 4.10,E,F). Surface expression of CXCR4 was confirmed by confocal microscopy (Fig. 4.11,A-H). CXCR4-immunoreactivity was exclusively localized to the surface of cell bodies and neurites (Fig. 4.11,A-C,H) and was not found in the cytoplasm (Fig. 4.11,D-G).

The novel receptor to SDF-1, RDC1, was expressed in 95.02% (± 4.98 SEM) of P6 DRG neurons (Fig. 4.9,B-D). RDC1-immunoreactivity was moderately expressed on neurites (arrows) and was prominent on neuronal cell bodies (arrowheads) after 24 h *in vitro*, where it was colocalized with CXCR4 (Fig. 4.12,A-C). On neurites, RDC1 was evenly distributed and displayed a granular pattern (Fig. 4.12,A,D). Expression of RDC1 in DRG neurons did not decrease during cultivation and remained prominent on both cell bodies and neurites after 48-72 h *in vitro* (Fig. 4.12,D-F). Directly after plating (2-5 h), CXCR4-immunoreactivity was prominently localized to cellular protrusions (arrows) of DRG neurons as well as to sites where processes emerged from the cell body (arrowheads) or branching occurred (Fig. 4.13,A;D). RDC1 was colocalized with CXCR4 on DRG neurons after 5 h *in vitro*. At this time point, RDC1 was evenly distributed in the cellular periphery and was prominent in the central regions of cell bodies (Fig. 4.13,B-D).

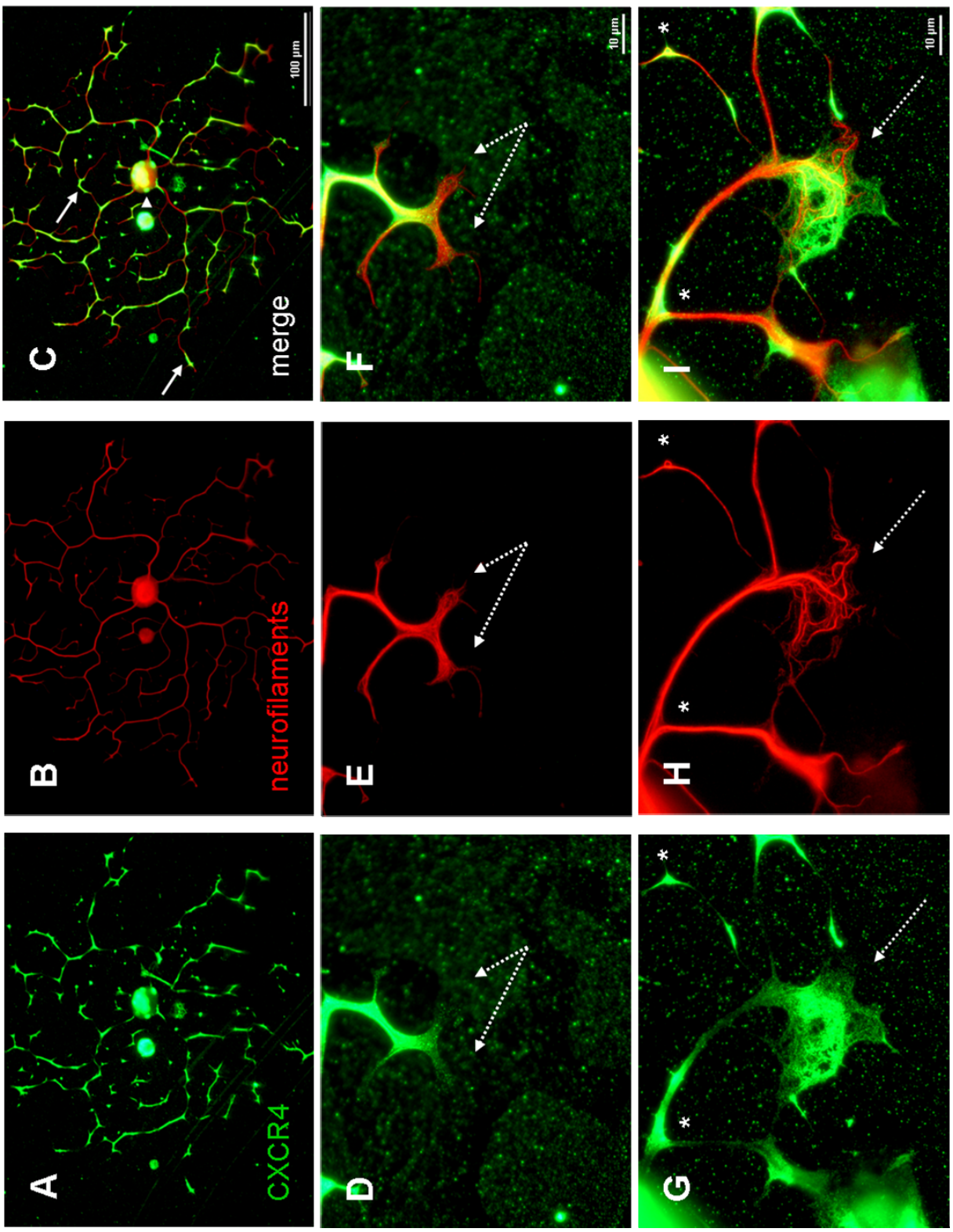

Fig. 4.8. (see also next page)

(see also previous page)

Fig. 4.8. CXCR4 is expressed in cultured DRG neurons. CXCR4 is expressed in P6 DRG neurons and is distributed in a characteristic pattern (A,C) on neurites (arrows) and cell bodies (arrowhead) counterstained for neurofilaments (B) after 24 h *in vitro*. On neurites, CXCR4-immunoreactivity is predominantly located adjacent to growth cones (dotted arrows) and near branching points (asterisks) and adjacent to growth cones (D-I). Regions to which CXCR4 is predominantly localized are further characterized by a splayed configuration of neurofilament (E,F,H,I). Pictures chosen for presentation (A-I) are representative of eight independent experiments (n = 8).

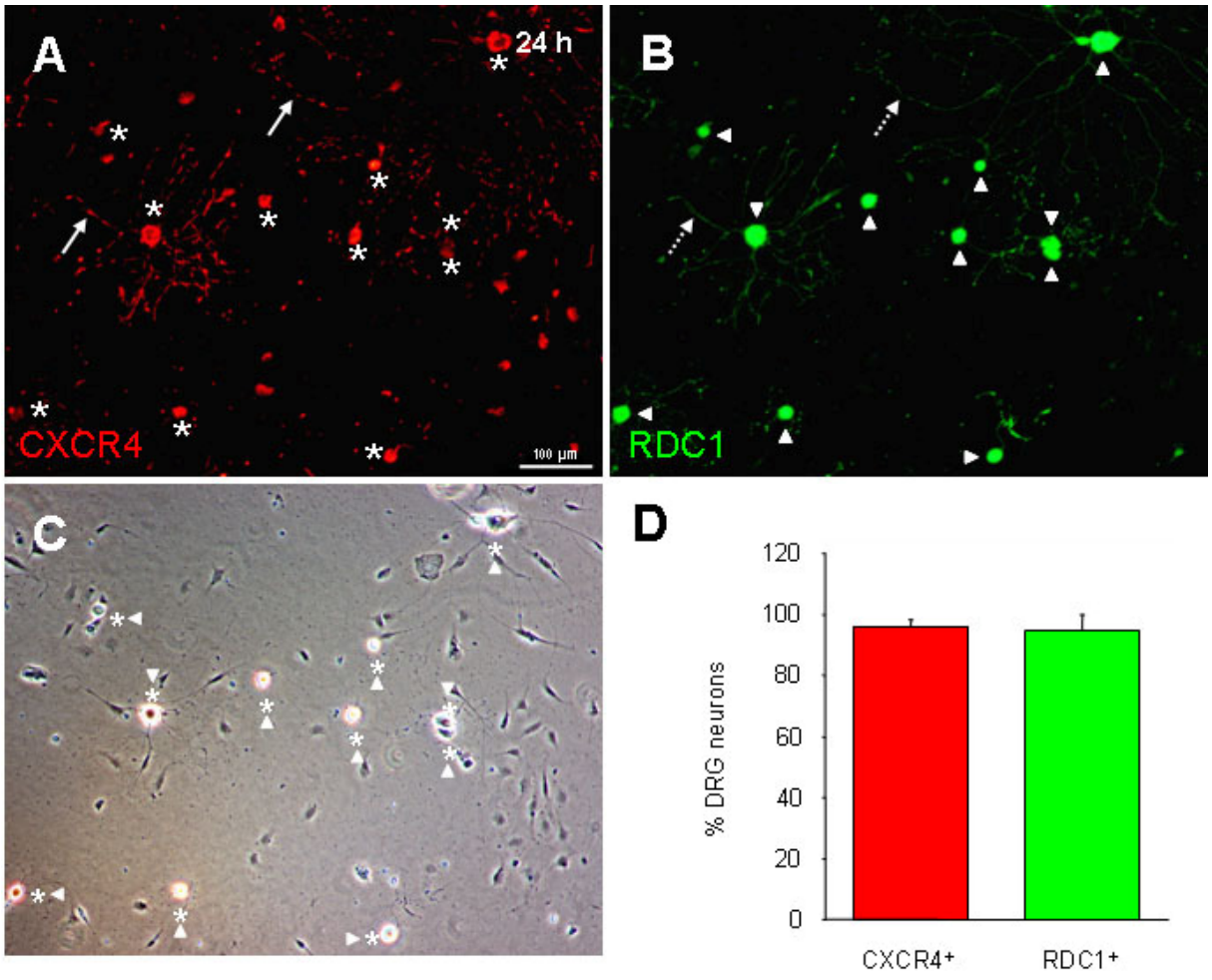

Fig. 4.9. CXCR4 and RDC1 are expressed in cultured DRG neurons. CXCR4 (A) and RDC1 (B) are expressed in the majority of P6 DRG neurons (C,D) after 24 h *in vitro*. Both receptor molecules are coexpressed in cultured DRG neurons after 24 h, and CXCR4- and RDC1-immunoreactivity are differently distributed on neurites and cell bodies *in vitro* (A,B). CXCR4-immunoreactivity on neuronal cell bodies is indicated by asterisks (A,C), while on neurites it is indicated by arrows (A). RDC1-immunoreactivity on cell bodies is indicated by arrowheads (B,C), while on neurites it is indicated by dashed arrows (B). Pictures chosen for presentation are representative of three (A-C) independent experiments (n = 3). Results (mean ± SEM) are from three (D) independent experiments (n = 3) and are expressed as percentage of neurons displaying intense fluorescent labelling of nuclei following staining for both CXCR4 and RDC1.

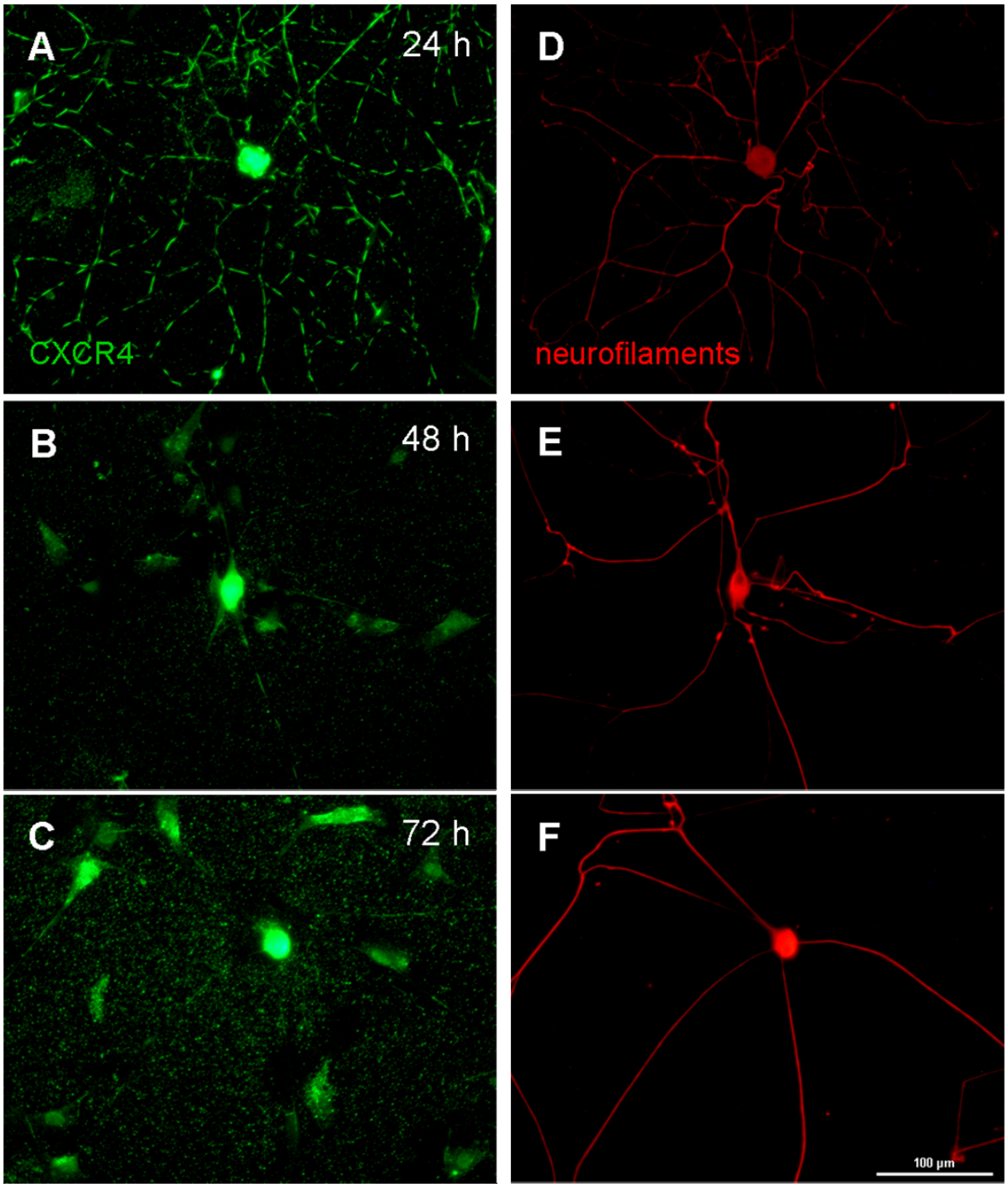

Fig. 4.10. CXCR4 expression and distribution in cultured DRG neurons is time-dependent. CXCR4 is prominently expressed in P6 DRG neurons on both cell bodies and neurites (A) counterstained for neurofilaments (D) after 24 h *in vitro*. During cultivation, CXCR4-immunoreactivity decreases on neurites, but remains prominent on cell bodies, after 48 h (B) or after 72 h (C), respectively. Immunoreactivity following staining for neurofilaments remains unaltered after 48-72 h *in vitro* (E,F). Pictures chosen for presentation are representative of five (A-F) independent experiments (n = 5).

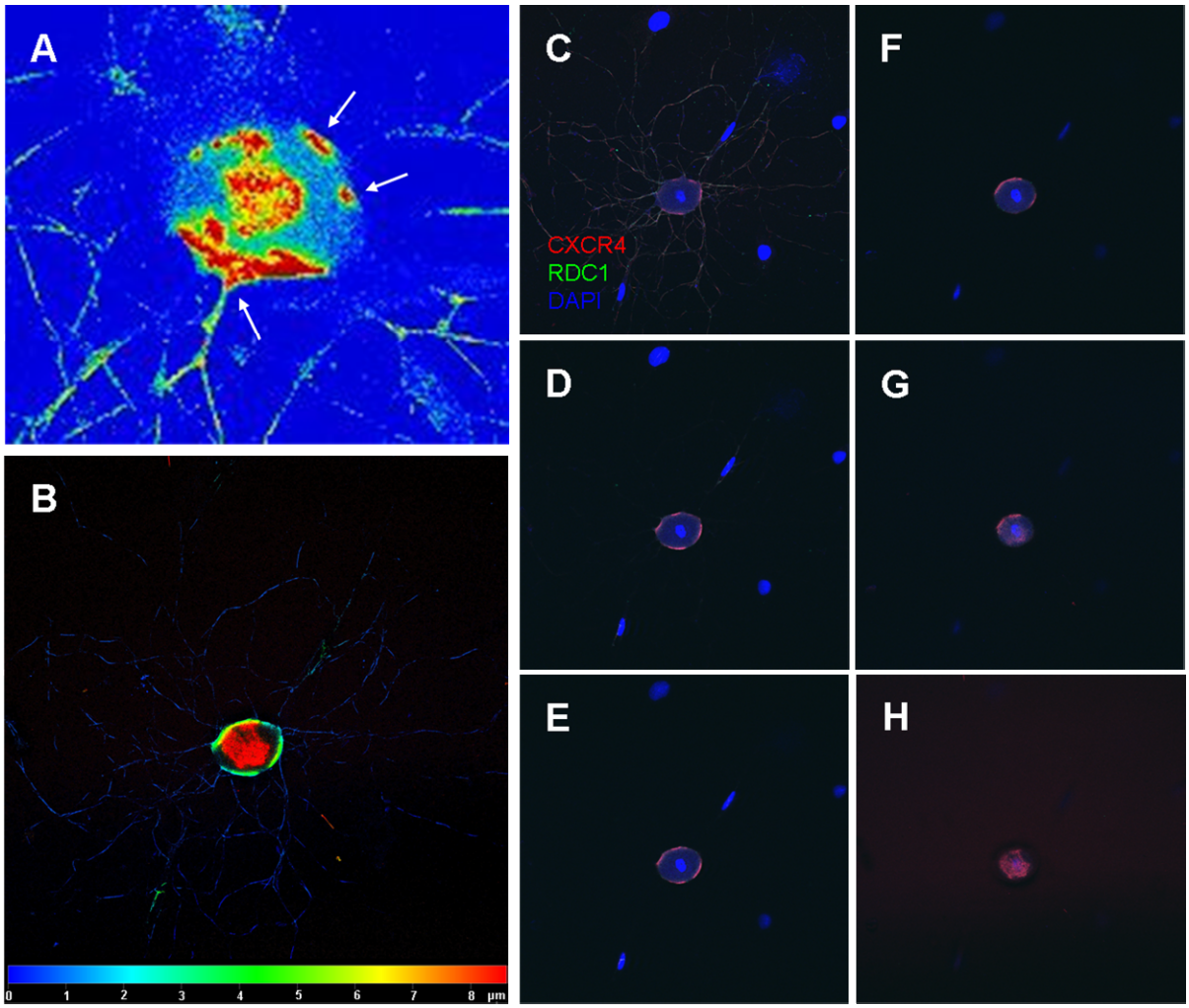

Fig. 4.11. CXCR4 is surface expressed in DRG neurons. Confocal laser scan microscopy imaging reveals CXCR4 surface expression in DRG neurons on both neurites and cell bodies (A-C,H). CXCR4-immunoreactivity is distributed in a patchy pattern on the outer membrane surface (A, arrows), but not in the cytoplasm (D-G), of neuronal cell bodies after 24 h *in vitro*.

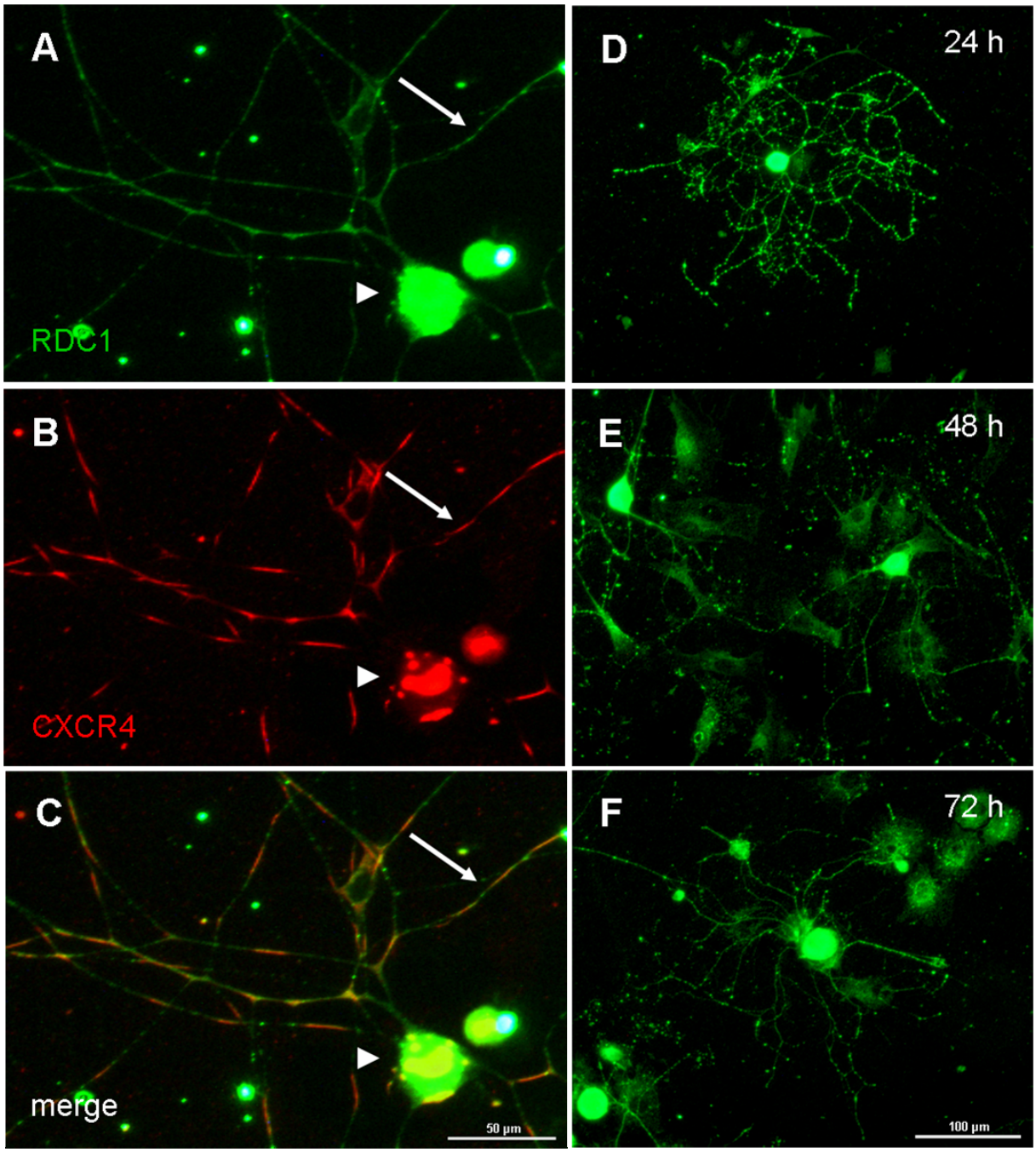

Fig. 4.12. CXCR4 and RDC1 are coexpressed in cultured DRG neurons. RDC1 (A) and CXCR4 (B) are coexpressed in P6 DRG neurons after 24 h *in vitro* (C). While CXCR4-immunoreactivity is distributed in a patchy pattern on neurites (arrows) and neuronal cell bodies (arrowheads), RDC1 expression appears even to granular. Expression and distribution of RDC1 display no time-dependent alterations during *in vitro* cultivation (D-F). RDC1-immunoreactivity on both cell bodies and neurites remains prominent after 48-72 h *in vitro*. Pictures chosen for presentation are representative of five (A-F) independent experiments (n = 5).

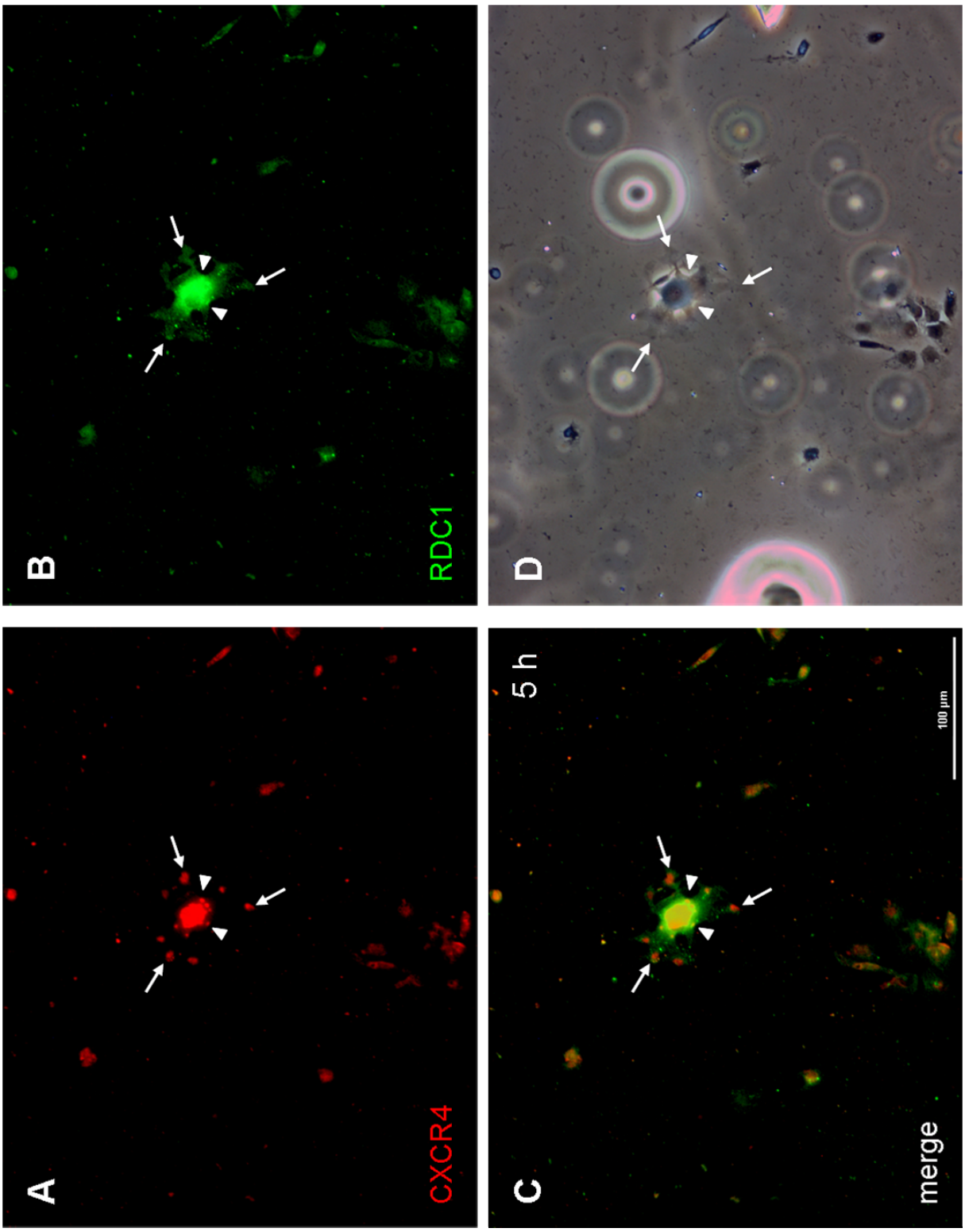

Fig. 4.13. (see also next page)

(see also previous page)

Fig. 4.13. CXCR4 displays a characteristic patterning in P6 DRG neurons directly after plating. CXCR4 (A,D) is distributed in a characteristic pattern in DRG neurons *in vitro* 5 h after cell plating. Thereby, it is predominantly localized in cellular protrusions (arrows) and at sites where processes emerge from the cell body (arrowheads). CXCR4 (A) and RDC1 (B) are coexpressed (C) in DRG neurons at directly after plating. No characteristic patterning is observed for RDC1 in DRG neurons 5 h after cell plating. Pictures chosen for presentation are representative of three (A-D) independent experiments (n = 3).

4.3.2 Schwann cells

As for DRG neurons, the Schwann cell fraction of dissociated P6 DRGs was assessed for expression and distribution of CXCR4 and RDC1.

CXCR4 was prominently expressed in a fraction of Schwann cells (asterisks) after 24 *in vitro* (Fig. 4.14,A,B,E). Thereby, CXCR4-immunoreactivity was localized to distinct cellular regions or the cell periphery, where it displayed a filament-like distribution (Fig. 4.14,F, arrows, G, arrowhead). Unlike CXCR4 expression in P6 DRG neurons, expression of this receptor in Schwann cells was not markedly decreased in the course of cultivation, but was prominent after 48 h or 72 h, respectively (data not shown). RDC1 and CXCR4 were coexpressed in a fraction of Schwann cells after 24 h *in vitro* (Fig. 4.14,F) as well as on cell bodies of P6 DRG neurons (Fig. 4.14,A-C, arrowheads). Coexpression of both receptors was maintained after 48-72 h (data not shown). Thereby, RDC1-immunoreactivity was observed in a larger fraction of cells, as compared to CXCR4. While RDC1 was weakly expressed at early stages of cultivation, expression of this receptor increased in the course of *in vitro* incubation (data not shown). Unlike CXCR4, RDC1 displayed an even or granular distribution (Fig. 4.14,C,D,F, dashed arrows, G, arrow) in Schwann cells, and RDC1 expression was, albeit moderately, observed in the majority of cells after 24-72 h *in vitro*. Simultaneously, expression of CXCR4, but not RDC1, was markedly diminished on neurites of P6 DRG neurons after 48 h *in vitro* (data not shown). Distribution of both CXCR4- and RDC1-immunoreactivity in Schwann cells was similar to a corresponding patterning of CXCR4 and RDC1 in processes of DRG neurons after 24 h *in vitro* (Fig. 4.15,A-C).

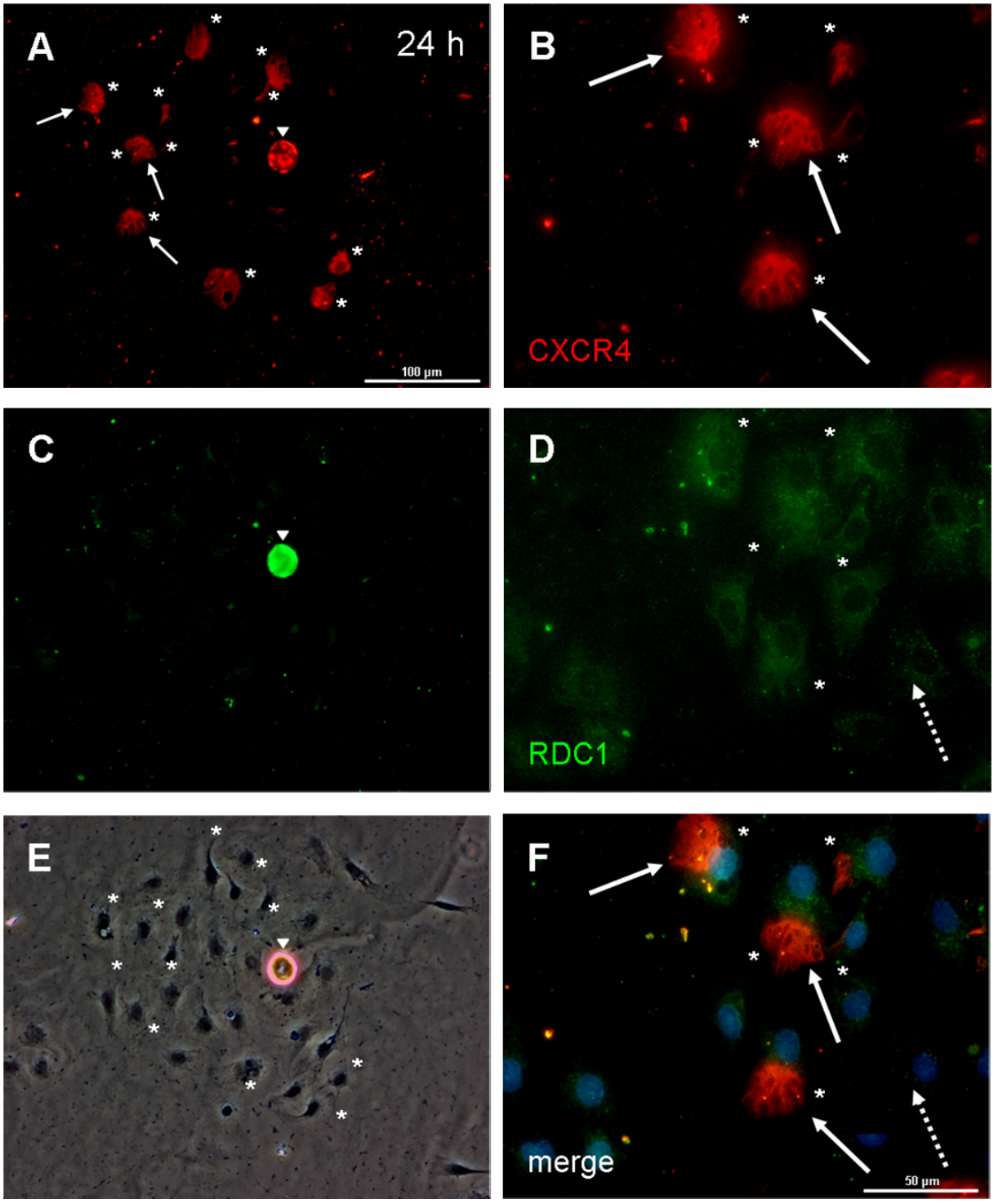

Fig. 4.14. (I, see also next page)

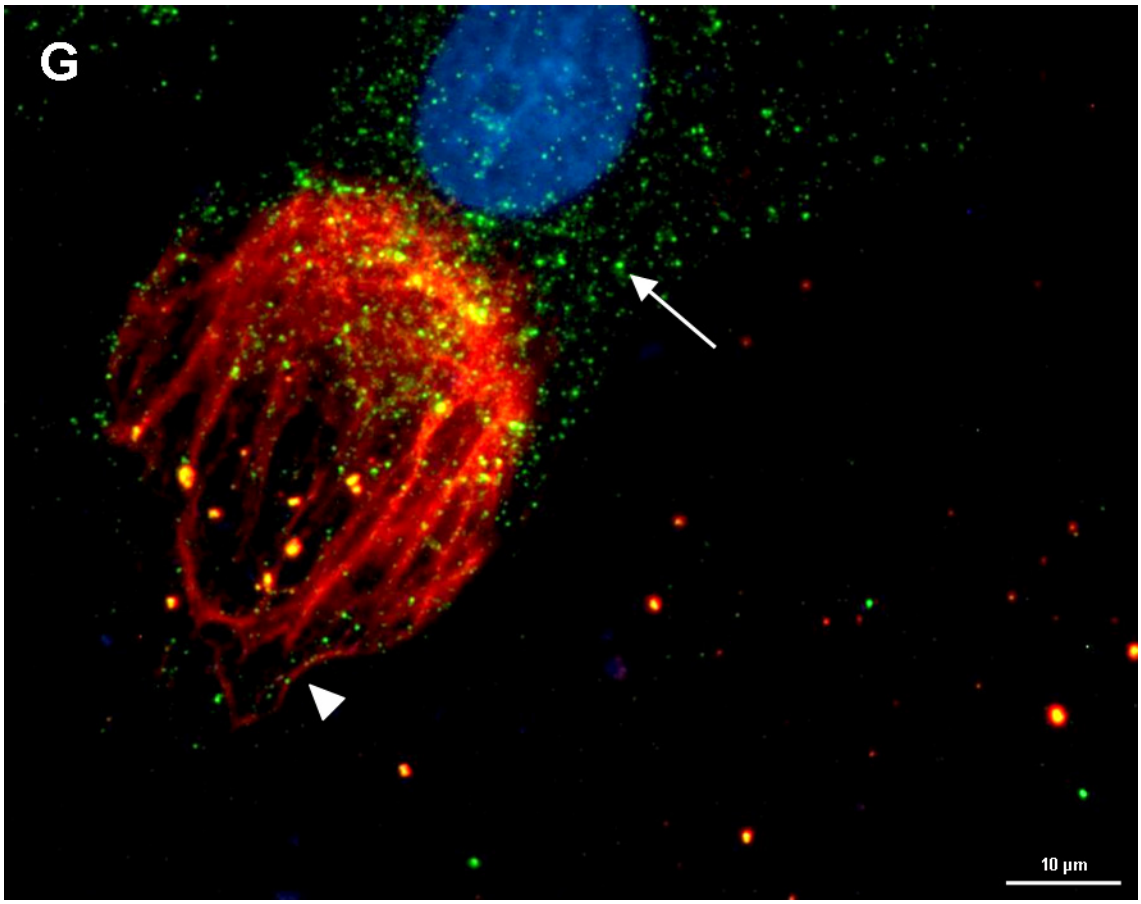

(II, see also previous page)

Fig. 4.14. CXCR4 and RDC1 are expressed in Schwann cells (I). CXCR4 is expressed in a fraction of Schwann cells (asterisks) and in neurons (arrowheads) of dissociated P6 DRGs after 24 h *in vitro* (A,B,E). CXCR4-immunoreactivity displays filament-like distribution in distinct cellular regions of Schwann cells (E, arrows,G, arrowheads). RDC1 shows weak expression in the majority of Schwann cells and in neuronal cells bodies (arrowheads) at early stages of cultivation, where it is distributed in an even or granular (dashed arrow) manner (C,D,E). RDC1 and CXCR4 are coexpressed (F,G) in Schwann cells after 24 h *in vitro*. Pictures chosen for presentation are representative of three (A-G) independent experiments (n = 3).

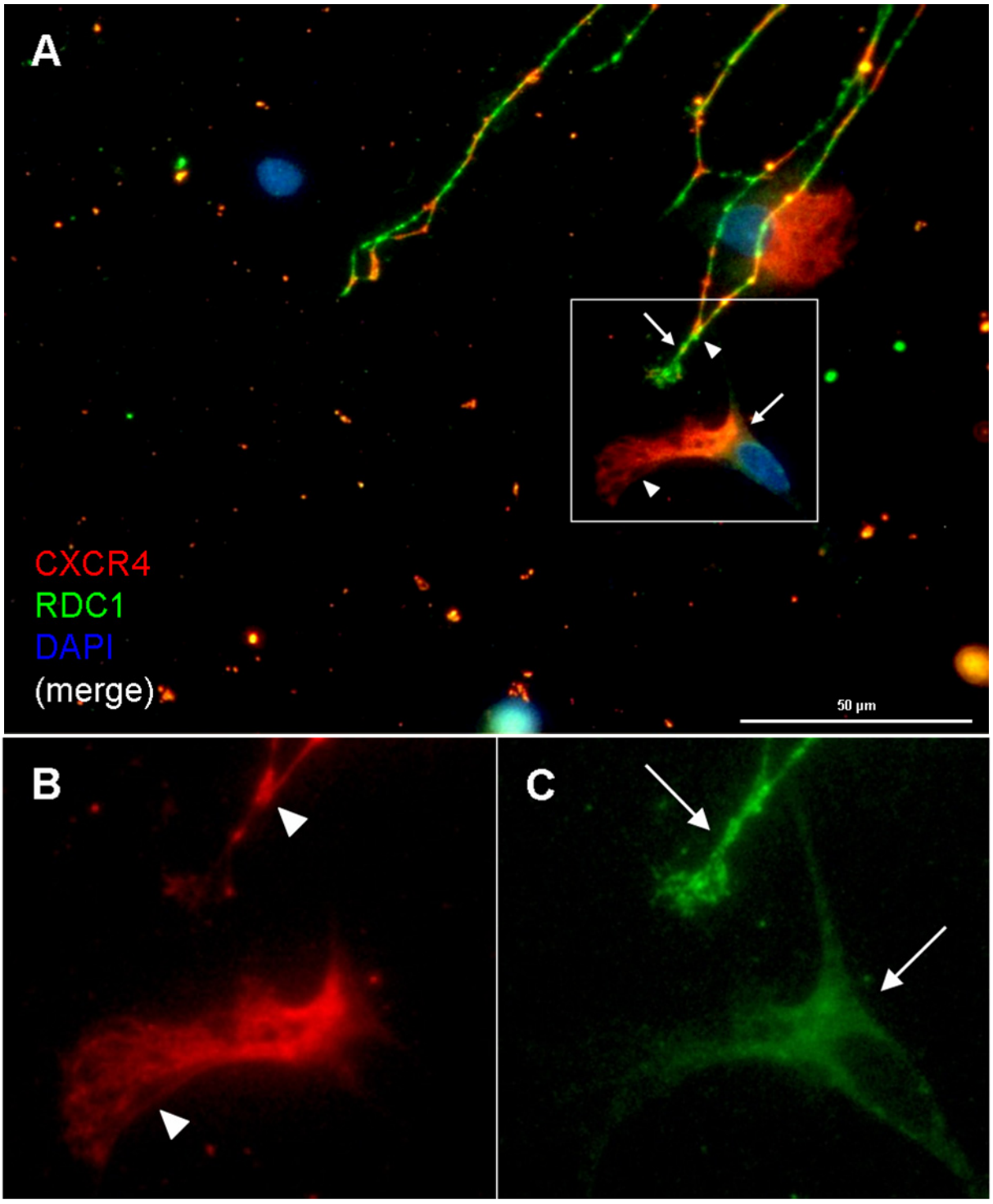

Fig. 4.15. CXCR4 and RDC1 are expressed in Schwann cells (II). Spatial distribution of CXCR4 (arrowheads) and RDC1 (arrows) in Schwann cells is similar to expression and distribution of both receptors in neurites and cell bodies of DRG neurons (A-C). Pictures chosen for presentation are representative of three (A-C) independent experiments (n = 3).

4.3.3 Cortical neurons

Analysis of CXCR4- and RDC1-immunoreactivity in cultured E15 cortical neurons revealed a receptor-specific pattern of expression and distribution *in vitro*.
CXCR4 and RDC1 were coexpressed in all cells of a certain preparation at each time point tested (Fig. 4.16,A-F). Thereby, CXCR4-immunoreactivity was prominent on the longest cellular process (Fig. 4.16,A,D, arrows; Fig. 4.17, arrows) and the proximal part of cell bodies (Fig. 4.16,A,D, arrows; Fig. 4.17, dashed arrows) after 24 h *in vitro*. Expression of CXCR4 slightly increased during cultivation and was moderately present on cell bodies and a fraction of cellular processes after 96-120 h *in vitro* (Fig. 4.18,A-C). RDC1-immunoreactivity was prominent on the majority of cellular processes (Fig. 4.16,C,D, arrowheads) and total cell bodies (Fig. 4.16,C,D, arrowheads; Fig. 4.17, arrowheads) after 24 h *in vitro*. Expression of this receptor increased during cultivation and was markedly stronger, compared to early time points of *in vitro* incubation and to CXCR4 expression, after 96-120 h (Fig. 4.18,A-E). While CXCR4- and RDC1-immunoreactivity on cellular processes displayed a granular distribution at early stages of cultivation (Fig. 4.16,D,E; Fig. 4.17, asterisks), both receptors were evenly expressed at later time points (Fig. 4.18,A,D).

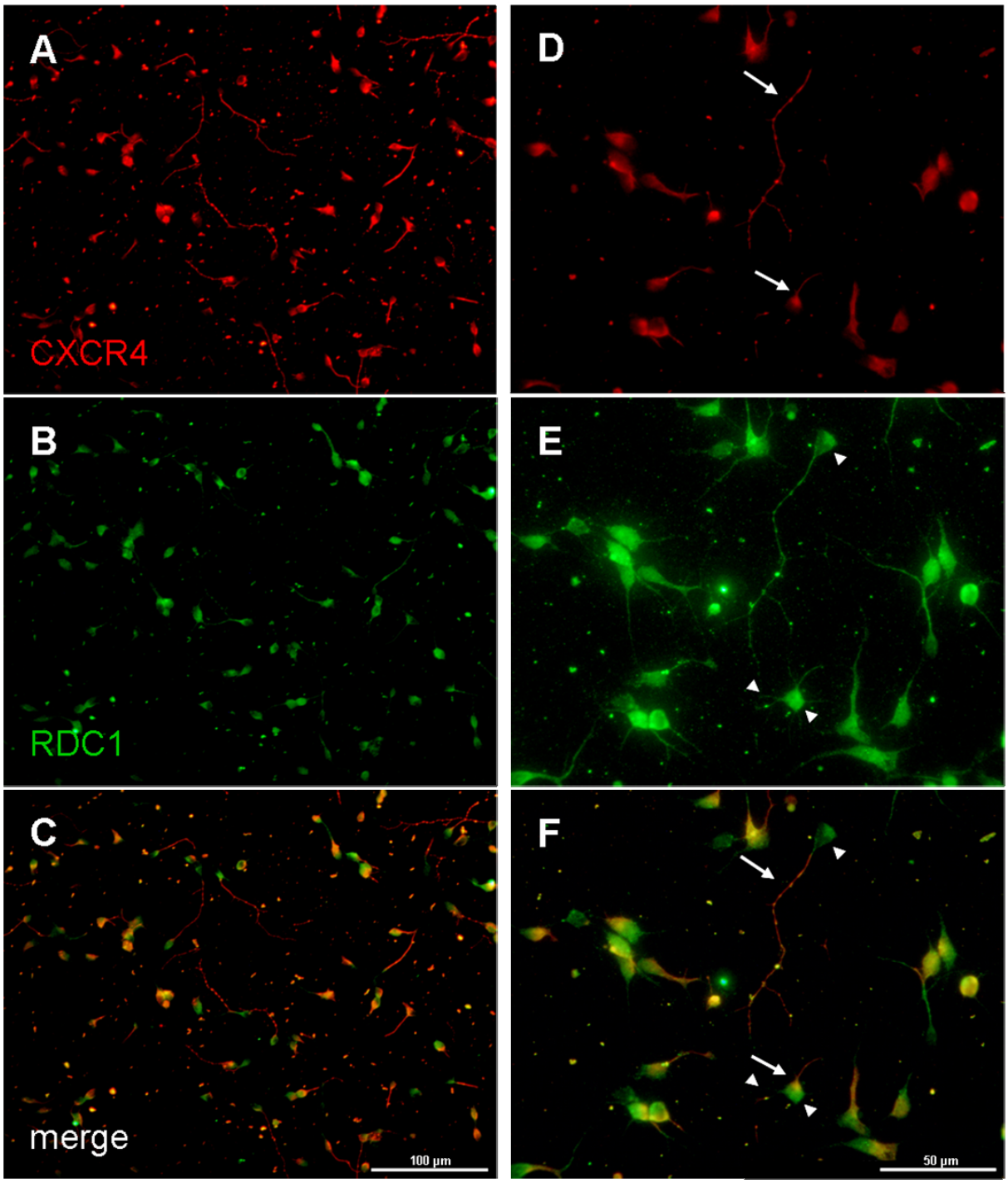

Fig. 4.16. CXCR4 and RDC1 are expressed in cortical neurons (I). CXCR4 (A,D,F) is expressed in E15 cortical neurons, where it is mapped to the longest neuronal process and the proximal part of cell bodies after 24 h *in vitro* (arrows). RDC1-immunoreactivity (B,E,F) is moderately to prominenlty present on processes and cell bodies of cortical neurons (arrowheads). RDC1 is coexpressed with CXCR4 (C,F) in the majority of cells at early stages of cultivation. Pictures chosen for presentation are representative of two (A-F) independent experiments (n = 2).

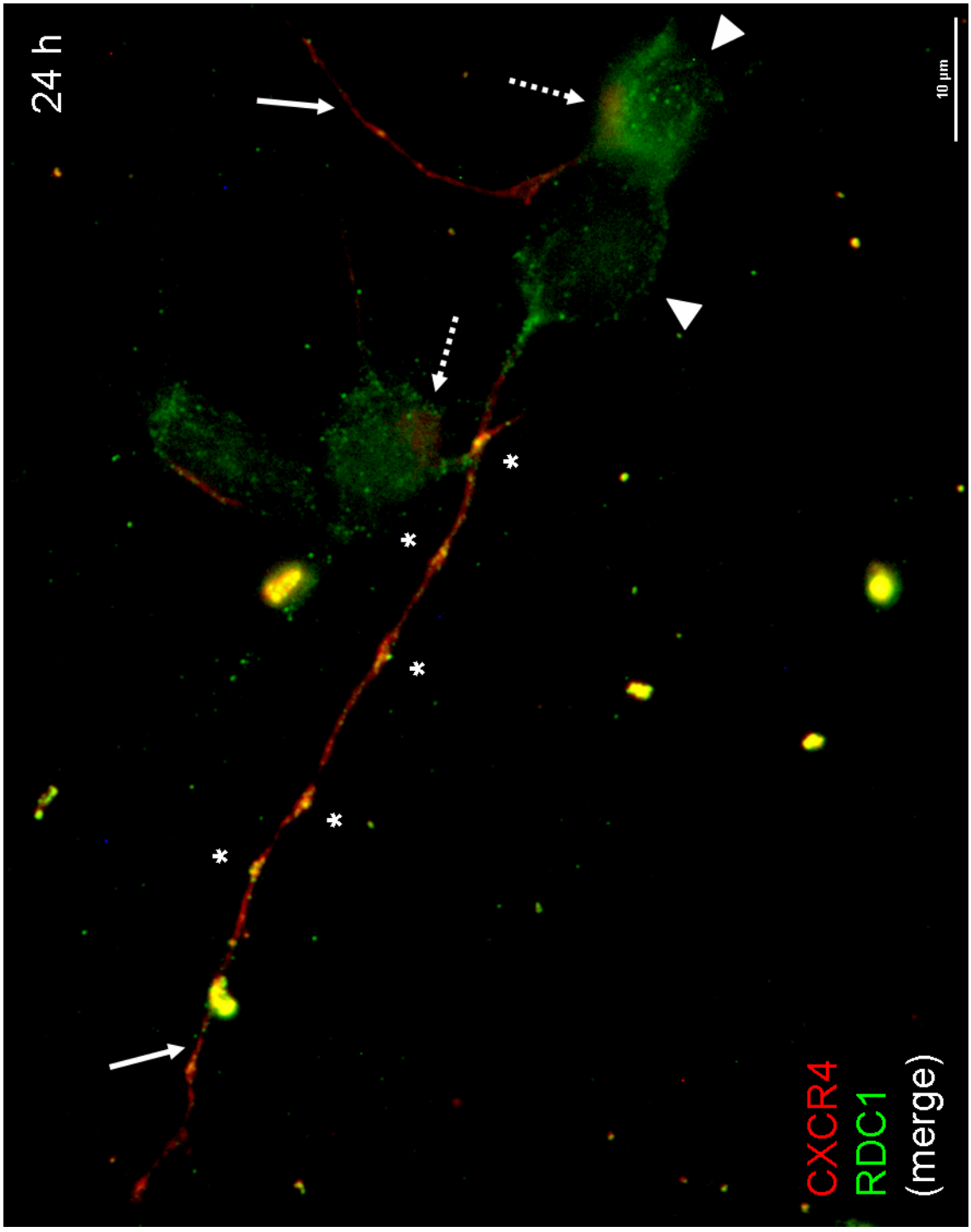

Fig. 4.17. (see also next page)

Fig. 4.17. CXCR4 and RDC1 are differentially distributed in cortical neurons. CXCR4 and RDC1 are coexpressed in E15 cortical neurons after 24 h *in vitro*. CXCR4-immunoreactivity is prominent on specific cellular processes (arrows) and the proximal part of cell bodies (dashed arrows), while RDC1 displays even or granular distribution on the whole neuronal cell body (arrowheads). Colocalization of CXCR4 and RDC1 in specific regions of cellular processes is indicated by asterisks. The picture chosen for presentation is representative of two independent experiments (n = 2).

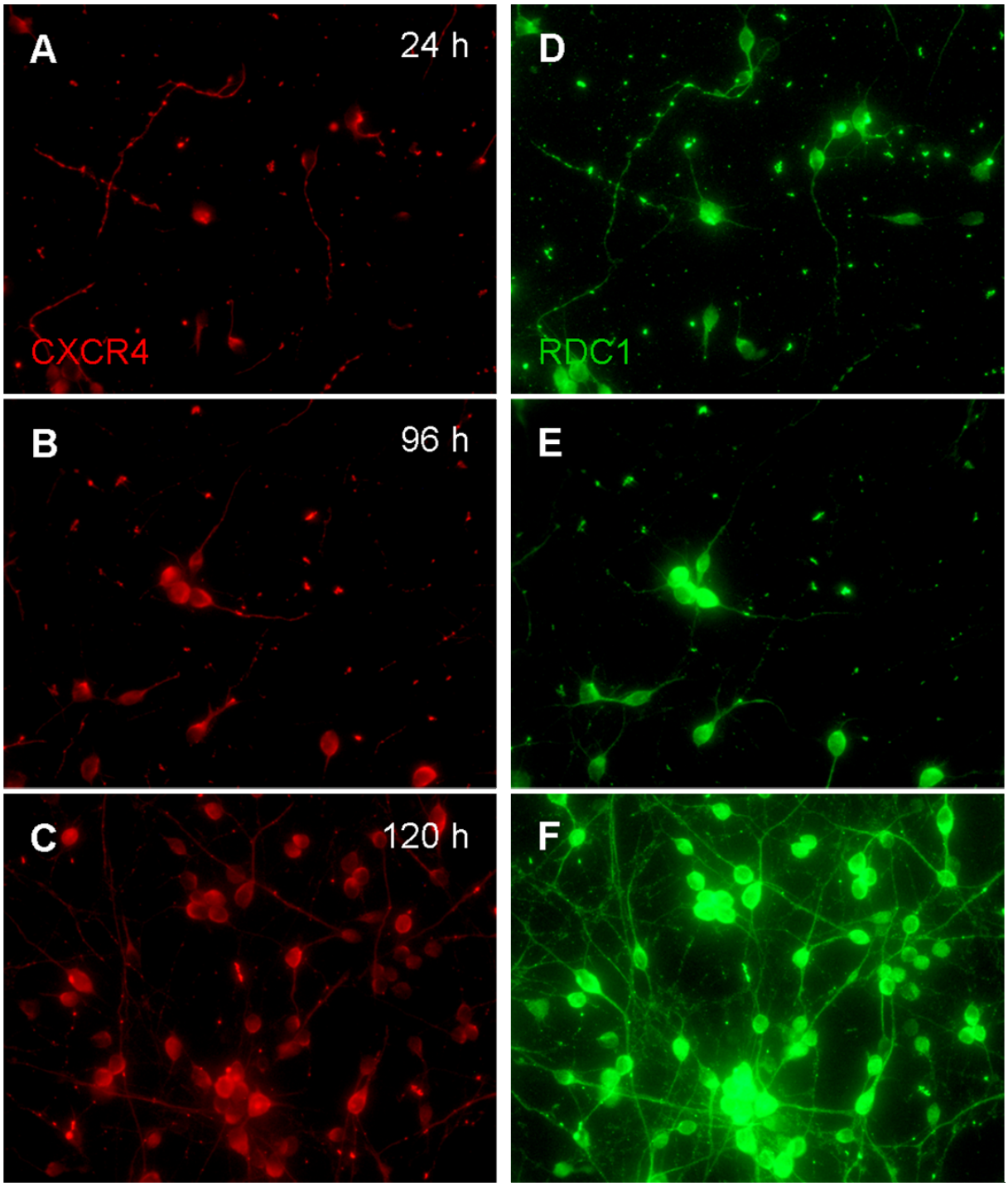

Fig. 4.18. CXCR4 and RDC1 are expressed in cortical neurons (II). CXCR4-immunoreactivity (A-C) is moderately present in E15 cortical neurons after 24 h *in vitro* (A) and increases during cultivation (B,C). RDC1 is coexpressed with CXCR4 in cortical neurons. RDC1-immunoreactivity (D-F) increases during *in vitro* incubation and is strongly expressed in neuronal processes and cell bodies after 96-120 h. Pictures chosen for presentation are representative of two (A-F) independent experiments (n = 2).

4.3.4 Leptomeningeal fibroblasts

CXCR4 and RDC1 were coexpressed in cultivated E15 leptomeningeal fibroblasts *in vitro*. During cultivation, CXCR4- and RDC1-immunoreactivity displayed marked differences with regard to the cellular distribution of receptor molecules. Both CXCR4 and RDC1 were weakly to moderately expressed in meningeal fibroblasts after 1 DIV (Fig. 4.21,A,C,E,F). While CXCR4 displayed an even distribution (arrows), RDC1 expression appeared granular (arrowheads) at early stages of cultivation (Fig. 4.21, B,D,F). After 2 DIV, CXCR4-immunoreactivity was predominantly located in cellular processes and the fibroblast periphery (arrows), but rarely showed an even distribution (asterisks) in the whole cell (Fig. 4.22,A,B,E,F). RDC1 was coexpressed with CXCR4 in meningeal fibroblasts after 2 DIV, where it was either evenly distributed or, conversely, was prominently located in the central region (arrowheads) of cells (Fig.4.22,C-F). Distribution of CXCR4-immunoreactivity in fibroblasts after 2 DIV was similar to CXCR4-expression in DRG neurons at early stages of *in vitro* cultivation (Fig. 4.22,G,H; Fig. 4.13,A,C). Unlike CXCR4, distribution of RDC1 displayed less or no time-dependent alterations in cellular localization in leptomeningeal fibroblasts. Characteristic distribution of both receptor molecules remained stable for up to 5 DIV (Fig. 4.23,A-F). Prominent localization of both receptors in central regions of meningeal fibroblasts at late stages of cultivation was presumably not due to region-specific distribution, but presumably represented artefacts of long-term *in vitro* incubation.

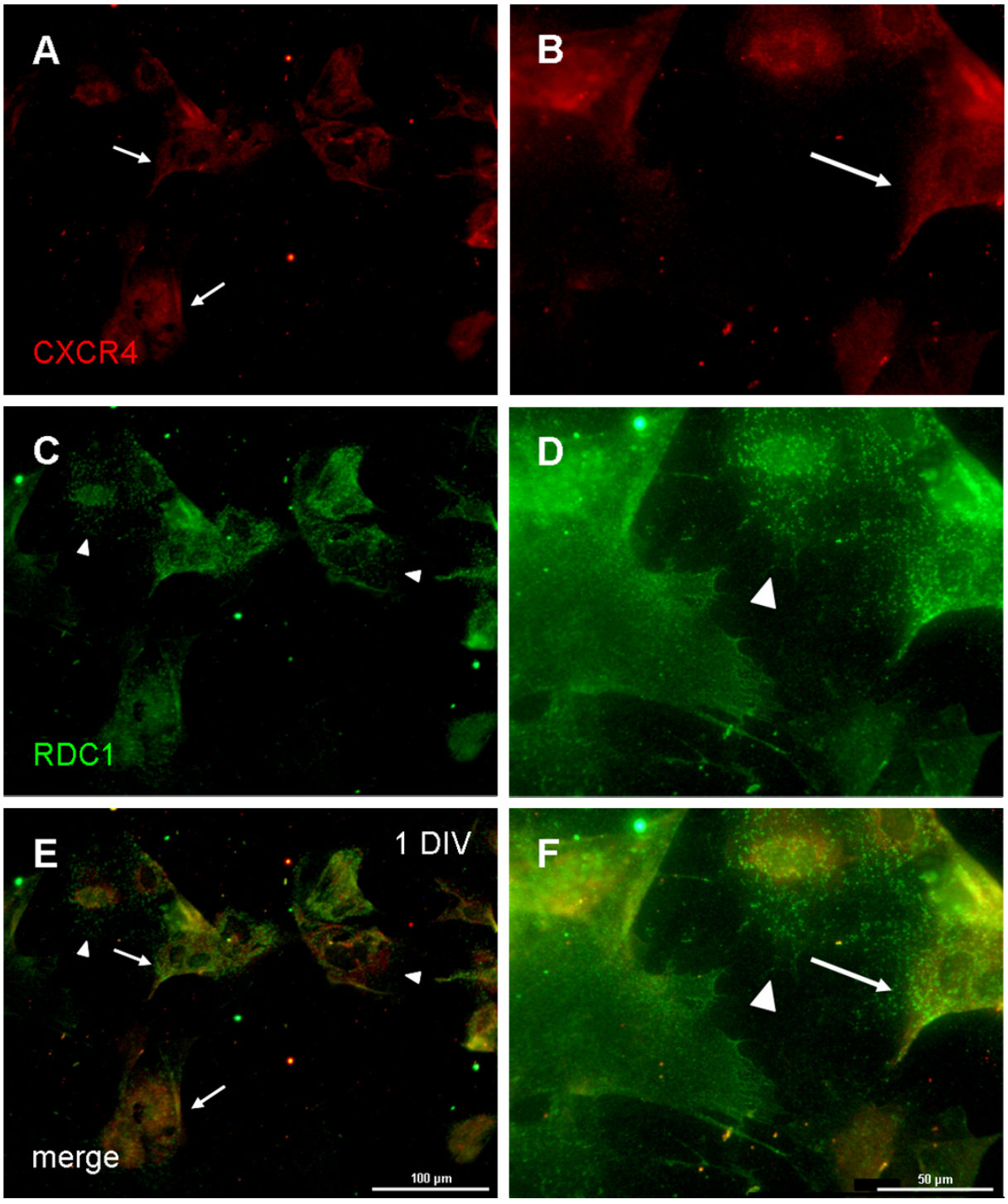

Fig. 4.19. CXCR4 and RDC1 are coexpressed in cultured leptomeningeal fibroblasts. CXCR4 (A,B) and RDC1 (C,D) are weakly to moderately expressed in E15 leptomeningeal fibroblasts and are colocalized (E,F) after 1 DIV. CXCR4-immunoreactivity is weakly and evenly expressed (arrows) at early time points of cultivation. Unlike CXCR4, RDC1 displays a granular distribution (arrowheads) after 1 DIV. Pictures chosen for presentation are representative of two (A-F) independent experiments (n = 2).

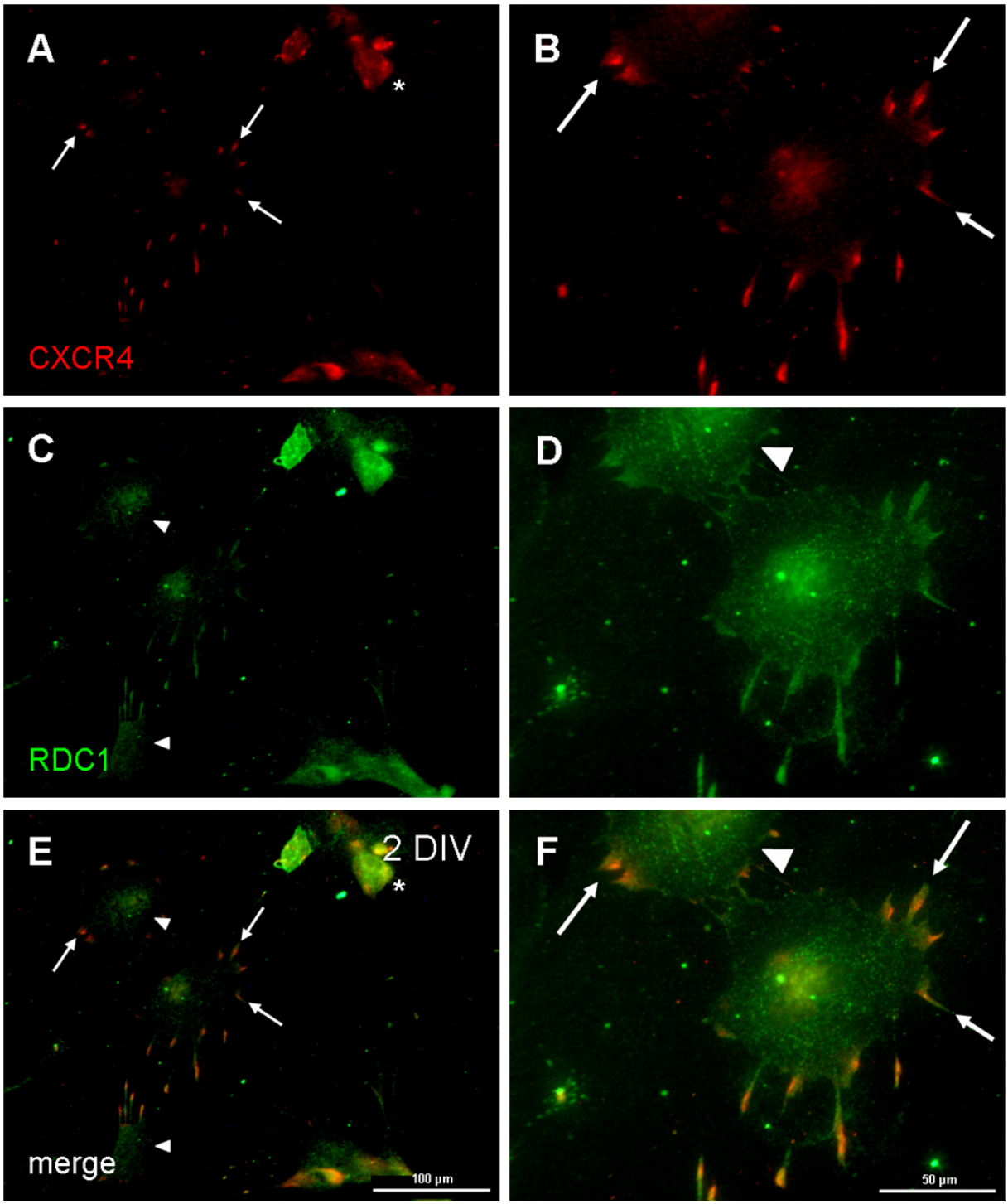

Fig. 4.20. (I, see also next page)

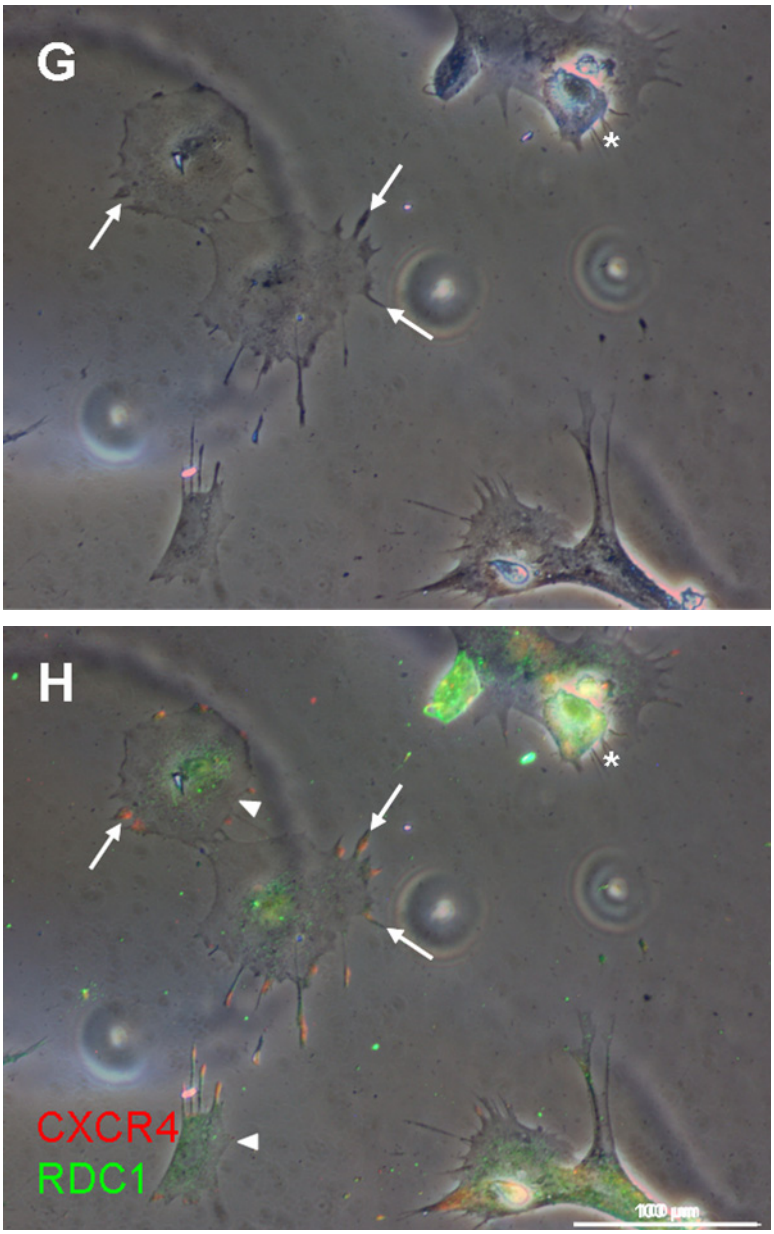

(II, see also previous page)

Fig. 4.20. CXCR4 and RDC1 display characteristic patterning in leptomeningeal fibroblasts. After 2 DIV, CXCR4-immunoreactivity mainly displays a region-specific patterning (arrows), but rarely an even distribution (asterisks) on meningeal fibroblasts (A,B,H). RDC1 (C,D,H) is coexpressed with CXCR4 (E,F,H) after 2 DIV *in vitro*. CXCR4-immunoreactivity is preferentially localized to peripheral regions and areas and filopodia-like structures (G,H) after 2 DIV. RDC1-immunoreactivity is moderate in peripheral regions (arrowheads), but prominent in central regions, of fibroblasts. Pictures chosen for presentation are representative of two (A-H) independent experiments (n = 2).

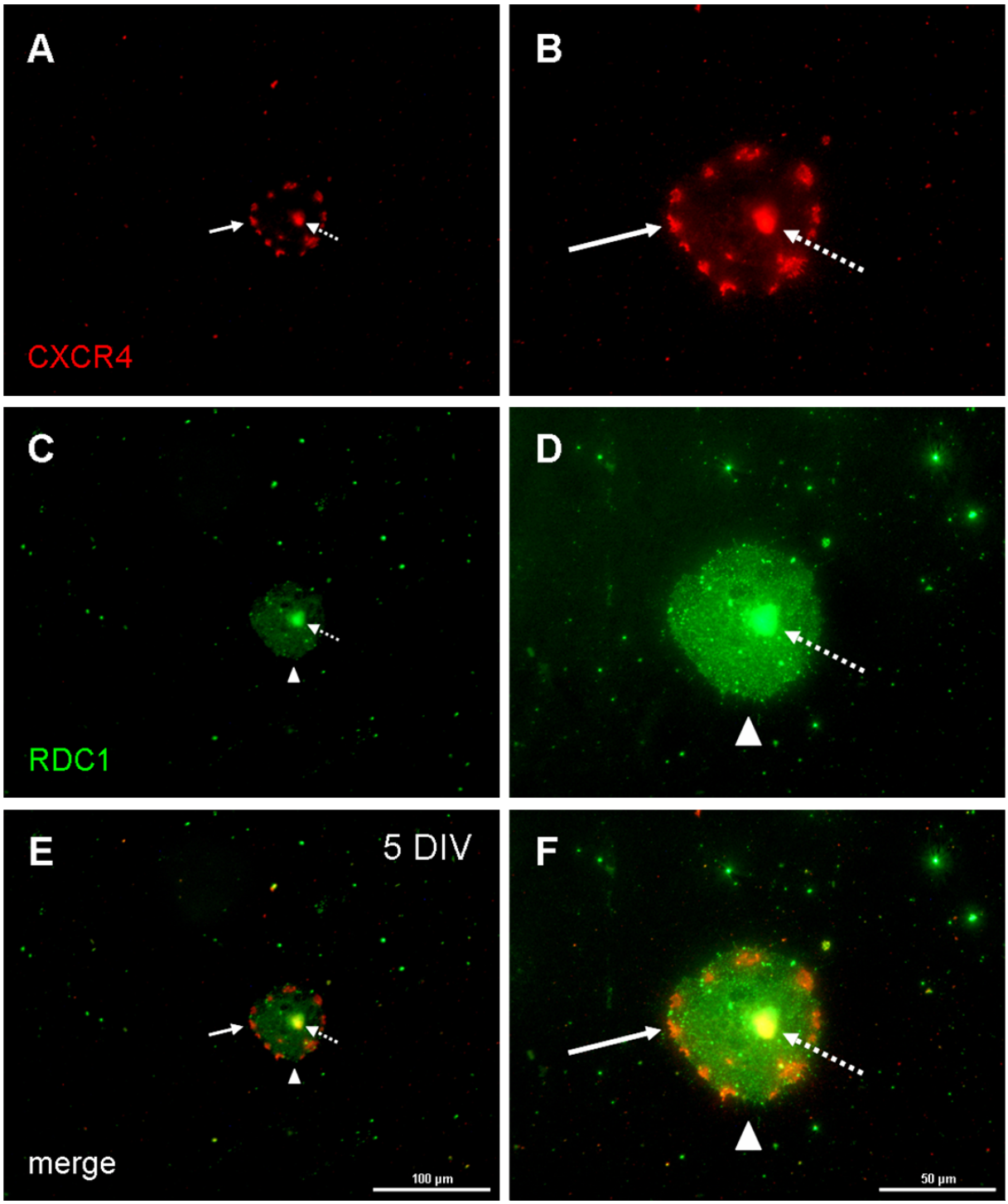

Fig. 4.21. Receptor patterning in meningeal fibroblasts remains stable at late stages of cultivation. Region-specific localization of CXCR4-immunoreactivity (A,B, arrows) is unaltered after 5 DIV. RDC1 (C,D) is moderately to prominently expressed (arrowheads) in fibroblasts after 5 DIV. CXCR4 and RDC1 are coexpressed (E,F) in meningeal fibroblasts at late stages of cultivation. Prominent localization of both receptors in central regions of cells (dashed arrows) likely represents an artefact after long-term *in vitro* incubation. Pictures chosen for presentation are representative of two (A-F) independent experiments (n = 2).

4.3.5 HeLa cells

CXCR4 and RDC1 were coexpressed in HeLa cells at 1 DIV as well as 5 DIV (Fig. 4.19,E,F, Fig. 4.20,E,F). CXCR4-immunoreactivity was predominantly localized to the central regions of cells (arrows) at early stages of cultivation (Fig. 4.19,A,B). After 5 DIV, this receptor was evenly distributed in Hela cells and was prominent in the periphery of cells (arrows), where it was mapped to the cell periphery, cellular protrusions and filopodia-like formations (Fig. 4.20,A,B). RDC1-immunoreactivity was evenly or granularly (arrowheads) distributed in HeLa cells after 1 DIV (Fig. 4.19,C,D). Similar to CXCR4, RDC1 was prominent in central regions of cells at early stages of *in vitro* incubation (Fig. 4.19,A-F). After 5 DIV, RDC1-immunoreactivity was mainly mapped to central regions of HeLa cells (arrowheads), but was weak in the cell periphery (Fig. 4.20,C,D).

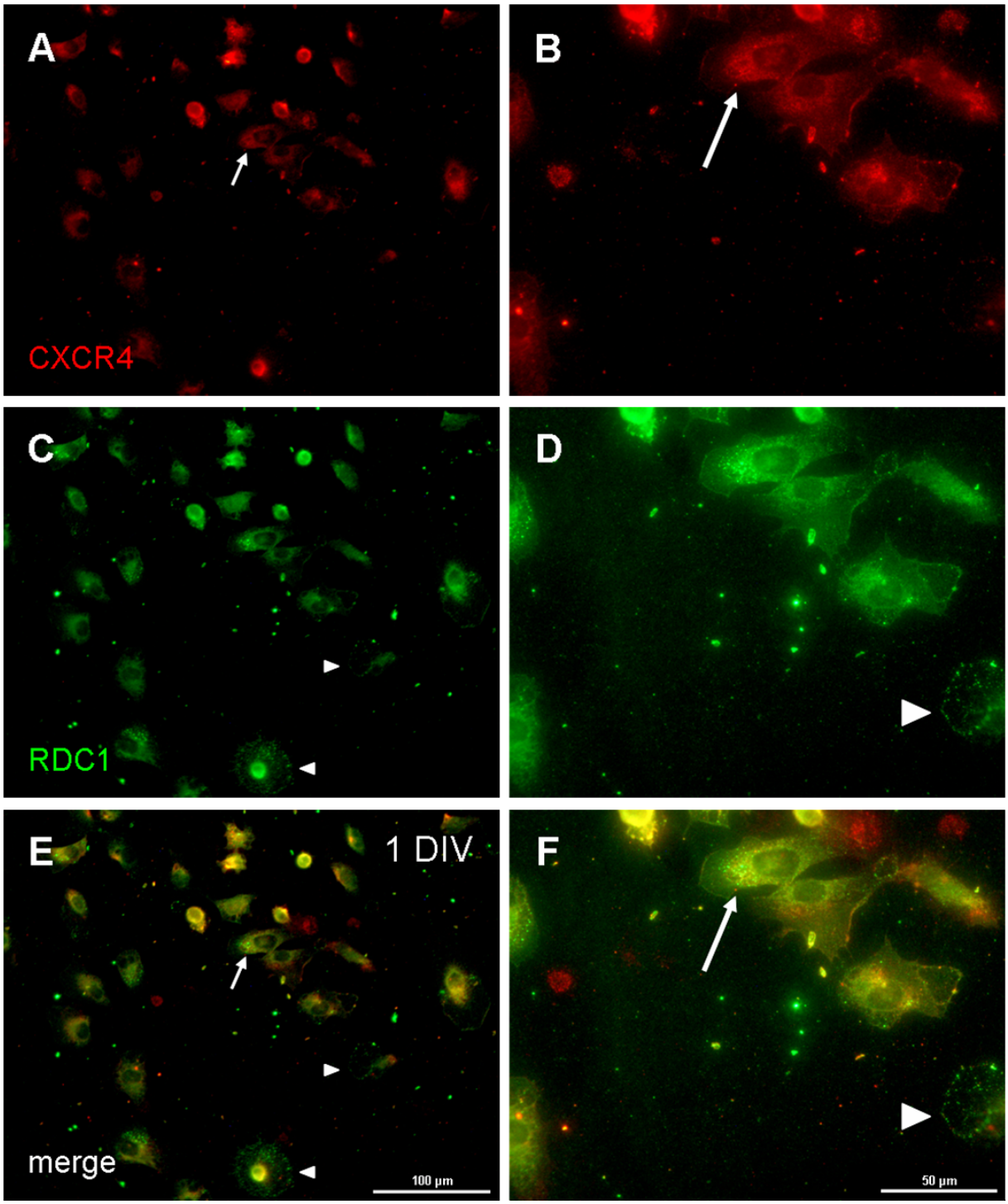

Fig. 4.22. CXCR4 and RDC1 are coexpressed in HeLa cells (I). CXCR4-immunoreactivity (A,B) is predominantly localized to central regions of HeLa cells (arrows) after 1 DIV (A,B). RDC1-immunoreactivity (C,D) displays an even or granular (arrowheads) distribution in the cell periphery and is colocalized with CXCR4 (E,F) in central regions of cells at early stages of cultivation. Pictures chosen for presentation are representative of two (A-F) independent experiments (n = 2).

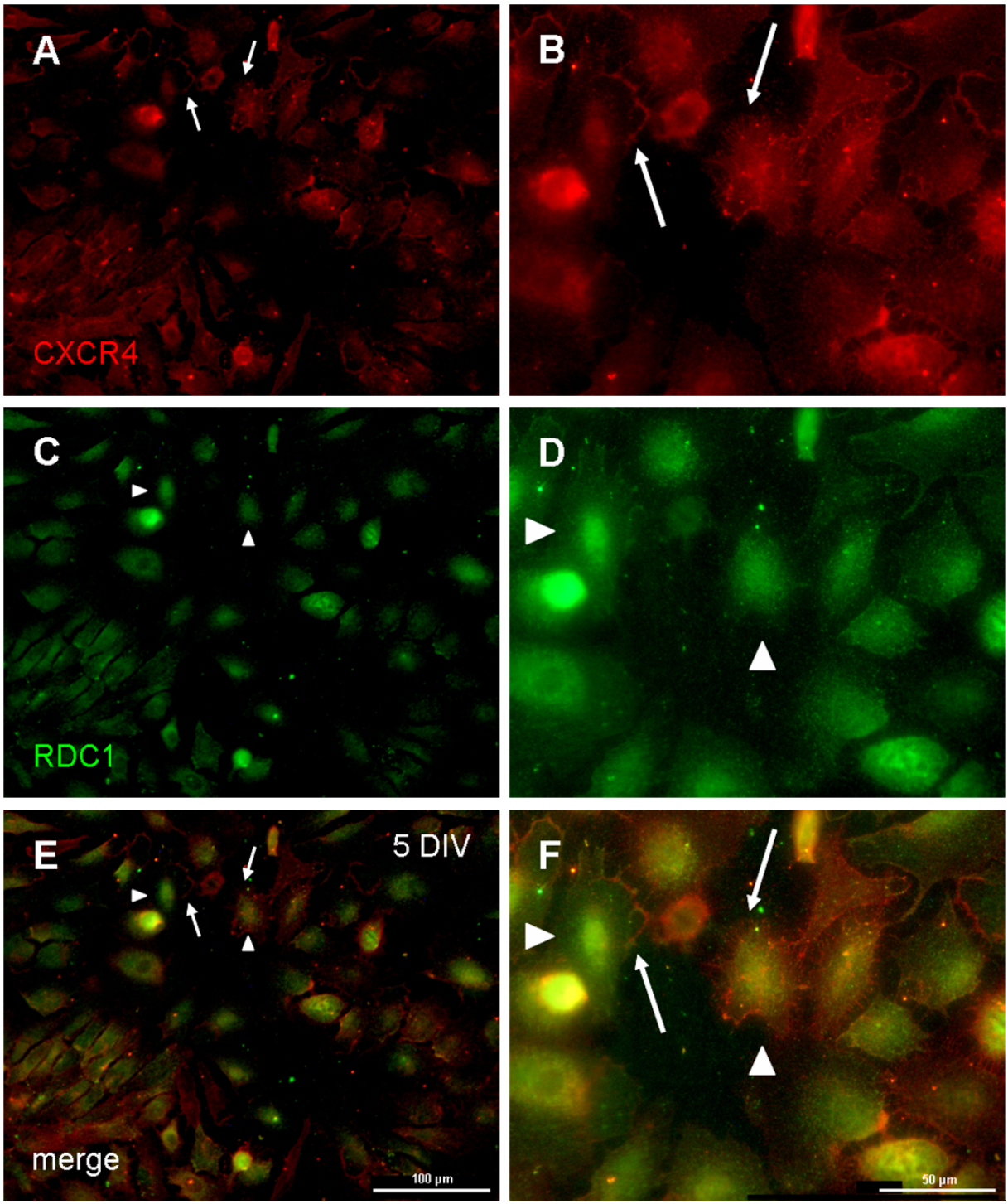

Fig. 4.23. CXCR4 and RDC1 are coexpressed in HeLa cells (II). CXCR4-immunoreactivity (A,B) is evenly distributed in HeLa cells after 5 DIV or is localized to the cell periphery and filopodia (arrows). RDC1 (C,D) is expressed in HeLa cells after 5 DIV (arrowheads). While both CXCR4 and RDC1 are colocalized (E,F) in central regions of cells at late stages of cultivation, RDC1-immunoreactivity is only weakly present in the cell periphery. Pictures chosen for presentation are representative of two (A-F) independent experiments (n = 2).

4.4 SDF-1 is expressed in Schwann cells and neurons of P6 DRGs *in vitro*

To assess whether SDF-1 is expressed by cultured cells used for both the neurite outgrowth assay and the assay for detection of CREB phosphorylation and translocation into nuclei, dissociated P6 DRGs were stained for all known isoforms of this chemokine using an antibody directed against the common N-terminal domain (Fig 4.24). It was found that SDF-1 was abundantly expressed in the Schwann cell fraction of DRGs, where it was prominent in cell bodies (arrowheads) as well as in cellular processes (arrows) after 24 h *in vitro*. Conversely, expression of SDF-1 was only weak in the neuronal fraction of dissociated P6 DRGs. In neurons, SDF-1 expression was mainly limited to cell bodies (asterisks) and was not detected in neurites after 24 h *in vitro*.

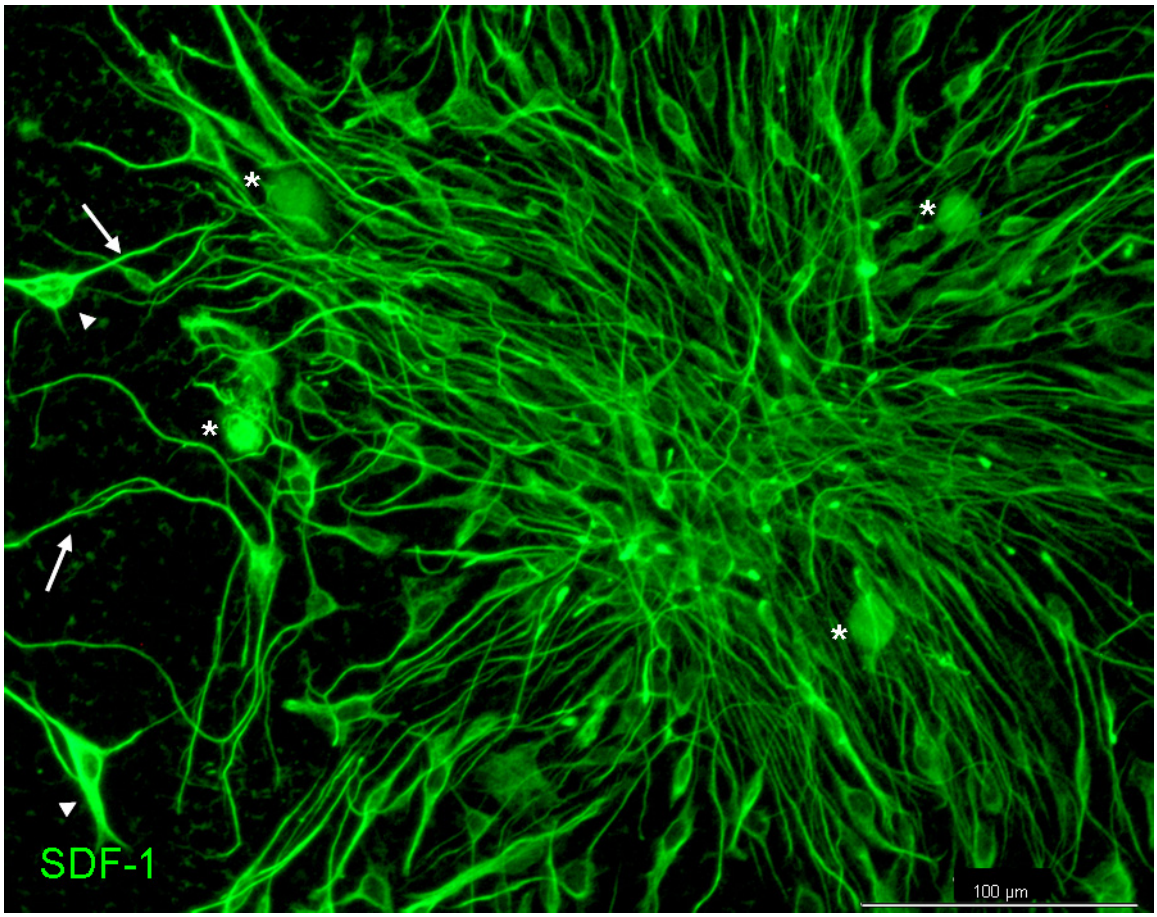

Fig. 4.24. SDF-1 is expressed in dissociated P6 DRGs. In the Schwann cell fraction of dissociated P6 DRGs, cellular processes (arrows) and cell bodies (arrowheads) display prominent expression of SDF-1 after 24 h *in vitro*. Conversely, SDF-1 is only weakly present in cell bodies of neurons (asterisks).

4.5 CXCR4 on the surface of DRG neurons is internalized following application of SDF-1α

To assess a functional interaction of SDF-1α with both CXCR4 and RDC1, P6 DRG neurons were stained for either receptor without pretreatment or following SDF-1α-treatment at a concentration of 100 ng/ml or 200 ng/ml, respectively, for 2 h *in vitro*. Receptor internalization indicating the interaction of SDF-1α with CXCR4 or RDC1 was analyzed by fluorescence microscopy (Fig. 4.25,A-L). CXCR4-immunoreactivity was prominent on cell bodies and neurites of untreated DRG neurons after 24 h *in vitro* (Fig. 4.25,A,D), while RDC1 was prominent on cell bodies, but was only moderately expressed on neurites (Fig. 4.25,B,D). Both CXCR4 and RDC1 were coexpressed in P6 DRG neurons after 24 h *in vitro* (Fig. 4.25,C,D). Following treatment with high doses (200 ng/ml) of SDF-1α, CXCR4-immunoreactivity was markedly downregulated on neurites, whereas on cell bodies no or only weak downregulation was observed (Fig. 4.25,I,K,L). Expression and distribution of RDC1 displayed no alterations following application of SDF-1α (Fig. 4.25,J,K,L). Treatment with low doses of this chemokine had no effect on both CXCR4- and RDC1-immunoreactivity in P6 DRG neurons (Fig. 4.25,E-H).

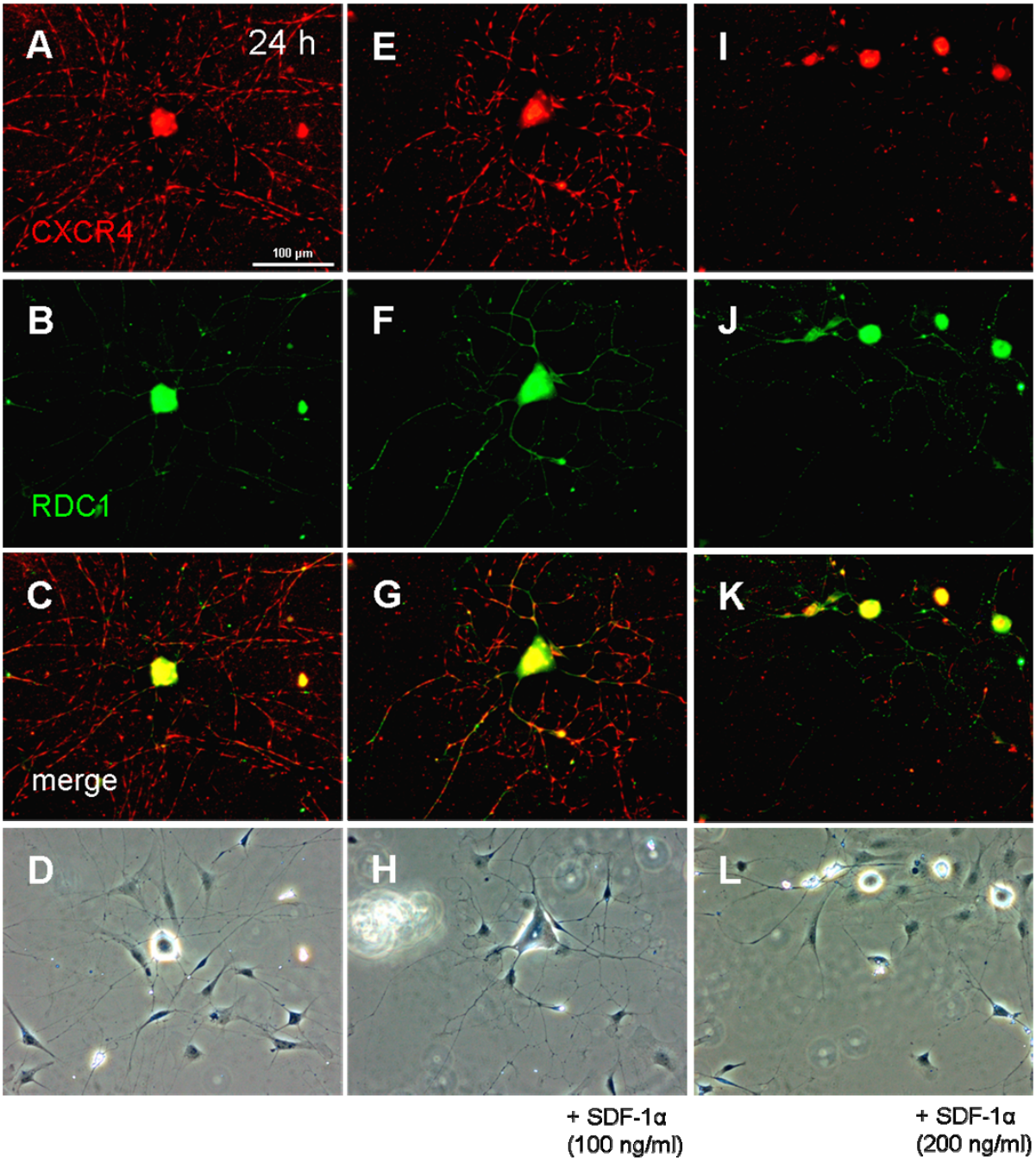

Fig. 4.25. CXCR4 is internalized following application of SDF-1α. CXCR4 (A) and RDC1 (B) are coexpressed on neurites and cell bodies (C,D) of P6 DRG neurons after 24 h *in vitro*. Treatment of cells with low doses of SDF-1α for 2 h does not effect the presentation of both CXCR4 and RDC1 on the surface of DRG neurons (E-H). CXCR4-immunoreactivity on neurites, but not cell bodies, is downregulated following application of high doses of SDF-1α (I,K,L). Treatment with this chemokine at high concentrations does not effect the presentation of RDC1 on both neurites and cell bodies of DRG neurons *in vitro* (J,K,L).

4.6 Elevation of intracellular Ca^{2+} following application of different SDF-1 isoforms

Elevation of intracellular Ca^{2+} levels is a key event of SDF-1-mediated signalling. It is triggered by interaction of the N-terminus of this chemokine with its cognate receptor, CXCR4, in a PTX sensitive, G_i protein-dependent manner. Thus, the ability to elicit physiological Ca^{2+} responses in CXCR4 expressing cells is a measuring unit of functionality of SDF-1 variants sharing a common N-terminal domain. To test for Ca^{2+} elevating properties of custom-designed rat SDF-1γ, this isoform was applied to CXCR4 overexpressing HeLa cells in an assay which monitored changes in free cytosolic Ca^{2+}. SDF-1γ-mediated responses were calculated and compared to responses induced by commercially available SDF-1α.

4.6.1 SDF-1 isoforms γ and α mediate elevation of intracellular Ca^{2+} levels

Application of SDF-1γ triggered elevation of intracellular Ca^{2+} levels in CXCR4 overexpressing HeLa cells in a dose-dependent manner at a concentration of 50–300 nM (Fig. 4.26,A, bars 2,5,8,11,B). SDF-1γ mediated Ca^{2+} elevation was significant, compared to application of bath solution alone, at a concentration of 100-300 nM (Fig. 4.26,A, compare bars 4 to 5,7 to 8, 10 to 11,B). Ca^{2+} responses effected by SDF-1γ peaked at 300 nM, at which concentration this isoform activated Ca^{2+} influx in 44.9% of cells and triggered Ca^{2+} influx with a mean amplitude of 0.673 ratio units ($\pm$ 0.129 SEM) shortly after application of this chemokine (Fig. 4.26,B, Fig. 4.27,A, bar 4,B, left graph, Fig. 4.28,A, bar 8). Ca^{2+} influx mediated by SDF-1γ was markedly lower than following application of ATP, at a concentration of 50-200 nM of this isoform (Fig. 4.26,A, compare bars 2 to 3,5 to 6,8 to 9,B). At 300 nM, SDF-1γ mediated responses slightly peaked elevation of intracellular Ca^{2+} levels by ATP with respect to the proportion of cells displaying Ca^{2+} influx (Fig. 4.26,A, compare bars 11 to 12,B). Ca^{2+} responses triggered by SDF-1γ were similar to SDF-1α-mediated effects concerning the general course of trend plots, but differed with respect to both the proportion of cells displaying Ca^{2+} influx as well as the amplitude of the elicited responses, respectively, at a concentration of 50-300 nM of applied chemokine (Fig. 4.26,A-D).

Application of SDF-1α induced significant elevation of intracellular Ca^{2+} levels in CXCR4-overexpressing HeLa cells in a dose-dependent manner similar to SDF-1γ at a concentration of 50-300 nM, compared to application of bath solution alone (Fig. 4.26,C, compare bars 1 to 2,4 to 5,7 to 8,10 to 11,D). Thereby, the proportion of cells displaying Ca^{2+} influx peaked at 100 nM with 68.2% of responsive cells (Fig. 4.27,A, bar 6,B, right graph). Conversely, mean amplitudes of SDF-1α mediated Ca^{2+} responses were highest (1.220 ratio units $\pm$ 0.298 SEM) at a concentration of 200 nM (Fig. 4.28,A, bar 14,C). Compared to application of SDF-1α, elevation of intracellular Ca^{2+} levels triggered by SDF-1γ was markedly reduced at lower concentrations of chemokine (Fig. 4.26,A-D, Fig. 4.27,A, Fig. 4.28,C). Ca^{2+} responses following application of higher concentrations of chemokine were similar for both isoforms. At a concentration of 300 nM, the proportion of Ca^{2+} responsive cells, but not the mean amplitude, was higher following application of SDF-1γ, compared to SDF-1α mediated Ca^{2+} increase (Fig. 4.27,A, compare bar 4 to 8, Fig. 4.28,A, compare bar 8 to 16).

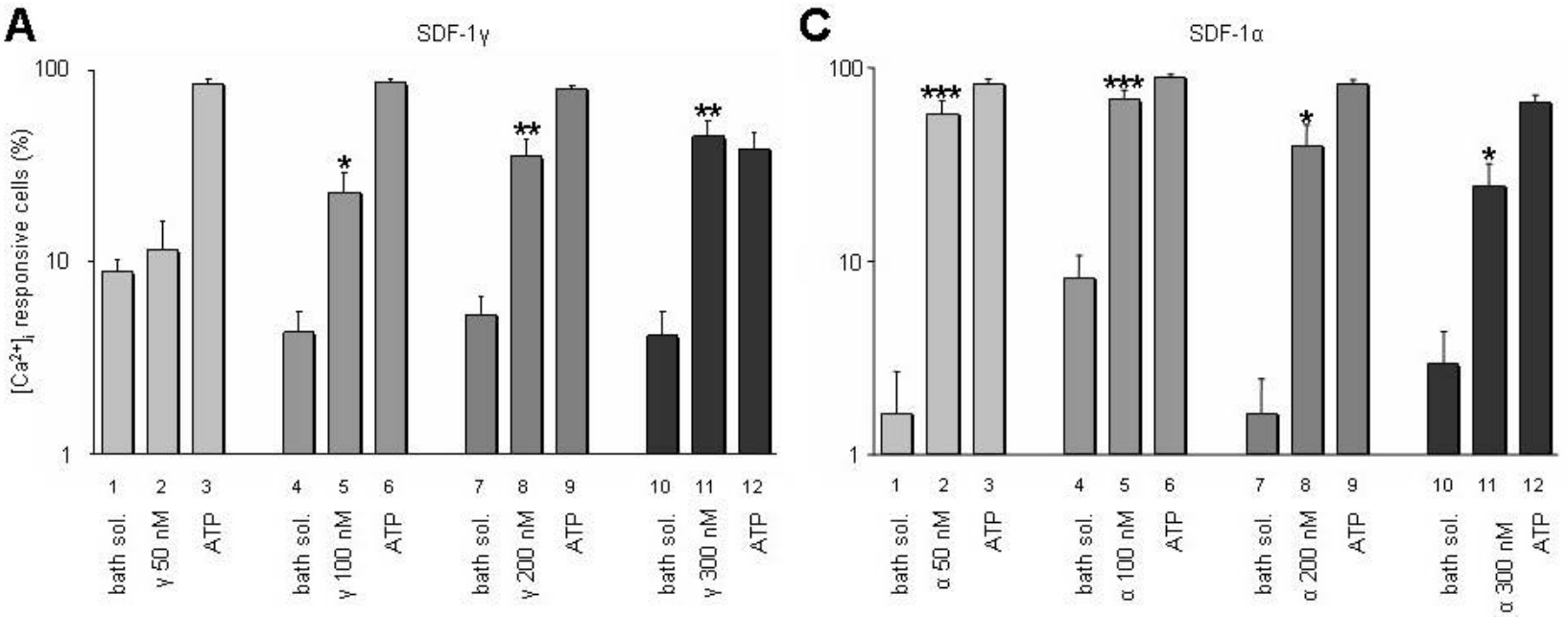

B

$[Ca^{2+}]_i$ responsive cells (%)	chemokine concentration SDF-1γ			
	50 nM	100 nM	200 nM	300 nM
bath solution	8.9	4.8	5.3	4.2
SDF-1γ	11.5	23.1	35.6	44.9
ATP	85.4	85.8	79.6	39.0
p-value	0.69281	0.015798	0.00142	0.00314

D

$[Ca^{2+}]_i$ responsive cells (%)	chemokine concentration SDF-1α			
	50 nM	100 nM	200 nM	300 nM
bath solution	1.6	8.2	1.6	2.9
SDF-1α	57.7	68.2	39.8	24.5
ATP	82.7	89.3	83.0	66.1
p-value	0.00005	0.0000	0.02432	0.03509

Fig. 4.26. (see also next page)

(see also previous page)

Fig. 4.26. SDF-1 isoforms elicit elevation of intracellular Ca^{2+} levels (I). Application of SDF-1γ triggers elevation of intracellular Ca^{2+} levels (A, bars 2,5,8,11, B) in CXCR4 overexpressing HeLa cells in a dose-dependent manner. SDF-1γ-induced Ca^{2+} influx is significant at higher concentrations of this isoform, compared to application of bath solution alone (A, bars 1,4,7,10, B). Following application of SDF-1α (C, bars 2,5,8,11, D,) a significant increase in intracellular Ca^{2+} levels is observed as compared to control conditions (C, 1,4,7,10, D). SDF-1 isoforms display concentration-dependent differences in their capacity to elevate intracellular Ca^{2+} levels (A-D). As a control, intracellular Ca^{2+} levels were upregulated following stimulation with ATP (A, bars 3,6,9,12, B, bars 3,6,9,12, C,D). Results (mean ± SEM) are from at least ten (A-D) independent experiments ($n \geq 10$) and are expressed as percentage of HeLa cells displaying elevation of intracellular Ca^{2+} levels following application of either isoform of SDF-1. Values are normalized for percentage of responsive cells following application of bath solution. *$p<0.05$, **$p<0.01$, ***$p<0.001$ (student´s t-test), compared to control cells.

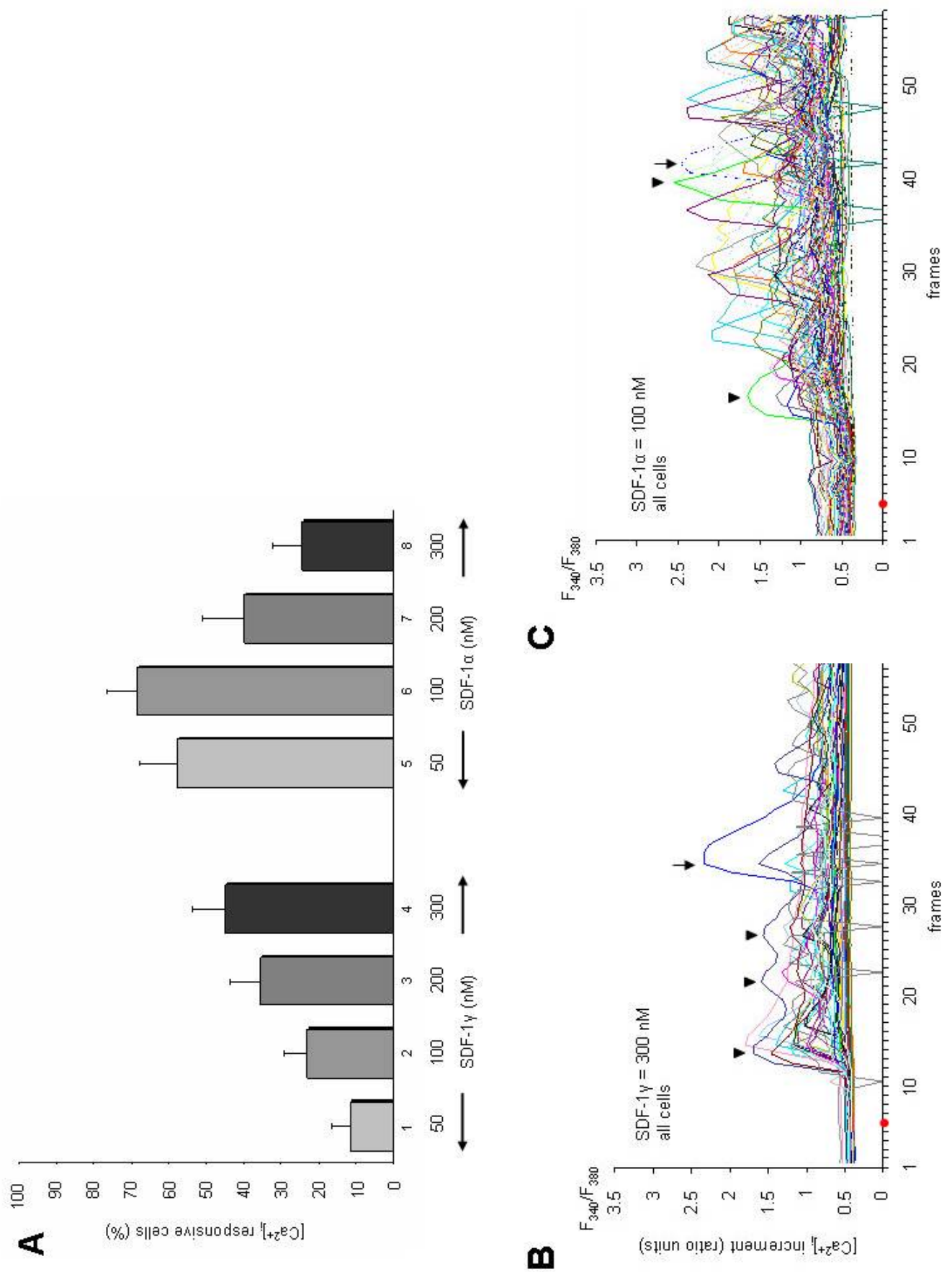

Fig. 4.27. (see also next page)

(see also previous page)

Fig. 4.27. SDF-1 mediated Ca^{2+} responses differ in an isoform-specific manner. The proportion of cells displaying Ca^{2+} influx following application of SDF-1γ (A, bars 1-3, B) is markedly reduced, compared to SDF-1α (A, bars 5-7, C), at low concentrations of this chemokine. Conversely, SDF-1γ elicits Ca^{2+} increase in a larger proportion of cells at high concentrations of applied chemokine, if compared to SDF-1α (A, bars 4,8, B). Ca^{2+} responses elicited by either isoform can be grouped in two categories and are characterized as oscillatory elevation or singular event, respectively (B,C). The time point of application is marked in red. Peaks of oscillatory responses are marked by arrowheads. Peaks of singular events are marked by arrows.

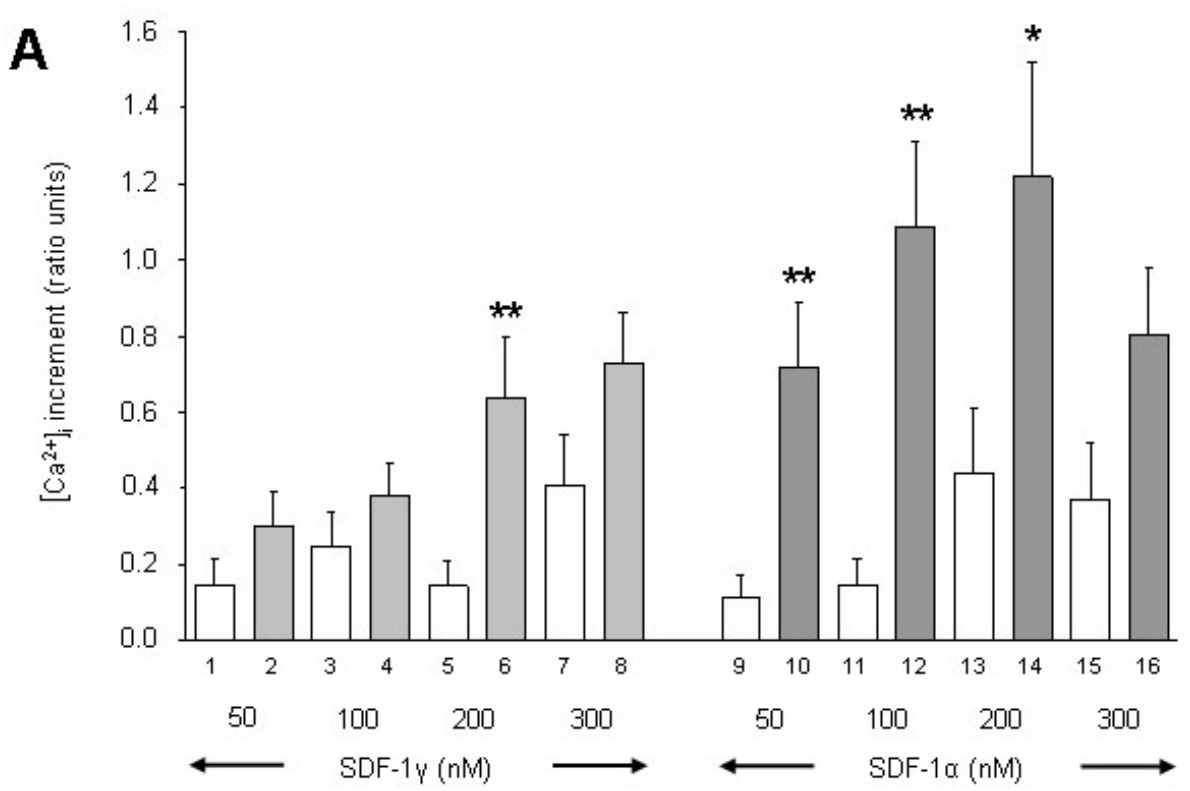

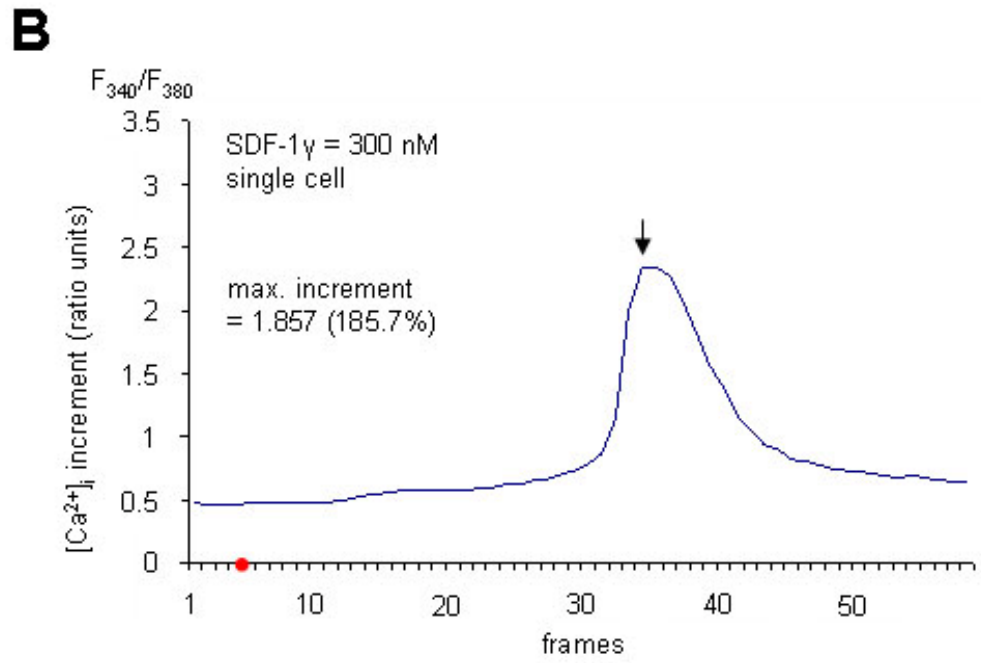

Fig. 4.28. (see also next page).

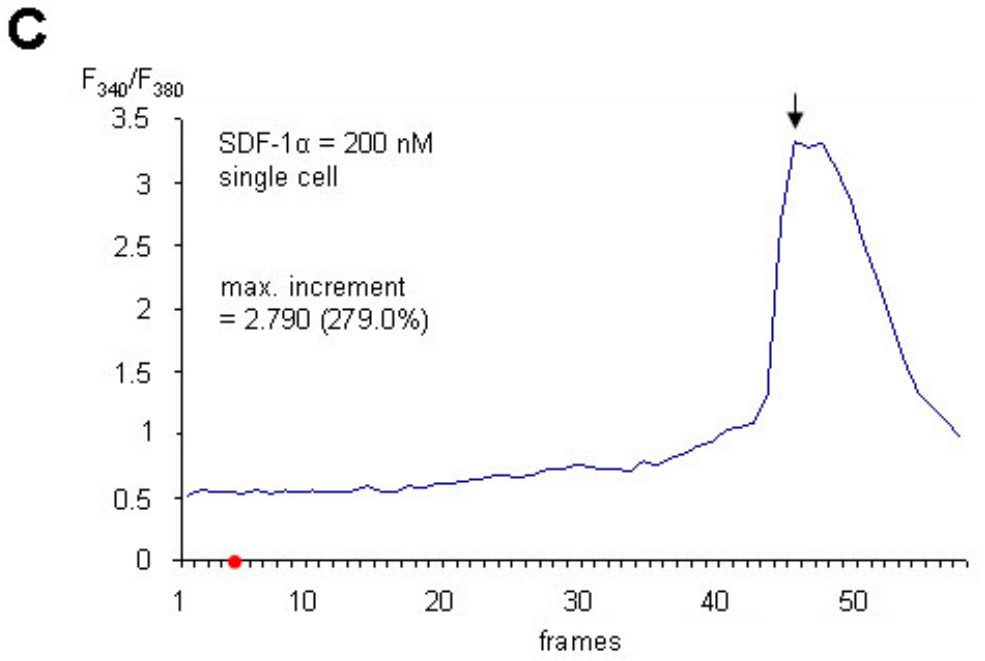

(see also previous page)

Fig. 4.28. SDF-1 isoforms elicit elevation of intracellular Ca^{2+} levels (II). Ca^{2+} influx elicited by SDF-1γ is strictly dose-dependent and is partially significant, compared to application of bath solution alone (A, bars 1-8). Mean amplitudes of SDF-1γ mediated Ca^{2+} influx are highest at 300 nM (A,B). Ca^{2+} responses mediated by application of SDF-1α are dose-dependent and are significant, compared to control conditions (A, bars 9-16). Mean amplitudes of SDF-1α mediated Ca^{2+} influx are highest at 200 nM (A,C). SDF-1 mediated Ca^{2+} responses differ in an isoform specific manner (A). The time point of application is marked in red. Peaks of singular events are indicated by arrows. Results (mean ± SEM) are from at least ten (A) independent experiments (n ≥ 10) and are expressed as percentage of HeLa cells displaying elevation of intracellular Ca^{2+} levels following application of either isoform of SDF-1. Values are normalized for percentage of responsive cells following application of bath solution. *p<0.05, **p<0.01, ***p<0.001 (student´s t-test), compared to control cells. Graphs of single cell Ca^{2+} responses chosen for presentation are representative of at least ten (B,C) independent experiments (n ≥ 10).

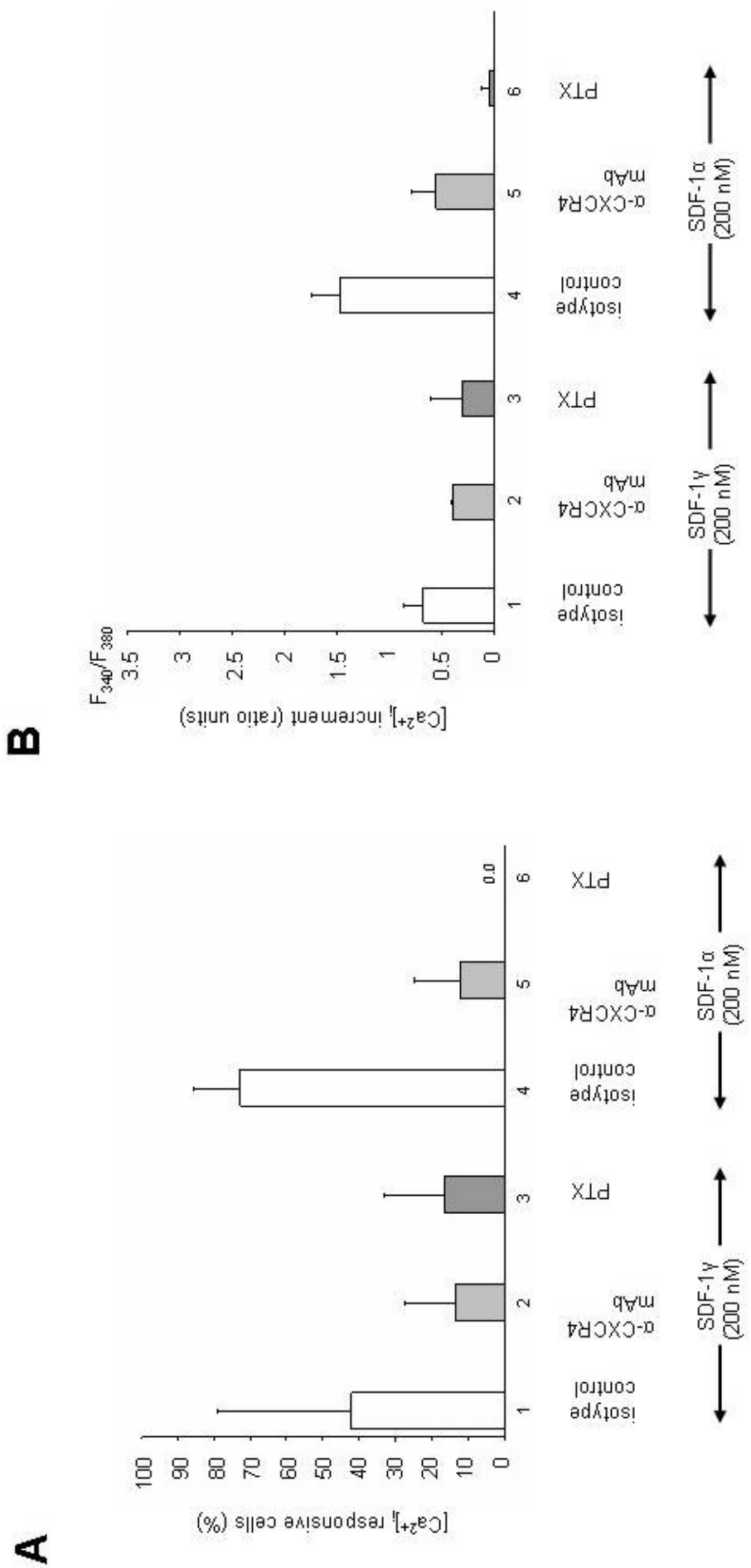

Fig. 4.29. (see also next page)

(see also previous page)

Fig. 4.29. SDF-1 mediated elevation of intracellular Ca^{2+} levels is abrogated by specific inhibitors to CXCR4 and G_i proteins (I). The number of Ca^{2+} responsive cells (A) as well as the mean amplitude of Ca^{2+} responses (B) following application of either SDF-1 isoform is decreased by preincubation with anti-CXCR4 antibody 12G5 clone (bars 2,5) or PTX (bars 3,6), compared to isotype control antibody treated cells (bars 1,4). Results (mean ± SEM) are from two (A,B) independent experiments (n = 2) and are expressed as percentage of HeLa cells displaying elevation of intracellular Ca^{2+} levels following application of either isoform of SDF-1. Values are normalized for percentage of responsive cells following application of bath solution (data not shown).

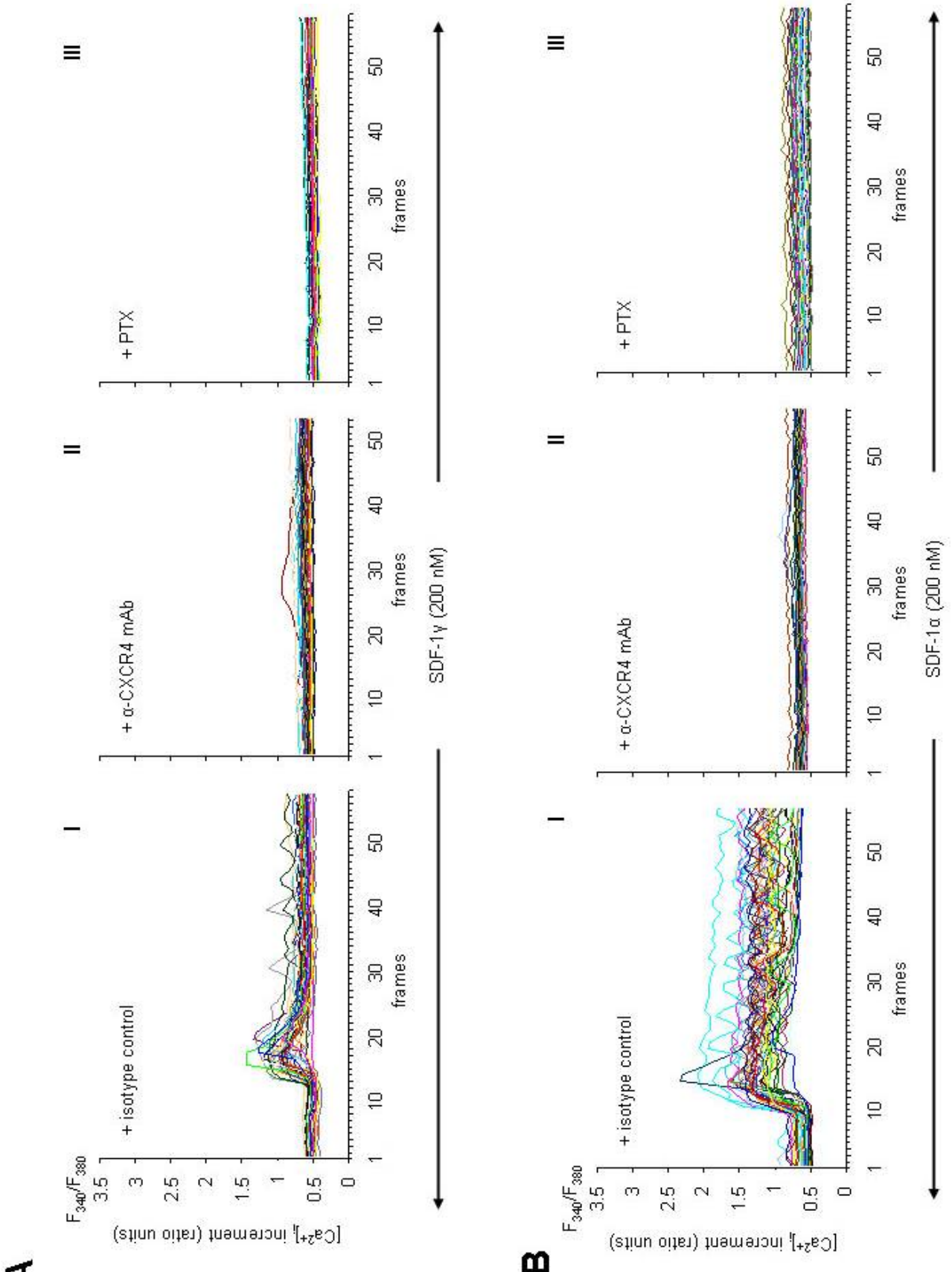

Fig. 4.30. (see also next page)

(see also previous page)

Fig. 4. 30. SDF-1 mediated elevation of intracellular Ca^{2+} levels is abrogated by specific inhibitors to CXCR4 and G_i proteins (II). The number of Ca^{2+} responsive cells as well as the mean amplitude of Ca^{2+} responses following application of either SDF-1γ (A) or SDF-1α (B) are decreased by preincubation with anti-CXCR4 antibody 12G5 clone (A II, B II) or PTX (A III, B III), compared to isotype control antibody treated cells (A I, B I). Ca^{2+} responses are abrogated by inhibitors in an isoform-specific manner (A,B). Graphs of single experiment Ca^{2+} responses chosen for presentation are representative of two (A,B) independent experiments (n = 2).

4.6.2 SDF-1-mediated upregulation of intracellular Ca^{2+} is CXCR4-/G protein-dependent

Elevation of intracellular Ca^{2+} levels triggered by either SDF-1 isoform at a concentration of 200 nM was significantly decreased by pretreatment of cells with anti-CXCR4 antibody 12G5 clone or PTX, respectively, compared to cells following preincubation with isotype control antibody (Fig. 4.29, Fig. 4.30). Pretreatment with anti-CXCR4 antibody prior to application of chemokine resulted in a decreased proportion of cells displaying Ca^{2+} influx of 13.6% for SDF-1γ and 12.5% for SDF-1α as well as correspondingly decreased mean amplitudes of SDF-1 mediated Ca^{2+} responses of 0.397 ratio units (± 0.018 SEM) for SDF-1γ and 0.562 ratio units (± 0.220 SEM) for SDF-1α, respectively, compared to control conditions (Fig. 4.29,A, compare bars 1 to 2,4 to 5,B, compare bars 1 to 2,4 to 5, Fig. 4.30,A, compare I to II,B, compare I to II). As SDF-1α-mediated elevation of intracellular Ca^{2+} levels demonstratedly is dependent on G_i protein-activation, G_i protein-dependency of Ca^{2+} influx induced by application of SDF-1γ was tested. Pretreatment of cells with PTX prior to application of SDF-1γ led to an almost complete abrogation of Ca^{2+} response, similar to SDF-1α control cells (Fig. 4.29, A,B). The proportion of PTX treated cells displaying Ca^{2+} influx following application of chemokine was limited to 16.7% for SDF-1γ and 12.5% for SDF-1α, compared to isotype control-treated cells (Fig. 4.29,A, compare bars 1 to 3,4 to 6). Mean amplitudes of Ca^{2+} responses were markedly reduced to 0.306 ratio units (± 0.306 SEM) for SDF-1γ and 0.061 ratio units (± 0.061 SEM) for SDF-1α, respectively, as compared to isotype control conditions

(Fig. 4.29,B, compare bars 1 to 3,4 to 6, Fig. 4.30,A, compare I to III,B, compare I to III).

4.6.3 Ca^{2+} responses following application of SDF-1 are variable

Following application of either SDF-1γ or SDF-1α, two different types of Ca^{2+}-response were observed. Occurrence of either form of Ca^{2+}-response was not related to the SDF-1 isoform or the concentration applied (Fig. 4.27,B). Stimulation with SDF-1 resulted in either an oscillatory elevation of intracellular Ca^{2+} levels (arrowheads) or a singular event (arrows). While latter was characterized by rapid Ca^{2+} influx followed by a return to base levels, the oscillatory response repeatedly displayed a sustained increase and decrease of intracellular Ca^{2+} levels over the whole recording time.

5 Discussion

5.1 SDF-1 as a putative therapeutic target

Generally, the actions of the majority of chemokines are limited to the immune and hematopoietic system, and most members of this group are upregulated in the diseased state (Horuk, 1996; Murdoch and Finn, 2000; Murphy et al., 2000; Zlotnik and Yoshie, 2000). Conversely, the α-chemokine SDF-1 is constitutively and ubiquitously expressed (Yu et al., 2006). Through interaction with CXCR4, and probably also a novel receptor, RDC1, SDF-1 signals a multitude of highly diverse functions (Lazarini et al., 2003; Kucia et al., 2004; Balabanian et al., 2005). Studies on SDF-1- and CXCR4-deficient animals revealed that this chemokine acts as a key regulator of embryonic development (Ma et al., 1998; Tachibana et al., 1998; Zuo et al., 1998; .Lu et al., 2002; Vilz et al., 2005). Moreover, SDF-1 was recently identified to mediate important functions in the physiology and pathophysiology of the nervous system, where it was characterized in a dual role in neuronal apoptosis and survival as well as growth promotion and inhibition (Kaul and Lipton, 1999; Khan et al., 2004; Khan et al., 2005; Chalasani et al., 2003; Pujol et al., 2004). Apart from a supposable role in immune system pathology, the SDF-1/CXCR4 axis gained notice as a putative therapeutic target when SDF-1 was characterized to act as a molecular beacon in the chemotaxis of $CXCR4^+$ tumour cells (Geminder et al., 2001; Muller et al., 2001; Burger et al., 2006). The notion that SDF-1 exists in various C-terminally different isoforms raised the question whether these structural variations contribute to the functional diversity of this chemokine (Gleichmann et al., 2000; Yu et al., 2006). While known biological facets of SDF-1 could experimentally be attributed to the common N-terminal domain of the different transcripts, isoform-specific functions have yet to be determined.

5.1.1 Objective targets of SDF-1 analysis in this study

Several aspects have been investigated in this thesis. First, a possible role of SDF-1 and CXCR4 in adult mammalian CNS regeneration was analyzed. While functions for both ligand and receptor have been characterized in the embryonic nervous system, still little is known about possible implications in the adult CNS and PNS. Recently, SDF-1 was described to abrogate neurite outgrowth inhibitory effects of various chemorepellent molecules with a role in early nervous system development (Chalasani et al., 2003; Chalasani et al., 2007). Conversely, a role of this chemokine in the complex inhibitory environment of adult CNS myelin has not been identified to date. In this study, SDF-1 for the first time was demonstrated to mediate overcoming of myelin-induced outgrowth inhibition of P6 DRG neurons. Thus, findings presented here confirm and exceed recent reports on a growth promoting function in the nervous system. Moreover, an approach was undertaken to elucidate signalling events which are involved in SDF-1-mediated neurite outgrowth promotion. As SDF-1 was demonstrated to bind to and signal through both CXCR4 and RDC1, expression and distribution of these receptors was determined in myelin-sensitive DRG neurons as well as in various primary cells and cell lines. In a second part, the SDF-1 splice variant most recently characterized in rat, SDF-1γ, was compared to SDF-1α in its capacity to elevate cytosolic Ca^{2+}. While latter isoform has been extensively studied, SDF-1γ has not been functionally analyzed to date.

5.1.2 Nervous system regeneration as a possible field of application for SDF-1α

Facing the high annual numbers of patients suffering SCI, it has become a major goal of neurobiological research to overcome the impairment of the adult mammalian CNS to efficiently regenerate. As regeneration failure is caused by a vast number of different factors, targeting these factors holds the promise of promoting CNS repair processes and thus restoring sensory and motor skills of the affected individuals. Notably, two different factors have been characterized to conjoinedly constitute a major impediment to adult CNS regeneration, and have been extensively studied as promising targets for therapeutic intervention during the recent years (Filbin, 2003).

Several inhibitory components of CNS myelin have been identified, which are suggestedly either presented to damaged axons on the membrane surface of neighbouring cells or released upon damage of spinal cord white matter (Tang et al., 2001; Filbin, 2003). Recently, a possible mode of action was postulated which linked MAIs to cytoskeletal alterations and axonal growth arrest. According to this model, MAIs interact with a tripartite receptor complex to effect the cleavage of one of its components, $p75^{NTR}$ (Domeniconi et al., 2005). In the following, both kinase LIMK1 (LIM is an acronym of the three gene products Lin-11, Isl-1, and Mec-3) and phosphatase SSH suggestedly interrupt actin cyling through phosphorylation and deactivation of the actin depolymerizing factor cofilin (Hsieh et al., 2006). Approaches to target components of this inhibitory signalling pathway proved to provide important means to promote CNS regeneration (Higuchi et al., 2003; Kastin and Pan, 2005). In animal models of SCI, blocking MAIs by either application of predesigned antibodies or preimmunizing with myelin demonstratedly increased the regeneration efficiency of lesioned postnatal neurons (Thallmair et al., 1998; Huang et al., 1999; Keirstead et al., 1999; Kastin and Pan, 2005). Similar effects were observed if Rho GTPase activity was decreased by specific inhibitors or transfection of dominant negative forms of this protein (Kastin and Pan, 2005). Surprisingly, a deletion of genes coding for various inhibitors did not always effect increased CNS regeneration, as it had been expected (Li et al., 1996; Zheng et al., 2003).

Findings that outgrowth inhibition was restricted to post-embryonic developmental stages of the CNS strongly suggested an age-dependency in tolerance of negative guidance cues. Moreover, neuronal outgrowth capacities could be correlated to the amount of intracellular cAMP, as the developmental downregulation of neuronal cAMP was demonstrated to coincide with an increased sensitivity towards inhibitors (Cai et al., 2001; Spencer and Filbin, 2004). Thus, efforts were undertaken to restore the “embryonic intracellular settings” of adult CNS neurons. Thereby, axonal outgrowth was successfully increased by either direct injection of cAMP into the cell body or by application of adenylate cyclase activators such as forskolin. Neurotrophins were demonstrated to efficiently stimulate neuronal growth due to their cAMP elevating properties, while they could simultaneously counteract myelin-inhibitory proteins by competing for $p75^{NTR}$ as a component of the inhibitory tripartite receptor complex (Bregman et al., 1998; Cai et al., 1999). As the roles of certain effector molecules of cAMP are being slowly unravelled, future studies hold the

promise of a more exact manipulation of growth promoting signalling events (Cai et al., 2002; Mizuno et al., 2004).

5.1.2.1 SDF-1α in overcoming myelin-induced outgrowth inhibition

Molecules with a role in neurite outgrowth promotion are being investigated not only with respect to a possible therapeutic application, but also for their functions in developmental processes. Recently, the α-chemokine SDF-1 was identified to abolish growth cone collapse induced by sema3A, sema3C, slit-2, and robo (Chalasani et al., 2003; Chalasani et al., 2007). Thus, while SDF-1 was identified to abrogate the effect of chemorepellent molecules with a role in early nervous system development, a function in postnatal regeneration could not be demonstrated to date. In this thesis, SDF-1 is for the first time described to successfully abolish neurite outgrowth inhibition which is induced by a complex of diverse myelin components in an *in vitro* model of nervous system repair following injury. Unlike in earlier studies, where SDF-1 effects were demonstrated for only a few selected inhibitors, here experiments were performed on a crude fraction of adult CNS myelin. Furthermore, instead of embryonic cells with a reported capacity to regenerate, postnatal neurons were employed for outgrowth experiments. The model applied in this study thus mimicks more closely the effect of this chemokine in an *in vivo* situation of SCI, where high amounts of myelin debris, including MAIs, are present at the site of injury (Tang et al., 2001; Schwab et al., 2005).

Cells employed in the neurite outgrowth assay in this study were prepared from DRGs of P6 rats. DRG neurons have two processes, one extending into the periphery, and a central axon, which enters the spinal cord at the dorsal root entry zone, DREZ. DRG neurons provide a useful model system to examine nervous system regeneration *in vivo*, as they generally do not die after lesion of either process (Chong et al., 1999; Neumann and Woolf, 1999). Further, as the intrinsic regenerative capacities of both axonal branches differ, both growth promotion and regeneration can simultaneously be observed. While the peripheral process regenerates well, axonal regeneration through the DREZ into the spinal cord is only poor. Conversely, if the peripheral branch is inflicted with a conditioning lesion, CL, prior to an injury of the central axon, latter displays markedly improved outgrowth. Interestingly, DRG neurons were demonstrated to undergo a conversion in their sensitivity towards growth inhibitors sharply at P3/P4, which makes them a useful tool to study age-dependent neuronal outgrowth inhibition *in vivo* or *in vitro*,

respectively (DeBellard et al., 1996; Filbin, 2003). At P6, DRG neurons have already experienced the intrinsic neuronal switch leading to myelin-sensitivity.

5.1.2.2 SDF-1α restores postnatal neuronal outgrowth capacities

While P6 DRG neurons displayed excellent outgrowth on PDL/laminin-coated surfaces, this growth was largely reduced if surfaces were additionally coated with a crude fraction of adult CNS myelin, and the number of neurons growing three or more neurites of at least the cell body diameter was significantly decreased in presence of myelin after 24 h *in vitro* (Fig. 4.1; Fig. 4.2). However, this effect was not due to a reduced adherence on myelin, as a comparison of total cell numbers revealed that latter were even slightly elevated on myelin-coated surfaces, compared to laminin controls. Furthermore, the overall neuronal outgrowth performance was markedly impaired in presence of CNS myelin. On myelin, processes showed enhanced fasciculation and a limited tendency to form branches, compared to a regular pattern of neurites on laminin alone after 24 h *in vitro*. Myelin-induced outgrowth inhibition was markedly diminished by application of SDF-1α to cultured DRG neurons after 24 h *in vitro*. Observations on SDF-1α-mediated effects as presented here are in accordance with recent findings by Chalasani and colleagues (2003, 2007), where treatment of embryonic neurons with SDF-1 reduced axonal responsiveness to potent chemorepellents such as sema3A, sema3C, slit-2, and robo. In latter studies, application of SDF-1 led to both an increase in axonal length and abrogation of growth cone collapse in presence of chemorepellent molecules *in vitro*, while SDF-1 signalling was demonstrated to effect axonal pathfinding *in vivo*.

5.1.2.3 Preincubation with SDF-1α enhances neurite outgrowth promotion

In this thesis, it was found that growth promotion following application of SDF-1α was considerably enhanced when cells were pretreated with this chemokine prior to plating on myelin (Fig. 4.1; Fig. 4.2). After preincubation for 1 h in presence of this chemokine, the number of neurons growing out on myelin-coated slides was significantly increased after additional 23 h *in vitro*, compared to cells cultured without

SDF-1α or without pretreatment. In addition, SDF-1α-treated neurons on myelin generally displayed a markedly improved neurite patterning which was similar to laminin-only controls with respect to both the lengths of the neurites as well as the number of branching events, while fasciculation was largely reduced.
However, pretreatment of myelin-cultivated neurons alone was necessary, but not sufficient, as withdrawal of SDF-1α following pretreatment largely led to an abrogation of the mediated effects. Pretreatment with SDF-1α can thus be considered a priming process which facilitates subsequent outgrowth on myelin-coated surfaces. Interestingly, similar priming effects were observed by Cai and colleagues (1999, 2001; 2002), who noted increased axonal regeneration for cerebellar neurons pretreated with either BDNF or GDNF (Cai et al., 1999). Moreover, these findings were in accordance with earlier studies, where a CL of DRG peripheral branches was shown to be causative for improved outgrowth capacities of subsequently lesioned central processes (Neumann and Woolf, 1999; Neumann et al., 2002). Generally, priming of postnatal neurons was demonstrated to be a) mandatory for successful regeneration, as could be confirmed in this study, and b) was attributed to a concomitant elevation of intracellular cAMP levels. Conversely, priming of neurons with SDF-1 was reportedly not required to effectively trigger outgrowth promotion *in vitro* in other reports (Chalasani et al., 2003). In this study, the importance of preincubation was further underlined by the finding that even neurons which were pretreated in medium alone displayed slightly improved outgrowth.

5.1.2.4 SDF-1α-induced neurite outgrowth promotion: CXCR4-dependency

In earlier studies, SDF-1-induced axon regeneration was demonstrated to be CXCR4-dependent, as blocking of this receptor resulted in a decreased neuronal tolerance of growth inhibitors (Chalasani et al., 2003). However, SDF-1 was recently reported to interact with two different receptors, CXCR4 and RDC1, suggesting that SDF-1α-induced neurite outgrowth promotion might be transduced by either receptor molecule (Balabanian et al., 2005). To address this question, neurons cultured on myelin were pretreated with the anti-CXCR4 antagonist AMD3100, a potent bicyclam inhibitor of this receptor, prior to application of SDF-1α. Binding of AMD3100 to

CXCR4 was reported to involve residues in several transmembrane and extracellular domains (Zhang et al., 2002). While binding and activation of CXCR4 by SDF-1 results in a conformational shift of the hydrophobic core and cytoplasmic domains of the receptor to a state permissive for the formation of a high affinity ternary complex with G_α subunits, this conformational change is suggestedly blocked by antagonist-treatment (Ghanouni et al., 2001; Zhang et al., 2002; Trent et al., 2003).

Surprisingly, it was observed that a simultaneous treatment with both the antagonist and SDF-1α resulted in only a slight abrogation of the before described growth promoting effects at low doses of AMD3100, compared to chemokine-only controls (Fig. 4.3). Conversely, application of high doses of AMD3100 either alone or together with SDF-1α was observed to facilitate neurite outgrowth on myelin, compared to untreated cells, albeit this effect was not significant. Interestingly, intrinsic CXCR4-stimulatory properties of AMD3100 were noted earlier (Zhang et al., 2002; Trent et al., 2003). Thus, as targeting CXCR4 with either SDF-1α or AMD3100 generally increased neurite outgrowth promotion on myelin, this receptor is most possibly involved in mediating growth promoting effects as described in this study. Furthermore, while alternative receptor utilization could not be completely excluded, CXCR4-independent signalling pathways are unlikely to mainly contribute to SDF-1α-mediated neurite outgrowth promotion. Activation of this receptor by either ligand binding or induction of a conformational shift is presumably sufficient to overcome myelin inhibition, while cross-reaction of AMD3100 with other cell surface receptors can be excluded due to the high specificity of this inhibitor for its target receptor CXCR4 (Hatse et al., 2002). A role for CXCR4 in the transduction of SDF-1α-mediated signalling was further suggested by a functional interaction of SDF-1α and this receptor as demonstrated in this study by SDF-1α-induced internalization of CXCR4 (Fig. 4.25).

Unlike in other studies, application of NGF as a component of fully substituted medium was not sufficient to overcome myelin-associated outgrowth inhibition in the model presented in this thesis. Conversely, priming with this neurotrophin was reported to effectively promote regeneration of postnatal DRG neurons before (Cai et al., 1999). Interestingly, SDF-1α efficiently abrogated outgrowth-inhibitory effects in the same concentration range as was noted for various neurotrophins in studies by Gao and colleagues (2003).

5.1.3 SDF-1/CXCR4 downstream signalling in neurite outgrowth promotion

As reported before, research on CNS regeneration was strongly influenced by the notion that beside environmental factors the intrinsic state of the injured neuron is of additional importance for its regenerative behaviour (Blackmore and Letourneau, 2005). Furthermore, the cyclic nucleotide cAMP was recently characterized to act as a measuring unit for regenerative abilities of neuronal cells. Postnatal neurons become in the course of developmental downregulation of intracellular cAMP-levels increasingly sensitive to negative guidance cues (Cai et al., 2001; Gao et al., 2003; Gao et al., 2004). Indeed, in earlier reports on SDF-1α-induced axonal tolerance of growth inhibitors a role of this chemokine in the elevation of cytosolic cAMP was noted *in vitro* (Chalasani et al., 2003). It could further be established that regeneration promoting effects of both neurotrophins and db-cAMP are transcription-dependent and involve activation of transcription factors such as CREB (Gao et al., 2004).

5.1.3.1 SDF-1α-mediated resetting of outgrowth capacities coincides with an upregulation of intracellular cAMP levels: implications of CXCR4 and PKA

In order to investigate the signalling events involved in SDF-1α-mediated growth promotion, the regulation of intracellular cAMP levels was assessed following a short pulse of this chemokine by detection of cAMP-dependent phosphorylation of CREB and subsequent translocation into neuronal nuclei. Interestingly, a significant increase in the number of $pCREB^{+}$ nuclei following application of SDF-1α suggested a chemokine-dependent upregulation of cAMP in myelin-sensitive DRG neurons (Fig. 4.4; Fig. 4.5). Findings in this study on a cAMP/pCREB elevating role of SDF-1α in neuronal cells thus are in accordance with earlier studies, in which this event was related to SDF-1-induced neurite outgrowth promotion and pathfinding (Chalasani et al., 2003; Chalasani et al., 2007). In the absence of SDF-1α, the adenylate cyclase activator forskolin both led to a pronounced increase in cAMP/pCREB and mimicked the ability of this chemokine to induce neurite outgrowth promotion, as was

demonstrated in this study, thus further indicating a role for cAMP in SDF-1α-mediated overcoming of myelin inhibition.

To elucidate the signalling events which transduce SDF-1α-mediated elevation of pCREB-immunoreactivity, blocking experiments were performed with either the anti-CXCR4 antagonist AMD3100 or an inhibitor to the cAMP-dependent downstream effector molecule PKA, KT5720 (Fig. 4.6; Fig. 4.7). Interestingly, following preincubation with AMD3100 a pronounced upregulation of pCREB-immunoreactivity was observed in SDF-1α-treated cultures with respect to both time-independent mean maximum values as well as to overall mean values, compared to cells treated with SDF-1α alone or untreated control cells. While intrinsic CXCR4-stimulatory properties of this antagonist could not be excluded, upregulation of pCREB/cAMP in AMD3100-treated cultures might also be due to alternative signalling pathways induced by SDF-1α (Zhang et al., 2002; Trent et al., 2003). In this instance, application of an inhibitor to CXCR4 could supposedly channel activation of competing signalling pathways by SDF-1α. As no experiments were performed with AMD3100 alone, a positive role of this antagonist in CREB phosphorylation and translocation into nuclei could neither be confirmed nor rejected. Thus, blocking experiments employing AMD3100 remained inconclusive with respect to a role of CXCR4 in SDF-1α-induced upregulation of cAMP/pCREB. This was further emphasized by the finding that a slight downregulation of forskolin-mediated effects was observed in AMD3100-treated cells. However, findings on a possible CXCR4-stimulatory role of AMD3100 noted here are in accordance with observations on a neurite outgrowth promoting function of this antagonist as described earlier in this thesis.

The effector molecule PKA was reported to induce downstream phosphorylation and transcription activation upon elevation of intracellular cAMP levels. Amongst others, PKA was recently described to promote regeneration on myelin in a pCREB-dependent manner (Gao et al., 2004). To investigate a possible role of PKA in SDF-1α-mediated upregulation of pCREB/cAMP, the PKA inhibitor KT5720 was applied. After pretreatment with both KT5720 and SDF-1α, weak pCREB-downregulatory effects were observed for both time-independent mean maximum values and overall mean values, as compared to the effects following application of SDF-1α alone. While the observed downregulatory effect on SDF-1α-induced pCREB-

immunoreactivity was only moderate, these results hint to a role of PKA in upregulation of cAMP/pCREB. Surprisingly, no such effect of KT5720-treatment could be observed for a forskolin-dependent increase in pCREB-immunoreactivity.

5.1.3.2 A variable role of SDF-1α in cAMP/pCREB regulation

The findings presented in this study are only partially in accordance with recent observations, which noted SDF-1-induced CREB phosphorylation and translocation into the nuclei of sympathetic neurons to occur stably and reliably 30 min after application of this chemokine (Chalasani et al., 2003). Moreover, while in latter report upregulation of pCREB-immunoreactivity was demonstratedly CXCR4- as well as PKA-dependent, corresponding results could not be obtained in this thesis. Thus, further studies will be required to confirm the signalling pathways involved in SDF-1α-induced phosphorylation of CREB in postnatal DRG neurons. However, findings made in this study suggest that SDF-1α-mediated neurite outgrowth promotion on myelin and an increase of cAMP/pCREB might be independently regulated. While SDF-1α-induced activation of CXCR4 presumably promotes neurite outgrowth of myelin-sensitive neurons, upregulation of cAMP/pCREB following application of this chemokine is not necessarily functionally connected with latter event. Findings on a possible uncoupling of neurite outgrowth promotion and elevation of intracellular cAMP levels were already reported in earlier studies, where PKA inhibition was observed to have no effect on axon regeneration (Liu and Snider, 2001). Interestingly, latter study demonstrated that axon regeneration of embryonic as well as adult neurons largely depended on Jak/STAT signalling.

However, as earlier reports on a cAMP/pCREB elevating role of SDF-1 were performed on neuronal cells of a different age and origin than in this thesis (Chalasani et al., 2003), SDF-1 might therefore employ different modes of action to induce neurite outgrowth promotion and elevation of intracellular cAMP levels.

Furthermore, variations in experimental conditions supposedly contribute to diverging results. While in this study DRG neurons monitored for pCREB were cultivated in medium supplemented with FBS and NGF to equal treatment conditions with those applied in the neurite outgrowth assay, sympathetic neurons in earlier reports were grown in serum-free medium, probably to maximize cAMP-stimulatory effects. As

NGF alone is reportedly effectual to evoke an increase of cytosolic cAMP, the here observed low overall increase in the proportion of pCREB-positive nuclei following application of SDF-1α might mirror a permanent decrease of neuronal sensitivity to external stimuli in these cultures due to exposure to NGF, albeit the amount applied in this study was not sufficient to abolish myelin-associated neurite outgrowth inhibition (Chang et al., 2006). That the efficacy of agents to trigger signalling events can differ in an experiment-dependent manner was demonstrated earlier for db-cAMP, which failed to elicit detectable Erk activation in cells, if those were not serum deprived prior to conducting the experiment (Gao et al., 2003). The performance of assays such as CREB phosphorylation and translocation into nuclei in fully defined minimal medium thus might lead to a distortion of effects, even more as primary neurons were demonstrated to tolerate serum starvation and remain healthy for only a maximum length of time of approximately 6 h (Gao et al., 2003).

However, findings on a cAMP-elevating role of SDF-1 are contradictory to well described interactions of CXCR4 with members of the G_i protein-family. Dwinell and colleagues (2003) noted an abrogation of forskolin-mediated cAMP-elevation in intestinal epithelial cell lines following application of SDF-1. Moreover, enhancement of cerebellar granule cell proliferation induced by sonic hedgehog, SHH, during embryogenesis is demonstratedly due to a SDF-1-mediated decrease of cAMP and subsequent negative modulation of PKA-activity (Klein et al., 2001). Only recently evidence arose that SDF-1 might elevate intracellular cAMP through a CXCR4-dependent pathway, and a dual role of this chemokine has thus evolved (Chalasani et al., 2003). Notably, overall numbers of pCREB-positive nuclei were comparably low in untreated as well as in treated cells in this study, while the time required for reaching maximum elevation of pCREB-immunoreactivity was highly variable in individual cultures, probably due to cell preparation-dependent variations. Furthermore, an initial decrease in the number of nuclei displaying pCREB-immunoreactivity was repeatedly observed. A downregulatory effect of SDF-1α on levels of intracellular cAMP can therefore not be completely excluded.

5.1.4 Alternative contributors to neurite outgrowth promotion and upregulation of cAMP/pCREB

Besides a CXCR4-dependent upregulation of cytosolic cAMP, other signalling events might possibly contribute to SDF-1α-mediated effects as presented in this study. First, high variations between single experiments could be due to the presence of considerable, albeit variable, amounts of endogenous SDF-1 in P6 DRG cultures, as suggested by immunocytochemical analysis. In this study, this chemokine was demonstrated to be prominently expressed in the Schwann cell fraction of P6 DRGs, whereas neurons displayed only low levels of SDF-1 expression (Fig. 4.24). Thus, endogenous SDF-1 might distort the effects of externally added chemokine in both the neurite outgrowth assay and the pCREB assay. While only the α- and β-isoform of SDF-1 have been extensively studied to date (Fig. 2.1), up to six different variants were recently identified (Gleichmann et al., 2000; Yu et al., 2006). Moreover, the β- and γ-transcript were demonstrated to be inversely regulated during CNS and PNS postnatal development, and a role of certain isoforms in nervous system regeneration has been suggested (Gleichmann et al., 2000). Findings that CXCR4 forms oligomers as well as multimers in numerous cell types, further add to complexity (Sloane et al., 2005). This receptor heterogeneity is suggestedly causative to the multiple functions of CXCR4, which might implicate a G_i protein-independent upregulation of intracellular cAMP levels as well as an activation of so far unknown signalling pathways with a role in neurite outgrowth promotion. Moreover, further evidence exists that chemokine receptors do not exclusively interact with members of the G_i protein family to trigger downstream signalling events (Arai and Charo; 1996). Finally, while SDF-1 was for long considered to solely activate CXCR4, the identification of RDC1 as a novel receptor implicates an activation of additional signalling pathways. Both receptors are present on P6 DRG neurons, and could thus function in neurite outgrowth promotion in either an additive or a competitive manner. As the signal transduction cascade connected to RDC1 has not been characterized to date, it might proposedly contribute to SDF-1α-induced neurite outgrowth promotion and/or upregulation of cAMP/pCREB.

5.2 Spatio-temporal expression patterns of CXCR4 and RDC1 *in vitro*

As in earlier studies SDF-1-induced growth promoting effects were demonstrated to be CXCR4-dependent, the ability of SDF-1 to mediate neurite outgrowth promotion of myelin-sensitive DRG neurons suggested a neuronal expression of CXCR4 in these cells (Chalasani et al., 2003; Chalasani et al., 2007). However, the former VIP-receptor RDC1 was recently described to be activated by SDF-1, although data still are controversial (Balabanian et al., 2005; Infantino et al., 2005). To clarify the signalling pathways employed in this study, and to characterize RDC1 receptor expression in cultured rat neuronal cells, the spatial and temporal expression and distribution of CXCR4 and RDC1 was investigated in P6 DRG neurons.

5.2.1 Distinctive features of receptor patterning on myelin sensitive DRG neurons

Immunostaining of an extracellularly located epitope of CXCR4 revealed a prominent expression of this receptor in the majority of DRG neurons applied in this study after 24 h *in vitro* (Fig. 4.8-Fig. 4.13). As described before, CXCR4-immunoreactivity displayed a characteristic and time-dependent distribution, whereby it was preferentially localized at branching points and near growth cones of neurites. Furthermore, accessibility of this receptor for its ligand, SDF-1, was confirmed by confocal laser scan microscopy, which mapped CXCR4 exclusively to the cell surface of neurons. The alternative receptor for SDF-1, RDC1, was coexpressed with CXCR4 in P6 DRG neurons, but differed largely with respect to its cellular distribution and time-dependency of expression (Fig. 4.9; Fig. 4.12; Fig. 4.13). It can thus be concluded that SDF-1 activates two different receptors on DRG neurons and probably affects multiple signalling pathways. Interestingly, both receptors to SDF-1 showed an inverse regulation in myelin-sensitive DRG neurons in this study, which might imply a functional inversion during cultivation.

Our findings on a time-dependent characteristic distribution of CXCR4 especially in neuronal processes were supported by earlier observations on the cellular distribution of this receptor in developing hippocampal neurons at E18 (Pujol et al., 2005). It was found that CXCR4 was predominantly located at the leading edge of

growing neurites at early stages of cultivation, while later this receptor was more broadly distributed along cellular processes. Moreover, different staining intensities could be observed for axons and dendrites. SDF-1-stimulation of E18 hippocampal neurons in this model led to a reduction of both growth cone numbers and axonal outgrowth, but conversely increased axonal branching events, thus directly altering neuronal patterning. While morphogenic effects of CXCR4 in latter studies were mainly confined to axons, here, both immunocytochemical results and findings of the neurite outgrowth assay suggest a potential role for SDF-1 and CXCR4 in the overall neurite patterning of DRG neurons. Further findings which were made in this thesis on the distribution of CXCR4 in non-neuronal cells such as leptomeningeal fibroblasts as well as DRG neurons directly after plating, hint to CXCR4-dependent signalling as a general cellular means to direct the formation of cellular processes and protrusion (Fig. 4.14-Fig. 4.23). To these findings will be referred later.
In hippocampal neurons, CXCR4 was mostly located both at the periphery of perikarya and throughout cell body cytoplasm (Pujol et al., 2003). Conversely, in this thesis CXCR4-immunoreactivity in DRG neurons was mainly restricted to the cell surface, as was outlined before. Further, expression of CXCR4 was demonstrated to specifically decrease on cellular processes at late stages of cultivation, thus indicating a complementary spatio-temporal receptor distribution, as compared with RDC1. As CXCR4 in studies by Pujol and colleagues (2003) was investigated as part of a GFP-fusion protein, and as receptor staining was performed after membrane permeabilization, the observed pattern might not reflect the actual presentation of CXCR4 on the outer surface of neuronal membranes.

5.2.1.1 Spatio-temporal patterning of CXCR4 and RDC1 with a possible role in neurite outgrowth and branching

The distinctive localization of CXCR4 to structures which represent regions of directional growth in early stages of cultivation is suggestive of a role in neurite patterning. Especially in regions of neurite branching, CXCR4 was detected in flat structures of considerable spatial extension, which were further characterized to harbour splayed or loop-like formations of neurofilament in high resolution images (Fig. 5.1,A-C). In earlier reports, a direct visualization of fluorescently labelled axons

suggested that branch points of primary growth cones of cortical axons are demarcated by developing large complex morphologies and undergoing lengthy pausing behaviours (Halloran and Kalil, 1994). Moreover, growth cones of cortical neurons were demonstrated to develop corresponding morphologies *in vitro* while pausing (Fig. 5.1,D,E). After the growth cones had resumed their outgrowth, axon branches later developed from the left-behind remnants of these structures (Szebenyi et al., 1998). Large complex growth cones further were identified at choice points in the nervous system where the respective axons have to make directional decisions, such as crossing the midline, turning or branching (Mason and Erskine, 2000). While growth cones generally are to small (5-10 µm in diameter) to provide a microscopic resolution required to monitor local changes in cytoskeletal dynamics, their morphology in pausing states is characterized by considerable extensions of up to 50 µm in diameter (Dent et al., 2003). In this thesis, CXCR4-immunoreactivity in postnatal DRG neurons was localized to regions which matched pausing growth cones and areas of neurite branching with respect to both their size as well as neurofilament configuration (Fig. 5.1,A-E). As these structures represent regions of directional growth, it is thus suggested that CXCR4 might govern branching and/or lengthy neurite growth in these cells. As RDC1 was not prominently present at these sites at early stages of development, a role of this receptor in directional growth seems unlikely. A possible function of SDF-1 and CXCR4 in neurite outgrowth and pathfinding is supported by findings made in knock out animals. Brains of SDF-1 and CXCR4 deficient animals, respectively, exhibit severe malformation not only of the cerebellum (Ma et al., 1998; Zou et al., 1998), but also of hippocampal and neocortical structures (Lu et al., 2002; Stumm et al., 2002). Further, *in vitro* studies documented an either repellent or attractant role for SDF-1 in the chemotaxis of cultured hippocampal, cerebellar, and cortical neurons (Bagri et al., 2002; Zhu et al., 2002; Stumm et al., 2002), axon guidance (Lu et al., 2001; Xiang et al., 2002; Chalasani et al., 2003), and axon elongation (Arakawa et al., 2003). Branching mechanisms reportedly have implications for sprouting after injury, and preliminary results on axon sprouting in corticospinal tract-, CST-, lesioned rats following SDF-1-treatment are suggestive of a stimulatory function of this chemokine (Dent et al., 2003; Klapka et al., unpublished observations).

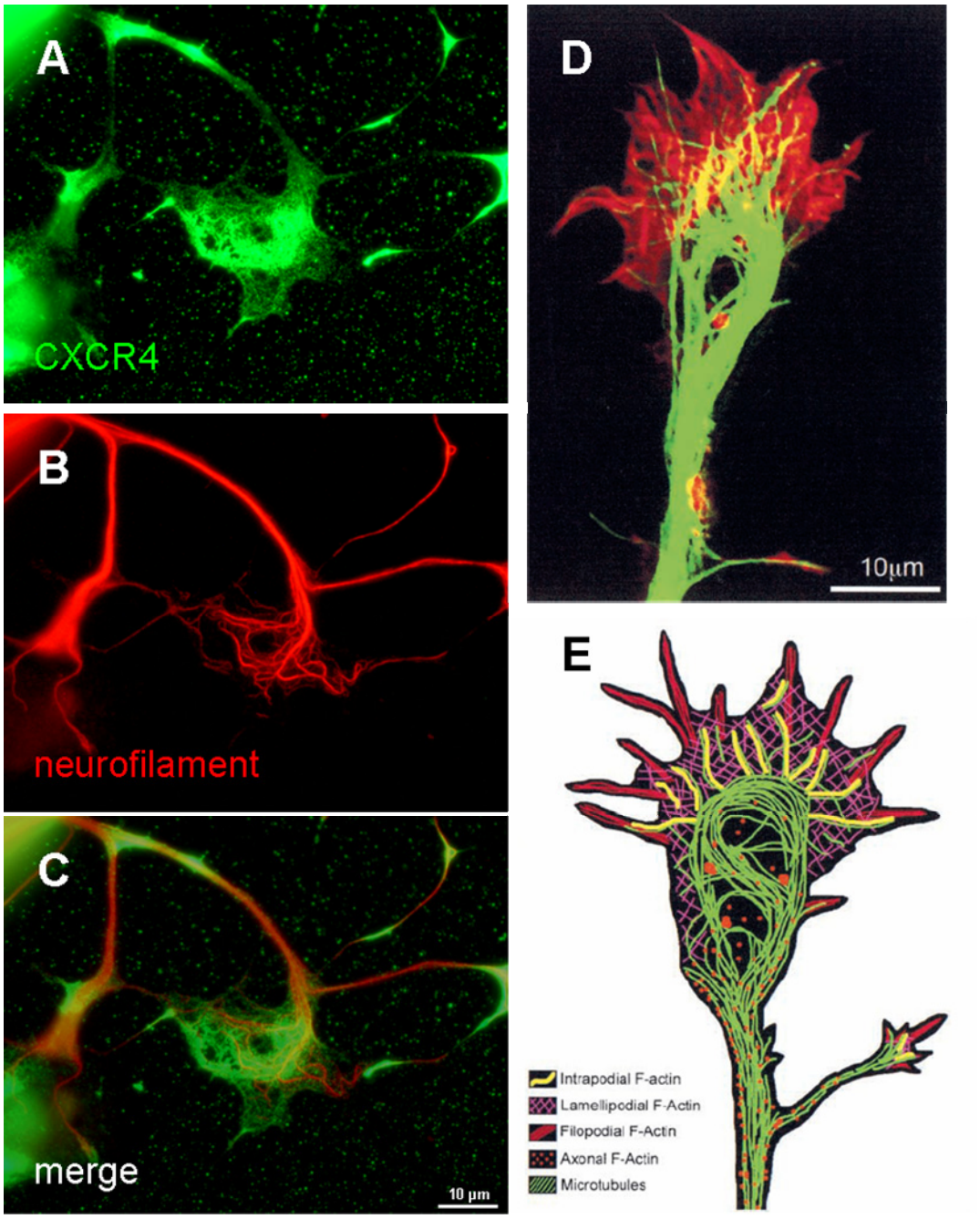

Dent et al., 2003 (mod.)

Fig. 5.1. The SDF-1/CXCR4 axis has a possible role in neurite outgrowth and branching. In P6 DRG neurons, CXCR4 is predominantly localized to regions of neurite branching and outgrowth (A-C). These structures have been reported to constitute areas of directional growth and display a characteristic configuration of neurofilaments *in vitro* (B,C), as well as of other cytoskeletal components (D,E). See text for details.

5.2.2 Spatio-temporal patterning of CXCR4 and RDC1 is present in both neuronal and non-neuronal cells

In cortical neurons, expression and distribution of both CXCR4 and RDC1 differed strongly in a preparation-dependent manner. Partially, CXCR4-immunoreactivity was restricted to the longest cellular process as well as to the respective proximal part of the cell body after 24 h *in vitro*. Conversely, while RDC1 was coexpressed with CXCR4, the former receptor was predominantly localized to small, dendrite-like processes and the opposing part of the cell body at early stages of incubation. Both CXCR4 and RDC1 expression increased during cultivation and was evenly distributed in the whole cortical neurons at late stages of *in vitro* incubation. The here presented findings on CXCR4- and RDC1- expression and distribution in cultured cortical neurons have to the present knowledge not been reported in literature before (Lazarini et al., 2003).

In both HeLa cells and meningeal fibroblasts, CXCR4 was preferentially localized to cellular protrusions such as lamellipodia, where it displayed a characteristic pattern similar to the receptor distribution that was observed in myelin-sensitive neurons. However, in HeLa cells a region-specific distribution of this receptor was prominent at late, but not early, stages of *in vitro* incubation. Similar, CXCR4 could be mapped to cellular processes and protrusions in meningeal fibroblasts after 2-5 DIV, but generally not as early as 1 DIV. In accordance with P6 DRG neurons, RDC1-immunoreactivity in both meningeal fibroblasts and HeLa cells was evenly distributed on the cell membrane surface at all stages of *in vitro* incubation, and a granular distribution of RDC1 was especially noted on HeLa cells.
The here presented findings thus indicate that a preferential localization of CXCR4 to regions such as of directional growth or outgrowth does not only apply for neuronal cells. While latter cells are characterized by a pronounced formation of cellular processes and extensive lengthy growth, CXCR4 seems to generally map to areas in which related events occur.

In this study, similar observations on receptor expression and distribution were further made in the Schwann cell fraction of dissociated P6 DRGs. Interestingly,

CXCR4 was present in a fraction, but not all Schwann cells, where it was coexpressed with RDC1 at all stages of cultivation. Thereby, RDC1 was present in a larger fraction of Schwann cells, compared to CXCR4. While RDC1-immunoreactivity displayed an even or granular distribution in Schwann cells, CXCR4 was localized to distinct cellular regions, which could represent areas of pronounced growth. Unlike expression of both receptors in neurites of P6 DRG neurons, no marked decrease or increase of either CXCR4- or RDC1-immunoreactivity was observed in Schwann cells.

5.2.3 SDF-1 and a possible function in cytoskeletal reorganization

Several cytoskeletal functions such as increased cell motility, adhesion to extracellular matrix proteins, morphological changes, and movement, have already been described to be regulated through SDF-1-mediated activation of CXCR4. SDF-1-induced changes in morphology thereby seem to be strictly cell-specific, as suggested by contradictory reports on the effects of SDF-1 on various tumour cell lines. While NCI-H446 small cell lung cancer, SCLC, cells displayed membrane ruffling as well as increased formation of neurite-like projections, filopodia, and uropodia, following application of SDF-1 (Kijima et al., 2002), Ba/F3 cells responded with less dramatic changes of cell morphology (Salgia et al., 1999). Effects on cytoskeletal components thereby are induced either by SDF-1 alone or in cooperation with other proteins such as the receptor tyrosine kinase, RTK, c-Kit (Kijima et al., 2002). Since long, SDF-1 has been known to excert chemotactic activity toward numerous cell types of the immune and hematopoietic system, such as T-lymphocytes or dendritic cells (Wang et al., 2000). Moreover, SDF-1 was demonstrated to govern the migration of germ cells as well as neuronal progenitors in the course of embryonic development (Doitsidou et al., 2002; Belmadani et al., 2005; Blaser et al., 2006). Only recently, this chemokine further was reported to direct tumour cells on their way to sites of metastasis (Muller et al., 2001; Burger et al., 2006).

Reorganization of the actin cytoskeleton is a central event in cell migration and is an early cellular response of chemotactic cells after chemokine stimulation. While the role of SDF-1 in chemotaxis-associated cytoskeletal rearrangements has recently

been extensively characterized for migrating blood cells, still little is known on whether these mechanisms might also apply for the events which lead to neurite formation and outgrowth. In a recently proposed model, SDF-1 directs Jurkat cell migration by LIMK1-dependent phosphorylation of the actin-depolymerizing and –severing protein cofilin (Nishita et al., 2002). While phosphorylation of cofilin was demonstrated to constitute a critical event in sema3A-induced growth cone collapse in DRG neurons and confers myelin-associated axon inhibition, activation of this signalling pathway by SDF-1 might conversely favour outgrowth (Aizawa et al., 2001; Hsieh et al., 2006). In accordance with these assumptions, SDF-1-induced cofilin-phosphorylation was reported to be transduced by Rac, whereas cofilin-mediated growth inhibition as conferred by myelin involves activation of RhoA (Nishita et al., 2002). Rho family small GTP-binding proteins, including Rho, Rac and Cdc42, play a central role in regulating actin cytoskeletal reorganization, and LIMK1 is phosphorylated and activated by ROCK and PAK, which are downstream effectors of Rho and Rac/Cdc42, respectively. Surprisingly, while both Rho-ROCK and Rac-PAK signalling pathways mediate phosphorylation and activation of LIMK1, these pathways effect antipodal cellular responses. As recently suggested, SDF-1-mediated phosphorylation of cofilin could lead to a more balanced actin cycling and thus supposedly effect either a stabilization of actin filaments in cellular protrusions or, conversely, promote outgrowth by enhancing the rapid turnover of actin (Nishita et al., 2002).

Thus, findings on a distinctive localization of CXCR4, but not RDC1, to structures of cell growth suggest a role for this receptor in the direction of cellular mechanisms such as cytoskeletal rearrangements. In this thesis, a similar spatio-temporal distribution for both CXCR4 and RDC1 was documented in a cell type-specific manner in neuronal as well as non-neuronal cells such as meningeal fibroblasts, Hela cells, cortical neurons,and both the Schwann cell fraction and neuronal fraction of P6 DRGs. Moreover, this is supported by observations on an early expression of CXCR4 receptor in primary cells, which temporally coincides with stages of pronounced outgrowth. In P6 DRG neurons, CXCR4 expression could be mapped to cellular protrusions directly after plating and attachment of cells. Thereby, CXCR4-immunoreactivity was most prominent at sites were cells had to make directional

decisions. Conversely, RDC1 displayed no pronounced cellular distribution at respective stages of cultivation.

The elevation of free cytosolic Ca^{2+} as a key signalling event in the interaction of SDF-1 and CXCR4 might further argument for a role in the direction of neurite branching and outgrowth. *In vivo* experiments in *Xenopus* spinal cord demonstrated that a downregulation of Ca^{2+} transients in growth cones accelerated axon outgrowth, whereas an increase in the number of Ca^{2+} transients decreased the rate of advance (Gomez and Spitzer, 1999). Conversely, at choice points where branching was likely to occur, growth cones generated higher frequencies of Ca^{2+} transients. While at present the mechanistical relationship between growth cone behaviour and morphology and Ca^{2+} increase in this structure is not fully understood, a role for chemokine-/chemokine receptor-induced Ca^{2+} elevation in branching and outgrowth can not be excluded. Notably, although L-type channels were demonstrated to mainly effect this type of Ca^{2+} increase, a contribution from intracellular stores could also be observed, and G_i protein-dependent depletion of intracellular stores has been characterized to predominantly govern the SDF-1-mediated increase of cytosolic Ca^{2+} levels. Albeit in this study no evidence was found for SDF-1-/CXCR4-mediated Ca^{2+} signalling in P6 DRG neurons, a function of the SDF-1/CXCR4 axis was clearly defined in the regulation of Ca^{2+} homeostasis in HeLa cells. Elevation of intracellular Ca^{2+} levels thereby was not limited to the α-isoform of this chemokine, but was further demonstrated for SDF-1γ, as reported in this study.

The anti-CXCR4 antibody applied in this study, 12G5 clone, was demonstrated to bind only to a subpopulation of CXCR4 molecules on numerous cell types (Baribaud et al., 2001; Sloane et al., 2005). According to recent findings, CXCR4 antigenic heterogeneity is attributable to conformational differences in the CXCR4 ECL domains, namely ECL2. These differences are presumably not due to posttranslational modifications, as they could be detected irrespective of the presence of targets of glycosylation, sulfation or G protein-coupling in the structure of this receptor, and suggestedly originate from CXCR4 multimerization. It might thus be argued that it can not clearly be stated whether the immunocytochemical stainings of CXCR4 presented in this study properly reflect the actual expression and distribution patterns of this receptor. However, as receptor heterogeneity has

predominantly, but not exclusively, been documented for cell lines and blood cells, implications for the present study are not clear. Furthermore, as anti-CXCR4 antibody 12G5 clone performed well in blocking of SDF-1-induced Ca^{2+} signalling, as reported below, it was concluded that no objections to an application of this antibody in the present study existed.

5.3 A common function of SDF-1 isoforms in elevation of intracellular Ca^{2+} levels

As the first SDF-1 isoform to be identified (Tashiro et al., 1993), SDF-1α has been widely studied and functionally characterized *in vivo* as well as *in vitro* (Lazarini et al., 2003; Kucia et al., 2004). During the recent years, a number of different isoforms with putative novel functions could be identified in various organisms (Tashiro et al., 1993; Gleichmann et al., 2000; Yu et al., 2006). SDF-1 transcripts are derived from a common mRNA precursor by means of alternative splicing, and while their proteins share a common N-terminal domain, they differ with respect to a C-terminal, isoform-specific, extension. The various isoforms are differentially expressed in a manner which is dependent on the developmental stage as well as on cell and tissue types, as could be demonstrated by quantitative PCR, Q-PCR, as well as isoform-specific *in situ* hybridization. Nonetheless, expression patterns still are controversial to date (Gleichmann et al., 2000; Tham et al., 2001; Stumm et al., 2002). The γ-variant of SDF-1 was recently identified in rat, and has not been characterized on a functional level yet. The C-terminal extension of SDF-1γ comprises 30 additional amino acids and thus represents the largest isoform in rat to date. In this thesis, custom-designed SDF-1γ was compared to commercially available SDF-1α in an *in vitro* assay to monitor the isoform-specific capacity to elevate intracellular Ca^{2+} levels. An increase of cytosolic Ca^{2+} levels by a depletion of internal stores was described as a key event in chemokine-induced intracellular signalling and indicates a functional interaction of ligand and receptor (Baggiolini et al., 1997; Murphy et al., 2000). Intracellular Ca^{2+} signalling is demonstratedly evoked by the common N-terminus of SDF-1-variants and has been extensively studied for the α-isoform in numerous cell types (Tilton et al., 2000; Lazarini et al., 2003; Roland et al., 2003; Kucia et al., 2004). As SDF-1α-mediated elevation of intracellular Ca^{2+} levels generally is uniform, variations following application of a certain isoform are therefore indicative of a C-terminus-

specific response. Here, a general capacity of both SDF-1γ and SDF-1α was revealed to trigger an upregulation of cytosolic Ca^{2+} levels in a concentration-dependent manner (Fig. 4.26-Fig. 4.30). Albeit Ca^{2+} responses were similar with respect to their general features, isoform-specific differences could be observed.

Generally, Ca^{2+} increase mediated by the α-transcript was significantly higher at low concentrations of this chemokine, compared to SDF-1γ. However, trend plots of Ca^{2+} responses were demonstrated to be similar for the two different variants. Interestingly, at higher concentrations responses triggered by either the α- or γ-isoform were equal, or were even more pronounced for SDF-1γ. ATP-mediated Ca^{2+} influx was slightly decreased after a preceding stimulation with both splice variants at high concentrations. Whether this was due to a protein overload of cells or a sustained activation of competing intracellular pathways, was not determined.

Findings on isoform-specific variations in the intensities of Ca^{2+} responses as described in this study are not necessarily due to C-terminal differences in protein sequence and structure. Mass spectroscopic analysis revealed a high discrepancy in the respective amount of full length protein for both isoforms. In the case of SDF-1γ, only 30-50% of all molecules carried an intact N-terminal domain, while the remaining portion was N-terminally truncated by several amino acids. Thereby, damage was presumed to originate from production errors due to protein length and extreme hydrophobicity.

In order to investigate a reported CXCR4-dependency of SDF-1 induced Ca^{2+} signalling, and as a means to assess a possible participation of SDF-1γ C-terminal domain, blocking experiments were performed. Cells were pretreated with either an anti-CXCR4 antibody (12G5 clone) or PTX. While the antibody was directed against the SDF-1 binding site(s) of the receptor, PTX abrogated receptor functions by uncoupling G_i protein-signalling. Both SDF-1γ- and SDF-1α-mediated elevation of intracellular Ca^{2+} levels displayed an efficient downregulation following preincubation with either antibody or PTX, while an isotype control antibody proved ineffective. As noted before, isoform-specific differences were also observed in blocking experiments. Interestingly, those were contradictory to the aforementioned limited ability of SDF-1γ to induce Ca^{2+} influx. Thereby, inhibitory effects following application of anti-CXCR4 antibody or PTX, respectively, were more pronounced for the α-variant, compared to the γ-isoform or the isotype control situation.

To date, a role for the amphiphilic C-terminal α-helix has exclusively been demonstrated for SDF-1α in binding to GAGs such as heparin (Luo et al., 1999; Cai et al., 2004). This event suggestedly stabilizes ligand-receptor interactions and was reported to increase SDF-1-induced chemotaxis and Ca^{2+} influx in T-lymphocytes. However, in other studies SDF-1α binding and signalling was demonstrated to occur through N-terminal peptides alone (Crump et al., 1997; Loetscher et al., 1998; Elisseeva et al., 2000). Against the background of the results presented in this study, it might be suggested that the extended C-terminal domain of SDF-1γ binds to GAGs on the cell surface of CXCR4-overexpressing HeLa cells. Thus, this could lead to a more sustained interaction of this ligand with receptor molecules which were not blocked by either anti-CXCR4 antibody or PTX. Alternately, elevation of intracellular Ca^{2+} levels following application of SDF-1γ might employ different or at least additional means of intracellular signalling which presumably is G_i protein-independent. It has to be noted that in blocking experiments mean Ca^{2+} responses were higher than was observed in experiments which were designed to solely compare SDF-1α and SDF-1γ effects. This can presumably be ascribed to a pretreatment effect which might result in a more efficient Ca^{2+} elevation, but could also be due to the lower n-numbers of this experimental setup. Generally, since the applied SDF-1 isoforms are of different origin, manufacturing by-products or sample contamination could easily be responsible for the observed variations.

5.4 Conclusions and further directions

The interactions of SDF-1 and its cognate receptor, CXCR4, are a well studied paradigm for chemokine and chemokine receptor biology within the boundaries of the immune system and beyond. Surprisingly, an increased understanding of their functions is accompanied by the notion that both this ligand and receptor often represent an exception to the general rules which have been described for the chemokine system (Murdoch, 2000). Here, a role for SDF-1α in overcoming myelin-induced outgrowth inhibition of postnatal mammalian PNS neurons was characterized and signalling events involved in SDF-1α-mediated growth promotion were investigated. It was found that myelin-sensitive DRG neurons displayed a significantly reduced outgrowth performance on a surface coated with CNS myelin, and that this effect could be reverted and growth was restored following application of SDF-1α in a dose-dependent manner. Moreover, SDF-1α-mediated effects were significantly enhanced if cells were pretreated with this chemokine prior to plating on myelin. Blocking of CXCR4 led to a partial, albeit not complete, abrogation of SDF-1α-induced neurite outgrowth promotion, thus probably suggesting the involvement of an additional signal transduction pathway activated by this chemokine.

Neuronal navigation and outgrowth are highly complex processes, in which external guidance cues are transduced across the membrane by specific receptors to activate intracellular signalling pathways and regulatory mechanisms for cytoskeletal rearrangements. It has become evident that many of these pathways might be similar to those involved in directional migration of non-neuronal cells such as cells of the hematopoietic system, albeit guidance cues and receptors are likely to differ. Cell migration, which plays an essential role in a variety of physiological and pathophysiological events, could be demonstrated to be dependent on the interactions of SDF-1 and CXCR4 in such different processes as the metastatic destination of cancer cells, germ cell migration, or stem cell homing. Reorganization of actin components of the cytoskeleton is a central event in migration and an early cellular response of chemotactic cells after chemokine stimulation. In this thesis, CXCR4-immunoreactivity in DRG neurons was localized to regions which matched pausing growth cones and areas of neurite branching at early stages of cultivation. As these structures represent regions of directional growth, CXCR4 might

suggestedly govern neurite branching or formation of cellular processes. Findings on expression and distribution of this receptor in various primary cells and cell lines supported this suggestion, which is especially convincing with respect to recent observations on a role for SDF-1 in LIMK1/cofilin-dependent actin rearrangements. Thus, cytoskeletal rearrangements upon SDF-1-induced activation of LIMK1 might not only be applicable to migrating cells, but could propose an explanation on how this chemokine directs neurite branching and outgrowth in presence of negative guidance cues.
Further studies will have to define the exact role SDF-1 plays in growth promotion and the signalling events herein involved. Possible experimental approaches might involve a permanent or temporary knock out or knock down of either of the cognate receptors to SDF-1, CXCR4 and RDC1, to investigate the role of these molecules in DRG neuron outgrowth and neurite patterning *in vitro*, and to allow for a more exact analysis of signalling events involved in SDF-1-induced outgrowth promotion.

In a second part, two different splice variants of SDF-1, SDF-1α and SDF-1γ, were characterized in their function to elevate the level of intracellular free Ca^{2+}. While SDF-1 isoforms differ considerably with regard to their C-terminal extension, still no distinctive features could be characterized for this region apart from a general supportive function. In this thesis, it could be demonstrated that rat splice variant SDF-1γ was functional and triggered intracellular Ca^{2+} increase similar to the α-isoform. The ability to elevate cytosolic Ca^{2+} could mainly be attributed to the N-terminal domain of both splice variants in both a CXCR4- and G_i protein-dependent manner. However, slight functional differences were observed for the γ–isoform in this study, which suggested that SDF-1γ-mediated Ca^{2+} increase might employ different or at least additional means of intracellular signalling. In recent studies, a function of the C-terminus in receptor activation was demonstrated for SDF-1α. As the SDF-1γ C-terminal region comprises 30 additional amino acids, a lack of function of this domain seems unlikely, regarding its high evolutionary conservation. However, while SDF-1 isoforms applied here were of different origin, further analysis of isoform-specific responses would require SDF-1 variants from a common source to eliminate production-dependent differences in future studies.

In the past, structural mutants of SDF-1 with altered binding and signalling properties have repeatedly been suggested as putative therapeutic tools. With respect to the diversity of molecular and functional properties of SDF-1 and CXCR4, targeting this system as a possible means of therapeutic intervention might be critical. Moreover, findings on various functional domains of SDF-1 clearly have to be considered in context with recent reports on cell-specific differences in CXCR4 expression, multimerization, and signalling. However, while SDF-1 might not directly find application as a therapeutic tool in CNS regeneration, studying this potent molecule might likely forward the understanding of the molecular machinery in CNS growth inhibition and promotion. Despite the identification of RDC1 as a novel receptor to SDF-1, CXCR4 might still be considered to represent the major partner in binding and signalling, and minute knowledge of ligand-receptor interactions might provide valuable insights into various cellular mechanisms.

6 Literature

Ahr B, Denizot M, Robert-Hebmann V, Brelot A, Biard-Piechaczyk M (2005). Identification of the cytoplasmic domains of CXCR4 involved in Jak2 and STAT3 phosphorylation. J Biol Chem 280:6692-6700.

Aizawa H, Kishi Y, Iida K, Sameshima M, Yahara I (2001).Cofilin-2, a novel type of cofilin, is expressed specifically at aggregation stage of *Dictyostelium discoideum* development. Genes Cells 6:913-921.

Allinen M, Beroukhim R, Cai L, Brennan C, Lahti-Domenici J, Huang H, Porter D, Hu M, Chin L, Richardson A, Schnitt S, Sellers WR, Polyak K (2004). Molecular characterization of the tumor microenvironment in breast cancer. Cancer Cell 6:17-32.

Amara A, Gall SL, Schwartz O, Salamero J, Montes M, Loetscher P, Baggiolini M, Virelizier JL, Arenzana-Seisdedos F (1997). HIV coreceptor downregulation as antiviral principle: SDF-1 alpha-dependent internalization of the chemokine receptor CXCR4 contributes to inhibition of HIV replication. J Exp Med 186:139-146.

Araujo DM, Cotman CW (1993). Trophic effects of interleukin-4, -7 and -8 on hippocampal neuronal cultures: potential involvement of glial-derived factors. Brain Res 600:49-55.

Avigdor A, Goichberg P, Shivtiel S, Dar A, Peled A, Samira S, Kollet O, Hershkoviz R, Alon R, Hardan I, Ben-Hur H, Naor D, Nagler A, Lapidot T (2004). CD44 and hyaluronic acid cooperate with SDF-1 in the trafficking of human $CD34^+$ stem/progenitor cells to the bone marrow. Blood 103:2981-2989.

Baggiolini M, Dewald B, Moser B (1997). Human chemokines: an update. Annu Rev Immunol 15:675-705.

Bagri A, Gurney T, He X, Zou YR, Littman DR, Tessier-Lavigne M, Pleasure SJ (2002). The chemokine SDF-1 regulates migration of dentate granule cells. Development 129:4249-4260.

Bajetto A, Barbero S, Bonavia R, Piccioli R, Pirani P, Florio T, Schettini G (2001). Stromal cell-derived factor-1α induces astrocyte proliferation through the activation of extracellular signal-regulated kinases 1/2 pathways. J Neurochem 77:1226-1236.

Bajetto A, Bonavia R, Barbero S, Schettini G (2002). Characterization of chemokines and their receptors in the central nervous system: physiopathological implications. J Neurochem 82:1311-1329.

Balabanian K, Lagane B, Infantino S, Chow KYC, Harriague J, Moepps B, Arenzana-Seisdedos F, Thelen M, Bachelerie F (2005). The chemokine SDF-1/CXCL12 binds to and signal through the orphan receptor RDC1 in T lymphocytes. J Biol Chem 280:35760-35766.

Baptiste DC, Fehlings MG (2006). Pharmacological approaches to repair the injured spinal cord. J Neurotrauma 23:318-334.

Barbero S, Bonavia R, Bajetto A, Porcile C, Pirani P, Ravetti JL, Zona G, Spaziante R, Florio T, Schettini G (2003). Stromal cell-derived factor-1α stimulates human glioblastoma cell growth through the activation of both extracellular signal-regulated kinase 1/2 and Akt. Cancer Res 63:1969-1974.

Baribaud F, Edwards TG, Sharron M, Brelot A, Heveker N, Price K, Mortari F, Alizon M, Tsang M, Doms RW (2001). Antigenically distinct conformations of CXCR4. J Virol 75: 8957-8967.

Barlic, Andrews JD, Kelvin AA, Bosinger SE, DeVries ME, Xu L, Dobransky T, Feldman RD, Ferguson SSG, Kelvin DJ (2000). Regulation of tyrosine kinase activation and granule release through β-arrestin by CXCR1. Nat Immunol 1:227-233.

Bazan JF, Bacon KB, Hardiman G, Wang W, Soo K, Rossi D, Greaves DR, Zlotnik A, Schall TJ (1997). A new class of membrane-bound chemokine with a CX3C motif. Nature 385:640-644.

Belmadani A, Tran PB, Ren D, Assimacopoulos S, Grove EA, Miller RJ (2005). The chemokine Stromal cell-derived factor-1 regulates the migration of sensory neuron progenitors. J Neurosci 25:3995-4003.

Benson MD, Romero MI, Lush ME, Lu QR, Henkemeyer M, Parada LF (2005). Ephrin-B3 is a myelin-based inhibitor of neurite outgrowth. Proc Natl Acad Sci USA 102:10694-10699.

Blackmore M, Letourneau PC (2005). Changes within maturing neurons limit axonal regeneration in the developing spinal cord. J Neurobiol 66:348-360.

Blaser H, Reichman-Fried M, Castanon I, Dumstrei K, Marlow FL, Kawakami K, Solnica-Krezel L, Heisenberg CP, Raz E (2006). Migration of zebrafish primordial germ cells: a role for myosin contraction and cytoplasmic flow. Dev Cell 11:613-627.

Blight AR (2002). Miracles and molecules – progress in spinal cord repair. Nature Neurosci Supp 5:1051-1054

Bolin LM, Murray R, Lukacs NM, Strieter RM, Kunkel SL, Schall TJ, Bacon KB (1998). Primary sensory neurons migrate in response to the chemokine RANTES. J Neuroimmunol 81:49-57.

Bracken MB, Collins WF, Freeman DF, et al. (1984). Efficacy of methylprednisolone in acute spinal cord injury. JAMA 251:45-52.

Bracken MB, Shepard MJ, Collins WF, et al. (1990). A randomized, controlled trial of methylprednisolone or naxolone in the treatment of acute spinal-cord injury. Results of the Second National Acute Spinal Cord Injury Study. N Engl J Med 322:1405-1411.

Bracken MB, Shepard MJ, Collins WF, et al. (1992). Methylprednisolone or naxolone treatment after acute spinal cord injury: 1-year follow-up data. Results of the Second National Acute Spinal Cord Injury Study. J Neurosurg 76:23-31.

Bracken MB, Shepard MJ, Holford TR, et al. (1997). Administration of methylprednisolone for 24 or 48 hours or tirilazad mesylate for 48 hours in the treatment of acute spinal cord injury. Results of the Third National Acute Spinal Cord Injury Randomized Control Trial. National Acute Spinal Cord Injury Study. JAMA 277:1597-1604.

Bregman BS (1998). Transplants and neurotrophins increase regeneration and recovery of function after spinal cord injury. In Frontiers or Neural Development, K. Uyemura, ed. (Tokyo: Springer-Verlag).

Brittis PA, Flanagan JG (2001). Nogo domains and a Nogo receptor: implications for axon regeneration. Neuron 30:11-14.

Brösamle C, Huber AB, Fiedler M, Skerra A, Schwab ME (2000). Regeneration of lesioned corticospinal tract fibers in the adult rat induced by a, recombinant, humanized IN-1 antibody fragment. J Neurosci 20:8061-8068.

Bunge MB (2001). Bridging areas of injury in the spinal cord. Neuroscientist 7:325-339.

Burger JA, Kipps TJ (2006). CXCR4: a key receptor in the crosstalk between tumor cells and their microenvironment. Blood 107:1761-1767.

Cai D, Deng K, Mellado W, Lee J, Ratan RR, Filbin MT (2002). Arginase I and polyamines act downstream from cyclic AMP in overcoming inhibition of axonal growth MAG and myelin *in vitro*. Neuron 35:711-719.

Cai D, Qiu J, Cao Z, McAtee M, Bregman BS, Filbin MT (2001). Neuronal cyclic cAMP controls the developmental loss in ability of axons to regenerate. J Neurosci 21:4731-4739.

Cai D, Shen Y, DeBellard ME, Tang S, Filbin MT (1999). Prior exposure to neurotrophins blocks inhibition of axonal regeneration by MAG and myelin via a cAMP-dependent mechanism. Neuron 22:89-101.

Cai SH, Tan Y, Ren XD, Li XH, Cai SX, Du J (2004). Loss of C-terminal α-helix decreased SDF-1α-mediated signaling and chemotaxis without influencing CXCR4 internalization. Acta Pharmacol Sin 25:152-160.

Caroni P, Schwab ME (1988). Antibody against myelin-associated inhibitor of neurite growth neutralizes nonpermissive substrate properties of CNS white matter. Neuron 1:85-96.

Caroni P, Schwab ME (1988b). Two membrane protein fractions from rat central myelin with inhibitory proteins or neurite growth and fibroblast spreading. J Cell Biol 106:1281-1288.

Chabot D, Zhang P, Quinnan G, Broder C (1999). Mutagenesis of CXCR4 identifies important domains for human immunodeficiency virus type 1, X4 isolate envelope-mediated membrane fusion and virus entry and reveals cryptic coreceptor activity for R5 isolates. J Virol 73:6598-6609.

Chabot DJ, Chen H, Dimitrov DS, Broder CC (2000). N-linked glycosylation of CXCR4 masks coreceptor function for CCR5-dependent human immunodeficiency virus type 1 isolates. J Virol 74:4404-4413.

Chalasani SH, Kabelko KA, Sunshine MJ, Littman DA, Raper JA (2003). A chemokine, SDF-1, reduces the effectiveness of multiple axonal repellents and is required for normal axon pathfinding. J Neurosci 23:1360-1371.

Chalasani SH, Sabol A, Xu H, Gyda MA, Rasband K, Granato M, Chien CB, Raper JA (2007). Stromal cell-derived factor-1 antagonizes slit/robo signaling *in vivo*. J Neurosci 27:973-980.

Chang JH, Vuppalanchi D, van Niekerk E, Trepel JB, Schanen NC, Twiss JL (2006). PC12 cells regulate inducible cyclic AMP (cAMP) element repressor expression to differentially control cAMP element-dependent transcription in response to nerve growth factor and cAMP. J Neurochem 99:1517-1530.

Chen MS, Huber AB, van der Haar ME, Frank M, Schnell S, Spillmann AA, Christ F, Schwab ME (2000). Nogo-A is a myelin-associated neurite outgrowth inhibitor and an antigen for monoclonal antibody IN-1. Nature 403:434-439.

Cheng H, Cao Y, Olson L (1996). Spinal cord repair in adult paraplegic rats: partial restoration of hind limb function. Science 273:510-513.

Chong MS, Woolf CJ, Haque NSK, Anderson PN (1999). Axonal regeneration form injured dorsal roots into the spinal cord of adult rats. J Comp Neurol 410:42-54.

Claps CM, Corcoran KE, Cho KJ, Rameshwar P (2005). Stromal derived growth factor-1alpha as a beacon for stem cell homing in development and injury. Curr Neurovas Res 2:319-329.

Cook JS, Wolsing DH, Lameh J, Olson CA, Correa PA, Sadee W, Blumenthal EM, Rosenbaum JS (1992). Characterization of the RDC1 gene which encodes the canine homolog of a proposed human VIP receptor. FEBS 300:149-152.

Crump MP, Gong JH, Loetscher P, Rajarathnam K, Amara A, Arenzana-Seisdedos F, Virelizier JL, Baggiolini M, Sykes BD, Clark-Lewis I (1997). Solution structure and basis for functional activity of stromal cell-derived factor-1; dissociation of CXCR4 activation from binding and inhibition of HIV-1. EMBO 16:6996-7007.

Dealwis C, Fernandez EJ, Thompson DA, Simon RJ, Siani MA, Lolis E (1998). Crystal structure of chemically synthesized [N33A] stromal cell-derived factor 1alpha, a potent ligand for the HIV-1 “fusin” coreceptor. PNAS 95:6941-6946.

DeBellard ME, Tang S, Mukhopadhyay G, Shen YJ, Filbin MT (1996). Myelin-associated glycoprotein inhibits axonal regeneration from a variety of neurons via

interaction with a sialoglycoprotein. Mol Cell Neurosci 7:89-101.

Dent EW, Tang F, Kalil K (2003). Axon guidance by growth cones and branches: common cytoskeletal and signaling mechanisms. Neuroscientist 9:343-353.

Dickson BJ (2002). Molecular mechanisms of axon guidance. Science 298:1959-1964.

Doitsidou M, Reichmann-Fried M, Stebler J, Köprunner M, Dörries J, Meyer D, Esguerra CV, Leung TC, Raz E (2002). Guidance of primordial germ cell migration by the chemokine SDF-1. Cell 111:647-659.

Domeniconi M, Filbin MT (2005). Overcoming inhibitors in myelin to promote axonal regeneration. J Neurol Sci 233:43-47.

Domeniconi M, Zampieri N, Spencer T, Hilaire M, Mellado W, Chao MV, Filbin MT (2005). MAG induces regulated intramembrane proteolysis of the p75 neurotrophin receptor to inhibit neurite outgrowth. Neuron 46:849-855.

Doranz BJ, Orsini MJ, Turner JD, Hoffman TL, Berson JF, Hoxie JA, Peiper SC, Brass LF, Doms RW (1999). Identification of CXCR4 domains that support coreceptor and chmokine receptor functions. J Virol 73:2752-2761.

Dumont RJ, Verma S, Okonkwo DO, et al. (2001). Acute spinal cord injury. Part II: contemporary pharmacotherapy. Clin Neuropharmacol 24:265-279.

Dwinell MB, Ogawa H, Barrett KE, Kagnoff MF (2004). SDF-1/CXCL12 regulates cAMP production and ion transport in intestinal epithelial cells via CXCR4. Am J Physiol Gastrointest Liver Physiol 286:G844-G850.

Elisseeva EL, Slupsky CM, Crump MP, Clark-Lewis I, Sykes BD (2000). NMR studies of active N-terminal peptides of Stromal cell-derived factor-1. J Biol Chem 275:26799-26805.

El-Shazly A, Yamaguchi N, Masuyama K, Suda T, Ishikawa T (1999). Novel association of the Src family kinasesHck and c-Fgr, with CCR3 receptor stimulation: a possible mechanism for eotaxin-induced human eosinophil chemotaxis. Biochem Biophys Res Commun 264:163-170.

Endres MJ, Clapham PR, Marsh M, Ahuja M, Turner JD, McKnight A, Thomas JF, Stoebenau-Haggarty B, Choe S, Vance PJ, Wells TNC, Power CA, Sutterwala SS, Doms RW, Landau NR, Hoxie JA (1996). CD4-independent infection by HIV-2 is mediated by fusin/CXCR4. Cell 87:745-756.

Esch F, Lin KI, Hills A, Zaman K, Baraban JM, Chatterjee S, Rubin L, Ash DE, Ratan RR (1998). Purification of multipotent antideath activity from bovine liver and its identification as arginase: nitric oxide-independent inhibition of neuronal apoptosis. J Neurosci 18:4083-4095.

Farzan M, Babcock G, Vasilieva N, Wright PL, Kiprilov E, Mirzabekov T, Choe H (2002). The role of posttranslational modifications of the CXCR4 amino terminus in stromal-derived factor 1 alpha association and HIV entry. J Biol Chem 277:29484-29489.

Farzan M, Mirzabekov T, Kolchinsky P, Wyatt R, Cayayab M, Girard N, Girard C (1999). Tyrosine sulfonation of the amino terminus of CCR5 facilitates HIV-1 entry. Cell 96:667-676.

Fawcett JW, Asher RA (1999). The glial scar and central nervous system repair. Brain Res Bull 49:377-391.

Feng Y, Broder CC, Kennedy PE, Berger EA (1996). HIV-1 entry cofactor: Functional cDNA cloning of a seven transmembrane, G protein-coupled receptor. Science 272:872-877.

Fernandez EJ, Lolis E (2002). Structure, function, and inhibition of chemokines. Annu Rev Pharmacol Toxicol 42:469-499.

Filbin MT (2003). Myelin-associated inhibitors of axonal regeneration in the adult mammalian CNS. Nat Rev Neurosci 4:1-11

Flax JD, Aurora S, Yang C, Simonin C, Wills AM, Billinghurst LL, Jendoubi M, Sidman RL, Wolfe JH, Kim SU, Snyder EY (1998). Engraftable human stem cells respond to development cues, replace neurons, and express foreign genes. Nat Biotech 16:1033-1039.

Fraser CM, Chung FZ, Wang CD, Venter JC (1988). Site-directed mutagenesis of human β-adrenergic receptors: substitution of aspartic acid-130 by asparagines produces a receptor with high-affinity agonist binding that is uncoupled from adenylate cyclase. Proc Natl Acad Sci 85:5478-5482.

Gage FH, Ray J, Fisher LJ (1995). Isolation, characterization, and use of stem cells from the CNS. Annu Rev Neurosci 18:159-192.

Ganju RK, Brubaker SA, Meyer J, Dutt P, Yang Y, Qin S, Newman W, Groopman JE (1998). The α-chemokine, stromal cell-derived factor-1α, binds to the transmembrane G-protein-coupled CXCR-4 receptor and activates multiple signal transduction pathways. J Biol Chem 273:23169-23175.

Gao Y, Deng K, Hou J, Bryson JB, Barco A, Nikulina E, Spencer T, Mellado W, Kandel ER, Filbin MT (2004). Activated CREB is sufficient to overcome inhibitors in myelin and promote spinal axon regeneration in vivo. Neuron 44:609-621.

Gao Y, Nikulina E, Mellado W, Filbin MT (2003). Neurotrophins elevate cAMP to reach a threshold required to overcome inhibition by MAG through extracellular signal-regulated kinase-dependent inhibition of phosphodiesterase. J Neurosci 23:11770-11777.

Geisler FH, Dorsey FC, Coleman WP (2001). Recovery of motor function after spinal cord injury – a randomized, placebo-controlled trial with GM-1 ganglioside. N Engl J Med 324:1829-1838.

Geminder H, Sagi-Assif O, Goldberg L, Meshel T, Rechavi G, Witz IP, Ben-Baruch A

(2001). A possible role for CXCR4 and its ligand, the CXC chemokine stromal cell-derived factor-1, in the development of bone marrow metastases in neuroblastoma. J Immunol 167:4747-4757.

Ghanouni P, Steenhuis JJ, Farrens DL, Kobilka BK (2001). Agonist-induced conformational changes in the G-protein-coupling domain of the β_2 adrenergic receptor. Proc Natl Acad Sci USA 98:5997-6002.

Gilad GM, Gilad VH (1988). Early polyamine treatment enhances survival of sympathetic neurons after postnatal axonal injury or immunosympathectomy. Brain Res 466:175-181.

Gilad VH, Tetzlaff WG, Rabey JM, Gilad GM (1996). Accelerated recovery following polyamines and aminoguanidine treatment after facial nerve injury in rats.Brain Res 724:141-144.

Gillard SE, Lu M, Mastracci RM, Miller RJ (2002). Expression of functional chemokine receptors by rat cerebellar neurons. J Neuroimmunol 124:16-28.
Gleichmann M, Gillen C, Czardybon M, Bosse F, Greiner-Petter R, Auer J, Müller HW (2000). Cloning and characterization of SDF-1γ, a novel SDF-1 chemokine transcript with developmentally regulated expression in the nervous system. Eur J Neurosci 12:1857-1866.

Goldshmit Y, McLenachan A, Turnley A (2006). Roles of Eph receptors and ephrins in the normal and damaged adult CNS. Brain Res Rev

Gomez TM, Spitzer NC (1999). In vivo regulation of axon extension and pathfinding by growth-cone calcium transients. Nature 397:784-787.

Goshima Y, Sasaki Y, Nakayama T, Ito T, Kimura T (2000). Functions of semaphorins in axon guidance and neuronal regeneration. Jpn J Pharmacol 82:273-279.

Gosling J, Monteclaro FS, Atchison RE, Arai H, Tsou CL, Goldsmith MA, Charo IF

(1997). Molecular uncoupling of C-C chemokine receptor 5-induced chemotaxis and signal transduction form HIV-1 coreceptor activity. PNAS 94:5061-5066.

Gourmala NG, Buttini M, Limonta S, Sauter S, Boddeke HW (1997). Differential and time-dependent expression of monocyte chemoattractant protein-1 mRNA by astrocytes and macrophages in rat brain: effects of ischemia and peripheral lipopolysaccharide administration. J Neuroimmunol 74:35-44.

GrandPrè T, Nakamura F, Vartanian T, Strittmatter SM (2000). Identification of the Nogo inhibitor of axon regeneration as a reticulon protein. Nature 403:439-444.

Gupta SK, Pillarisetti K (1999). Cutting edge: CXCR4-Lo: molecular cloning and functional expression of a novel human CXCR4 splice variant. J Immunol 163:2368-2372.

Habib AA, Marton LS, Allwardt B, Gulcher JR, Mikol DD, Högnason T, Chattopadhyay N, Stefansson K (1998). Expression of the oligodendrocyte-myelin glycoprotein by neurons in the mouse central nervous system. J Neurochem 70:1704-1711.

Hall ED (1993). Lipid antioxidants in acute central nervous system injury. Ann Emerg Med 22:1022-1027.

Halloran MC, Kalil K (1994). Dynamic behaviours of growth cones extending in the corpus callosum of living cortical brain slices observed with video microscopy. J Neurosci 14:2161-2177.

Han Y, He T, Huang DR, Pardo CR, Ransohoff RM (2001). TNFα mediates SDF-1 induced NF-κB activation and cytotoxic effects in primary astrocytes. J Clin Invest 108:425-435.

Haribabu B, Richardson RM, Fisher I, Sozzani S, Peiper SC, Horuk R, Ali H, Snyderman R (1997). J Biol Chem 272:28726-28731.

Harrison JK, Jiang Y, Chen S, Xia Y, Maciejewski D, McNamara RK, Streit WJ, Salafranca MN, Adhikari S, Thompson DA, Botti P, Bacon KB, Feng L (1998). Role for neuronally derived fraktalkine in mediating interactions between neurons and CX3CR1-expressing microglia. Proc Natl Acad Sci USA 95:10896-10901.

Hasegawa Y, Fujitani M, Hata K, Tohyama M, Yamagishi S, Yamashita T (2004). Promotion of axon regeneration by myelin-associated glycoprotein and Nogo through divergent signals downstream of G_i/G. J Neurosci 24:6826-6832.

Hatse S, Princen K, Bridger G, De Clercq E, Schols D (2002). Chemokine receptor inhibition by AMD3100 is strictly confined to CXCR4. FEBS Lett 527:255-262.

He J, Chen Y, Farzan M, Choe H, Ohagen A, Gartner S, Busciglio J, Yang X, Hofmann W, Newman W, Mackay CR, Sodroski J, Gabuzda D (1997). CCR3 and CCR5 are co-receptors for HIV-1 infection of microglia. Nature 385:645-649.

Heesen M, Berman MA, Höpken UE, Gerard NP, Dorf ME (1997). Alternate splicing of mouse fusin/CXC chemokine receptor 4. Stromal cell-derived factor-1α is a ligand for both CXC chemokine receptor 4 isoforms. J Immunol 158:3561-3564.

Hesselgesser J, Halks-Miller M, DelVecchio V, Peiper SC, Hoxie J, Kolson DL, Taub D, Horuk R (1997). CD4-independent association between HIV-1 gp120 and CXCR4: functional chemokine receptors are expressed in human neurons. Curr Biol 7:112-121.

Hesselgesser J, Taub D, Baskar P, Greenberg M, Hoxie J, Kolson DL, Horuk R (1998). Neuronal apoptosis induced by HIV-1 gp120 and the chemokine SDF-1α is mediated by the chemokine receptor CXCR4. Curr Biol 8:595-598.

Higuchi H, Yamashita T, Yoshikawa H, Tohyama M (2002). Functional inhibition of the p75 receptor using a small interfering RNA. Biochem Biophys Res Com 301:804-809.

Hooper NM, Karran EH, Turner AJ (1997). Membrane protein secretases. Biochem J

321:265-279.

Horner PJ, Gage FH (2000). Regenerating the damaged central nervous system. Nature 407:963-970.

Horuk R (1994). Molecular properties of the chemokine receptor family. Trends Pharmacol Sci 15:159-165.

Horuk R (1998). Chemokines beyond inflammation. Nature 393:524-525.

Horuk R, Chitnis CE, Darbonne WC, Colby TJ, Rybicki A, Hadley TJ, Miller LH (1993). A receptor for the malarial parasite Plasmodium vivax: the erythrocyte chemokine receptor. Science 261:1182.

Horuk R, Martin AW, Wang ZX, Schweitzer L, Gerassimides A, Guo H, Lu ZH, Hesselgesser J, Perez HD, Kim J, Parker J, Hadley TJ, Peiper SC (1997). Expression of chemokine receptors by subsets of neurons in the central nervous system. J Immunol 158:2882-2890.

Horuk R, Ng HP (2000). Chemokine receptor antagonists. Med Res Rev 20:155-168.

Horuk R, Peiper SC (1996). Chemokines: molecular double agents. Curr Biol 6:1581-1582.

Hsieh SHK, Ferraro GB, Fournier AE (2006). Myelin-associated inhibitors regulate cofilin phosphorylation and neuronal inhibition through LIM kinase and slingshot phosphatase. J Neurosci 26:1006-1015.

Huang DW, McKerracher L, Braun PE, David S (1999). A therapeutic vaccine approach to stimulate axon regeneration in the adult mammalian spinal cord. Neuron 24:639-647.

Hulsebosch CE (2002). Recent advances in pathophysiology and treatment of spinal

cord injury. Adv Physiol Educ 26:238-255.

Imai T, Hieshima K, Haskell C, Baba M, Nagira M, Nishimura M, Kakizaki M, Takagi S, Nomiyama H, Schall TJ, Yoshie O (1997). Identification and molecular characterization of fraktalkine receptor CX_3CR1, which mediates both leukocyte migration and adhesion. Cell 91:521-530.

Imitola J, Raddassi K, Park KI, Mueller FJ, Nieto M, Teng YD, Frenkel D, Li J, Sidman RL, Walsh CA, Snyder EY, Khoury SY (2004). Directed migration of neural stem cells to sites of CNS injury by the stromal cell-derived factor 1alpha/CXC chemokine receptor 4 pathway. Proc Natl Acad Sci USA 101:18117-18122.

Infantino S, Moepps B, Thelen M (2005). Expression and regulation of the orphan receptor RDC1 and its putative ligand in human dendritic and B cells. J Immunol 176: 2197-2207.

Ingoglia NA, Sharma SC, Pilchman J, Baranowski K, Sturman JA (1982). Axonal transport and transcellular transfer of nucleosides and polyamines in intact and regenerating optic nerves of goldfish: speculation on the axonal regulation of periaxonal cell metabolism. J Neurosci 2:1412-1423.

Jacobs WB, Fehlings MG (2003). The molecular basis of neural regeneration. Neurosurgery 53:943-949.

Johnson PW, Abramov-Newerly W, Seilheimer B, Sadoul R, Tropak MB, Arquint M, Dunn RJ, Schachner M, Roder JC (1989). Recombinant myelin-associated glycoprotein confers neural adhesion and neural outgrowth function. Neuron 3:377-385.

Kastin AJ, Pan W (2005). Targeting neurite growth inhibitors to induce CNS regeneration. Curr Phar Des 11:1247-1253.

Kaul M, Lipton SA (1999). Chemokines and activated macrophages in HIV gp120-induced neuronal apoptosis. Proc Natl Acad Sci USA 96:8212-8216.

Keirstead HS, Ben-Hur T, Rogister B, O´Leary MT, Dubois-Dalcq M, Blakemore WF (1999). Polysialylated neural cell adhesion molecule-positive CNS precursors generate both oligodendrocytes and Schwann cells to remyelinate the CNS after transplantation. J Neurosci 19:7529-7536.

Kelm S, Pelz A, Schauer R, Filbin MT, Tang S, DeBellard ME, Schnaar RL, Mahony JA, Hartnell A, Bradfield P, Crocker PR (1994). Sialoadhesin, myelin-associated glycoprotein and CD22 define a new family of sialic acid-dependent adhesion molecules of the immunoglobulin superfamily. Curr Biol 4:965-972.

Kelner GS, Kennedy J, Bacon KB, Kleyensteuber S, Largaespada DA, Jenkins NA, Copeland NG, Bazan JF, Moore KW, Schall TJ, Zlotnik A (1994). Lymphotactin: a cytokine that represents a new class of chemokine. Science 266:1395-1399.

Khan MZ, Brandimarti R, Patel JP, Huynh N, Wang J, Huang Z, Fatatis A, Meucci O (2004). Apoptotic and antiapoptotic effects of CXCR4: is it a matter of intrinsic efficacy? Implications for HIV neuropathogenesis. AIDS Res Hum Retroviruses 20:1063-1071.

Khan MZ, Shimizu S, Patel JP, Nelson A, Le MT, Mullen-Przeworski A, Brandimarti R, Fatatis A, Meucci O (2005). Regulation of neuronal p53 activity by CXCR4. Mol Cell Neurosci 30:58-66.

Kijima T, Maulik G, Ma PC, Tibaldi EV, Turner RE, Rollins B, Sattler M, Johnson BE, Salgia R (2002). Regulation of cellular proliferation, cytoskeletal function, and signal transduction through CXCR4 and c-Kit in small cell lung cancer cells. Cancer Res 62:6304-6311.

Klein RS, Rubin JB, Gibson HD, DeHaan EN, Alvarez-Hernandez X, Segal RA, Luster AD (2001). SDF-1α induces chemotaxis and enhances Sonic hedgehog-induced proliferation of cerecellar granule cells. Development 128:1971-1981.

Kobe B, Kajava AV (2001). The leucin-rich repeat as a protein recognition motif.

Curr Opin Struct Biol 11:725-732.

Kolakowski LF, Lu B, Gerard C, Gerard NP (1995). Probing the "message:address" sites for chemoattractant binding to the C5a receptor. J Biol Chem 270:18077-18082.

Kucia M, Jankowski K, Reca R, Wysoczynski M, Bandura L, Allensdorf DJ, Zhang J, Ratajczak J, Ratajczak MZ (2004). CXCR4-SDF-1 signalling, locomotion, chemotaxis and adhesion. J Mol Histol 35:233-245.

Lacroix S, Tuszynski MH (2000). Neurotrophic factors and gene therapy in spinal cord injury. Neurorehabil Neural Repair 14:265-275.

Lacy M, Jones J, Whittemore SR, Haviland DL, Wetsel RA, Barnum SR (1995). Expression of the receptors for the C5a anaphylatoxin, interleukin-8 and FMLP by human astrocytes and microglia. J Neuroimmunol 61:71-78.

Lapham CK, Ouyang J, Chandrasekhar B, Nguyen NY, Dimitrov DS, Golding H (1996). Evidence for cell-surface association between fusin and the CD4-gp120 complex in human cell lines. Science 274:602-605.

Lapham CK, Zaitseva MB, Lee S, Romanstseva T, Golding H (1999). Fusion of monocytes and macrophages with HIV-1 correlates with biochemical properties of CXCR4 and CCR5. Nat Med 5:303-308.

Lapidot T, Kollet O (2002). The essential roles of the chemokine SDF-1 and its receptor CXCR4 in human stem cell homing and repopulation of transplanted immune-deficient NOD/SCID and NOD/SCID/B2m^{null} mice. Leukemia 16:1992-2003.

Law NM, Rosenzweig SA (1994). Characterization of the G protein-linked orphan receptor GPRN1/RDC1. Biochem Biophys Res Commun 201:458-465.

Lazarini F, Tham TM, Casanova P, Arenzana-Seisdedos F, Dubois-Dalcq M (2003). Role of the α-chemokine Stromal cell-derived factor-1 (SDF-1) in the developing and

mature central nervous system. Glia 42:139-148.

Lee JK, Kim JE, Sivula M, Strittmatter SM (2004). Nogo receptor antagonism promotes stroke recovery by enhancing axonal plasticity. J Neurosci 24:6209-6217.

Lefkowitz RJ, Shenoy SK (2005). Transduction of receptor signals by β-arrestins. Science 308:512-517.

Li J, Imitola J, Snyder EY, Sidman RL (2006). Neural stem cells rescue *nervous* Purkinje neurons by restoring molecular homeostasis of tissue plasminogen activator and downstream targets. J Neurosci 26:7839-7848.

Li M, Shibata A, Li C, Braun PE, McKerracher L, Roder J, Kater SB, David S (1996). Myelin-associated glycoprotein inhibits neurite/axon growth and causes growth cone collapse. J Neurosci Res 46:404-414.

Lieberam I, Agalliu D, Nagasawa T, Ericson J, Jessell TM (2005). A CXCL12-CXCR4 chemokine signaling pathway defines the initial trajectory of mammalian motor axons. Neuron 47:667-679.

Lindley IJD, Westwick J, Kunkel SL (1993). Nomenclature announcement – the chemokines. Immunol Today 14:24-24.

Liu T, Young PR, McDonnell PC, White RF, Barone FC, Feuerstein GZ (1993). Cytokine-induced neutrophil chemoattractant mRNA expressed in cerebral ischemia. Neurosci Lett 164:125-128.

Liu Y, Himes BT, Solowska J, Moul J, Chow SY, Park KI, Tessler A, Murray M, Snyder EY, Fischer I (1999). Intraspinal delivery of neurotrophin-3 using neural stem cells genetically modified by recombinant retrovirus. Exp Neurol 158:9-26.

Lu M, Grove EA, Miller RJ (2002). Abnormal development of the hippocampal dentate gyrus in mice lacking the CXCR4 chemokine receptor. Proc Natl Acad Sci USA 99:7090-7095.

Lu Q, Sun EE, Klein RS, Flanagan JG (2001). Ephrin-B reverse signaling is mediated by a novel PDZ-RGS protein and selectively inhibits G protein-coupled chemoattraction. Cell 105:69-97.

Luo J, Luo Z, Zhou N, Hall JW, Huang Z (1999). Attachment of C-terminus of SDF-1 enhances the biological activity of its N-terminal peptide. Biochem Biophys Res Com 264:42-47.

Ma Q, Jones D, Borghesani DR, Segal RA, Nagasawa T, Kishimoto T, Bronson RT, Springer TA (1998). Impaired B-lymphopoiesis, myelopoiesis, and derailed cerebellar neuron migration in CXCR4- and SDF-1-deficient mice. Proc Natl Acad Sci 95:9448-9453.

Maione TE, Gray GS, Hunt AJ, Scarpe RJ (1991). Inhibition of tumor growth in mice by an analogue of platelet factor 4 that lacks affinity for heparin and retains potent angiostatic activity. Cancer Res 51:2077-2083.

Mason C, Erskine L (2000). Growth cone form, behaviour, and interactions in vivo: retinal axon pathfinding as a model. J Neurobiol 44:260-270.

McKerracher L, David S, Jackson DL, Kottis V, Dunn RJ, Braun PE (1994). Identification of myelin-associated glycoprotein as a major myelin-derived inhibitor of neurite outgrowth. Neuron 13:805-811.

McKerracher L, Higuchi H (2006). Targeting Rho to stimulate repair after spinal cord injury. J Neurotrauma 23:309-317.

McManus CM, Brosnan CF, Berman JW (1998). Cytokine induction of MIP-1α and MIP-1β in human fetal microglia. J Immunol 160:1449-1455.

McQuarrie IG (1978). The effect of a conditioning lesion on the regeneration of motor axons. Brain Res 152:597-602.

Mennicken F, Maki R, de Souza EB, Quirion R (1999). Chemokines and chemokine receptors in the CNS: a possible role in neuroinflammation and patterning. TRENDS Pharmacol Sci 20:73-78.

Meucci O, Fatatis A, Simen AA, Bushell JJ, Gray PW, Miller RJ (1998). Chemokines regulate hippocampal neuronal signaling and gp-120 neurotoxicity. Proc Natl Acad Sci USA 95:14500-14505.

Mi S, Lee X, Shao Z, Thill G, Ji B, Relton J, Levesque M, Allaire N, Perrin S, Sands B, Crowell T, Cate RL, McCoy JM, Pepinsky RB (2004). LINGO-1 is a component of the Nogo-66 receptor/p75 signaling complex. Nat Neurosci 7:221-228.

Mikol DD, Alexakos MJ, Bayley CA, Lemons RS, Le Beau MM, Stefansson K (1990). Structure and chromosomal localization of the gene for the oligodendrocyte-myelin glycoprotein of mouse: primary structure and gene structure. Genomics 17:604-610.

Mikol SS, Stefansson K (1988). A phosphatidylinositol-linked peanut agglutinin-binding glycoprotein in central nervous system myelin and on oligodendrocytes. J Cell Biol 106:1273-1279.

Mizuno T, Yamashita T, Tohyama M (2004). Chimaerins act downstream from neurotrophins in overcoming the inhibition of neurite outgrowth produced by myelin-associated glycoprotein. J Neurochem 91:395-403.

Mochizuki H, Matsubara A, Teishima J, Mutaguchi K, Yasumoto H, Dahiya R, Usui T, Kamiya K (2004). Interaction of ligand-receptor system between stromal cell-derived factor-1 and CXC chemokine receptor 4 in human prostate cancer: a possible predictor of metastasis. Biochem Biophys Res Commun 320:656-663.

Monnier PP, Sierra A, Schwab JM, Henke-Fahle S, Mueller BK (2003). The Rho/ROCK pathway mediates neurite growth-inhibitory activity associated with the chondroitin sulfate proteoglycans of the CNS glial scar. Mol Cell Neurosci 22:319-330.

Moon LD, Asher RA, Rhodes KE, Fawcett JW (2001). Regeneration of CNS axons back to their target following treatment of adult rat brain with chondroitinase ABC. Nat Neurosci 4:465-466.

Moreau-Fauvarque C, Kumanogoh A, Camand E, Jaillard C, Barbin G, Boquet I, Love C, Jones EY, Kikutani H, Lubetzki C, Dusart I, Chédotal A (2003). The transmembrane semaphorine Sema4D/CD100, an inhibitor of axonal growth, is expressed on oligodendrocytes and upregulated after CNS lesion. J Neurosci 23:9229-9239.

Mukhopadhyay G, Doherty P, Walsh FS, Crocker PR, Filbin MT (1994). A novel role for myelin-associated glycoprotein as an inhibitor of axonal regeneration. Neuron 13:757-767.

Müller A, Homey B, Soto H, Ge N, Catron D, Buchanan ME, McClanahan T, Murphy E, Yuan W, Wagners SN, Barrera JL, Mohar A, Verastegui E, Zlotnik A (2001). Involvement of chemokine receptors in breast cancer metastasis. Nature 410:50-56.

Murdoch C (2000). CXCR4: chemokine receptor extraordinaire. Immunol Rev 177:175-184.

Murdoch C, Finn A (2000). Chemokine receptors and their role in inflammation and infectious diseases. Blood 95:3032-3043.

Murphy PM, Baggiolini M, Charo IF, Hebert CA, Horuk R, Matsushima K, Miller LH, Oppenheim JJ, Power CA (2000). International union of Pharmacology. XXII. Nomenclature for chemokine receptors. Pharmacol Rev 52:145-176.

Nagasawa T, Hirota S, Tachibana K, Takakura N, Nishikawa S, Kitamura Y, Yoshida N, Kikutani H, Kishimoto T (1994). Defects in B-cell lymphopoiesis and bone-marrow myelopoiesis in mice lacking the CXC chemokine PBSF/SDF-1. Nature 382:635-638.

Nagata S, Ishihara T, Robberecht P, Libert F, Parmentier M, Christophe J, Vassart

G (1992). RDC1 may not be VIP receptor. Trends Pharmacol Sci 13:102-103.

Nakamura H, Saheki T, Nakagawa S (1990). Differential cellular localization of enzymes of L-arginine metabolism in the rat brain. Brain Res 530108-112.

Neote K, Mak JY, Kolakowski LF, Schall TJ (1994). Functional and biochemical analysis of the cloned Duffy antigen: identity with the red blood cell chemokine receptor. Blood 84:44-52.

Neumann S, Bradke F, Tessier-Lavigne M, Basbaum AI (2002). Regeneration of sensory axons within the injured spinal cord induced by intraganglionic cAMP elevation. Neuron 34:885-893.

Neumann S, Woolf CJ (1999). Regeneration of dorsal column fibers into and beyond the lesion site following adult spinal cord injury. Neuron 23:83-91.

Nishita M, Aizawa H, Mizuno K (2002). Stromal cell-derived factor-1α activates LIM kinase 1 and induces cofilin phosphorylation for T-cell chemotaxis. Mol Cell Biol 22:774-783.

Onuffer JJ, Horuk R (2002). Chemokines, chemokine receptors and small-molecule antagonists: recent developments. TRENDS Pharmacol. Sci 23:495-467.

Orimo A, Gupta PB, Sgroi DC, Arenzana-Seisdedos F, Delaunay T, Naeem R, Carey V, Richardson A, Weinberg A (2005). Stromal fibroblasts present in invasive human breast carcinomas promote tumor growth and angiogenesis through elevated SDF-1/CXCL12 secretion. Cell 121:335-348.

Otani K, Abe H, Kadoya S (1994). Beneficial effect of methylprednisolone sodium succinate in the treatment of acute spinal cord injury [in Japanese]. Sekitsui Sekizui 7:633-647.

Peled A, Petit I, Kollet O, Magid M, Ponomaryov T, Byk T, Nagler A, Ben-Hur H, Many A, Shultz L, Lider O, Alon R, Zipori D, Lapidot T (1999). Dependence of

human stem cell engraftment and repopulation of NOD/SCID mice on CXCR4. Science 283:845-848.

Peng H, Huang Y, Rose J, Erichsen D, Herek S, Fujii N, Tamamura H, Zheng J (2004). Stromal cell-derived factor 1-mediated CXCR4 signaling in rat and human cortical neural progenitor cells. J Neurosci Res 76:35-50.

Prinjha R, Moore SE, Vinson M, Blake S, Morrow R, Christie G, Michalovich D, Simmons SL, Walsh FS (2000). Inhibitor of neurite outgrowth in humans. Nature 403:383-384.

Pujol F, Kitabgi P, Boudin H (2004). The chemokine SDF-1 differentially regulates axonal elongation and branching in hippocampal neurons. J Cell Sci 118:1071-1080.

Qiu J, Cai D, Dai H, McAtee M, Hoffman PN, Bregman BS, Filbin MT (2002). Spinal axon regeneration induced by elevation of cyclic AMP. Neuron 34:895-903.

Ramón y Cajal S (1928). Degeneration and regeneration of the nervous system. Oxford Univ Press, London.

Ramón-Cueto A, Plant GW, Avila J, Bunge MB (1998). Long-distance axonal regeneration in the transacted adult rat spinal cord is promoted by olfactory ensheathing glia. J Neurosci 18:3803-3815.

Rempel SA, Dudas S, Ge S, Gutierrez JA (2000). Identification and localization of the cytokine SDF-1 and its receptor, CXC chemokine receptor 4, to regions of necrosis and angiogenesis in human glioblastoma. Clin Cancer Res 6:102-111.

Roland J, Murphy BJ, Ahr B, Robert-Hebmann V, Delauzun V, Nye KE, Devaux C, Biard-Piechaczyk M (2003). Role of the intracellular domains of CXCR4 in SDF-1-mediated signaling. Blood 101:399-406.

Rosenberg LJ, Teng YD, Wrathall JR (1999). Effects of the sodium channel blocker tetrodotoxin on acute white matter pathology after experimental contusive spinal

cord injury. J Neurosci 19:6122-6133.

Rossi D, Zlotnik A (2000). The biology of chemokines and their receptors. Annu Rev Immunol 18:217-242.

Rubin JB, Kung AL, Klein RS, Chan JA, Sun YP, Schmidt K, Kieran MK, Luster AD, Segal RA (2003). A small-molecule antagonist of CXCR4 inhibits intracranial growth of primary brain tumors. Proc Natl Acad Sci USA 100:13513-13518.

Salgia R, Quackenbush E, Lin J, Souchkova N, Sattler M, Ewaniuk DS, Klucher KM, Daley GQ, Kraeft SK, Sackstein R, Alyea EP, von Andrian UH, Chen LB, Gutierrez-Ramos JC, Pendergast AM, Griffin JD (1999). The BCR/ABL oncogene alters the chemotactic response to stromal-derived factor-1α. Blood 94:4233-4246.

Savio T, Schwab ME (1990). Lesioned corticospinal tract axons regenerate in myelin-free rat spinal cord. PNAS 87:4130-4133.

Schnell L, Schwab ME (1990). Axonal regeneration in the rat spinal cord produced by an antibody against myelin-associated neurite growth inhibitors. Nature 343:269-272.

Schwab JM, Bernard F, Moreau-Fauvarque C, Chèdotal A (2005). Injury reactive myelin/oligodendrocyte-derived axon growth inhibition in the adult mammalian central nervous system. Brain Res Rev 49:295-299.

Schwab ME (2002). Repairing the injured spinal cord. Science 295:1029-1031.

Schwab ME, Bartholdi D (1996). Degeneration and regeneration of axons in the lesioned spinal cord. Physiol Rev 76:319-369.

Seiler N (2000). Oxidation of polyamines and brain injury. Neurochem Res 25:471-490.

Sekhon LH, Fehlings MG (2001). Epidemiology, demographics, and pathophysiology

of acute spinal cord injury. Spine 26:S2-S12.

Shimizu N, Soda Y, Kanbe K, Liu HY, Mukai R, Kitamura T, Hoshino H (2000). A putative G protein-coupled receptor, RDC1, is a novel coreceptor for human and simian immunodeficiency viruses. J Virol 74:619-626.

Shirozu M, Nakano T, Inazawa J, Tashiro K, Tada H, Shinohara T, Honjo T (1995). Structure and chromosomal localization of the human stromal cell-derived factor 1 (SDF1) gene. Genomics 28:495-500.

Siciliano SJ, Rollins TE, DeMartino J, Konteatis Z, Malkowitz L, Riper GV, Bondy S, Rosen H, Springer MS (1994). Two-site binding of C5a by its receptor: an alternative binding paradigm for G protein-coupled receptors. Proc Natl Acad Sci USA 91:1214-1218.

Sloane A, Raso V, Dimitrov DS, Xiao X, Deo S, Muljadi N, Restuccia D, Turville S, Kearney C, Broder CB, Zoellner H, Cunningham AL, Bendall L, Lynch GW (2005). Marked structural and functional heterogeneity in CXCR4: Separation of HIV-1 and SDF-1α responses. Immunol Cell Biol 83:129-143.

Smith MC, Luker KE, Garbow JR, et al. (2004). CXCR4 regulates growth of both primary and metastatic breast cancer. Cancer Res 64:8604-8612.

Spencer T, Filbin MT (2004). A role for cAMP in regeneration of the adult mammalian CNS. J Anat 204:49-55.

Spillmann D, Witt D, Lindahl U (1998). Defining the interleukin-8-binding domain of heparan sulphate. J Biol Chem 273:15487-15493.

Sreedharan SP, Robichon A, Peterson KE, Goetzl EJ (1991). Cloning and expression of the human vasoactive intestinal peptide receptor. Proc Natl Acad Sci USA 88:4986-4990.

Strieter RM, Polverini PJ, Arenberg DA, Walz A, Opdenakker G, Van Damme J,

Kunkel SL (1995). Role of C-X-C chemokines as regulators of angiogenesis in lung cancer. J Leukocyte Biol 57:752-762.

Stumm RK, Rummel J, Junker V, Culmsee C, Pfeiffer M, Krieglstein J, Höllt V, Schulz S (2002). A dual role for the SDF-1/CXCR4 chemokine receptor system in adult brain: isoform-selective regulation of SDF-1 expression modulates CXCR4-dependent neuronal plasticity and cerebral leukocyte recruitment after focal ischemia. J Neurosci 22:5865-5878.

Stys PK (2004). White matter injury mechanisms. Curr Mol Med 4:113-130.

Szebenyi G, Callaway JL, Dent EW, Kalil K (1998). Interstitial branches develop form active regions of the axon demarcated by the primary growth cone during pausing behaviours. J Neurosci 18:7930-7940.

Tachibana K, Hirota S, Iizasa H, Yoshida H, Kawabata K, Kataoka Y, Kitamura Y, Matsushima K, Yoshida N, Nishikawa SI, Kishimoto T, Nagasawa T (1998). The chemokine receptor CXCR4 is essential for vascularization of the gastrointestinal tract. Nature 393:591-594.

Takahashi A, Camacho P, Lechleiter JD, Herman B (1999). Measurement of intracellular calcium. Physiol Rev 79:1089-1125.

Tanabe S, Heesen M, Yoshizawa I, Berman MA, Yi L, Bleul CC, Springer TA, Okuda K, Gerard N, Dorf ME (1997). Functional expression of the CXC-chemokine receptor-4/fusin on mouse microglial cells and astrocytes. J Immunol 159:905-911.

Tang S, Qiu J, Nikulina E, Filbin MT (2001). Solubile myelin-associated glycoprotein released from damaged white matter inhibits axonal regeneration. Mol Cell Neurosci 18:259-269.

Tang S, Shen Y, Mukhopadhyay G, DeBellard ME, Crocker P, Filbin MT (1997). Myelin-associated glycoprotein, MAG, recognizes neurons via two epitopes, a sialic acid binding side at Arg118 and a distinct neurite binding epitope. J Cell Biol

138:1355-1366.

Tashiro K, Tada H, Heilker R, Shirozu M, Nakano T, Honjo T (1993). Signal sequence trap: a cloning strategy for secreted proteins and type I membrane proteins. Science 261:600-603.

Thallmair M, Metz GA, Z´Graggen WJ, Raineteau O, Kartje GL, Schwab ME (1998). Neurite growth inhibitors restrict plasticity and functional recovery following corticospinal tract lesion.

Tham TN, Lazarini F, Franceschini IA, Lachapelle F, Amara A, Dubois-Dalcq M (2001). Developmental pattern of expression of the alpha chemokine stromal cell-derived factor-1 in the rat central nervous system. Eur J Neurosci 13:845-856.

The National SCI Statistic Center, 1999

Tilton B, Ho L, Oberlin E, Loetscher P, Baleux F, Clark-Lewis I, Thelen M (2000). Signal transduction by CXC chemokine receptor 4: stromal cell-derived factor-1 stimulates prolonged protein kinase B and extracellular signal-regulated kinase 2 activation in T lymphocytes. J Exp Med 192:313-324.

Trent JO, Wang ZX, Murray JL, Shao W, Tamamura H, Fujii N, Peiper SC (2003). Lipid bilayer simulations of CXCR4 with inverse agonists and weak partial agonists. J Biol Chem 278:47136-47144.

Vila-Coro AJ, Rodriguez-Frade JM, De Ana AM, Moreno-Ortiz MC, Martinez AC, Mellado M (1999). The chemokine SDF-1α triggers CXCR4 dimerization and activates the JAK/STAT pathway. FASEB J 13:1699-1710.

Vilz TO, Moepps B, Engele J, Molly S, Littman DR, Schilling K (2005). The SDF-1/CXCR4 pathway and the development of the cerebellar system. Eur J Neurosci 22:1831-1839.

Vourc´h P, Andres C (2004). Oligodendrocyte myelin glycoprotein (OMgp):

evolution, structure and function. Brain Res Rev 45:115-124.

Wang J, Sun Y, Song W, Nor JE, Wang CY, Taichman RS (2003). Diverse signaling pathways through the SDF-1/CXCR4 axis in prostate cancer cell lines leads to altered patterns of cytokine secretion and angiogenesis. Cell Signal 17:1578-1592.

Wang JF, Park IW, Groopman JE (2000). Stromal cell-derived factor-1α stimulates tyrosine phosphorylation of multiple focal adhesion proteins and induces migration ofhematopoietic progenitor cells: role of phosphoinositol-3 kinase and protein kinase C. Blood 95:2505-2513.

Wang KC, Koprivica V, Kim JA, Sivasankaran R, Guo Y, Neve RL, He Z (2002). Oligodendrocyte-myelin glycoprotein is a Nogo receptor ligand that inhibits neurite outgrowth. Nature 417:941-944.

Wang X, Yue TL, Barone FC, Feuerstein GZ (1995). Monocyte chemoattractant protein-1 messenger RNA expression in rat ischemic cortex. Stroke 26:661-665.

Webb LM, Ehrengruber MU, Clark-Lewis I, Baggiolini M, Rot A (1993). Binding to heparan sulfate or heparin enhances neutrophil responses to interleukin 8. Proc Natl Acad Sci USA 90:7158-7162.

Xiang Y, Li Y, Zhang Z, Cui K, Wang S, Yuan XB, Wu CP, Poo MM, Duan S (2002). Nerve growth cone guidance mediated by G protein-coupled receptors. Nat Neurosci 5:843-848.

Yamashita T, Higuchi H, Tohyama M (2002). The p75 receptor transduces the signal from myelin-associated glycoprotein to Rho. J Cell Biol 157:565-570.

Yancey KB, Lawley TJ, Dersookian M, Harvath L (1989). Analysis of the interaction of human C5a ans C5a des Arg with human monocytes and neutrophils: flow cytometric and chemotaxis studies. J Invest Dermatol 92:184-189.

Yiu G, He Z (2006). Glial inhibition of CNS axon regeneration. Nature Rev Neurosci

7:617-627.

Yu L, Cecil J, Peng SB, Schrementi J, Kovacevic S, Paul D, Su EW, Wang J (2006). Identification and expression of novel isoforms of human stromal cell-derived factor 1. Gene 374:174-179.

Zhang L, Huang Y, He T, Cao Y, Ho DD (1996). HIV-1 subtype and second-receptor use. Nature 383:768.

Zhang WB, Navenot JM, Haribabu B, Tamamura H, Hiramatu K, Omagari A, Pei G, Manfred JP, Fujii N, Broach JR, Peiper SC (2002). A point mutation that confers constitutive activity to CXCR4 reveals that T140 is an inverse agonist and that AMD3100 and ALX40-4C are weak partial agonists. J Biol Chem 277:24515-24521.

Zheng B, Ho C, Li S, Keirstead H, Steward O, Tessier-Lavigne M (2003). Lack of enhanced spinal regeneration in Nogo-deficient mice. Neuron 38:213-224.

Zheng J, Thylin MR, Ghorpade A, Xiong H, Persidsky Y, Cotter R, Niemann D, Che M, Zheng YC, Gelbard HA, Shepard RB, Swartz JM, Gendelman HE (1999). Intracellular CXCR4 signaling, neuronal apoptosis and neuropathogenic mechanisms of HIV-1-associated dementia. J Neuroimmunol 98:185-200.

Zhou Y, Larsen PH, Hao C, Yong VW (2002). CXCR4 is a major chemokine receptor on glioma cells and mediates their survival. J Biol Chem 277:49481-49487.

Zhu Y, Yu T, Zhang XC, Nagasawa T, Wu JY, Rao Y (2002). Role of the chemokine SDF-1 as the meningeal attractant for embryonic cerebellar neurons. Nat Neurosci 5:719-720.

Zlotnik A, Yoshie O (2000). Chemokines: a new classification system and their role in immunity. Immunity 12:121-127.

Zou YR, Kottmann AH, Kuroda M, Taniuchi I, Littman DR (1998). Function of the chemokine receptor CXCR4 in hematopoiesis and in cerebellar development. Nature 393:595-599.

7. Abbreviations

(p)CREB	(phosphorylated) cAMP responsive element binding protein
ATP	adenosine triphosphate
BDNF	brain-derived neurotrophic factor
BSA	bovine serum albumin (fraction V)
cAMP	cyclic adenosine monophosphate
CCR5	CC chemokine receptor 5
Cdc42	cell division cycle 42
CNS	central nervous system
CSPG	chondroitin sulphate proteoglycan
CXCL12	CXC chemokine ligand 12
CXCR4	CXC chemokine receptor 4
DAB	diaminobenzidine
DARC	Duffy antigen receptor for chemokines
DMEM	Dulbecco´s modified Eagle medium
DREZ	dorsal root entry zone
DRG	dorsal root ganglion
EAE	experimental allergic encephalitis
ECD	extracellular domain
ECL	extracellular loop
ECM	extracellular matrix
ERK	extracellular-signal regulated kinase
FAK	kocal adhesion kinase
FBS	foetal bovine serum
5´dFUrd	5´-fluoro-2´-desoxyuridine
Forene (Isofluran)	1-chloro-2,2,2-trifluoroethyldifluoromethylether
Fura 2-AM	Fura-2 pentakis(acetoxymethyl)ester
GAG	glycosaminoglycan
GDNF	glial cell line-derived neurotrophic factor
GDP	guanidine diphosphate
GPCR	G protein-coupled receptor

GPI	glycosylphosphatidylinositol
GTP	guanidine triphosphate
HIV	human immunodeficiency virus
ICL	intracellular loop
IDC	intracellular domain
Ig	immunoglobulin
Jak	Janus kinase
LIM	acronym of Lin-11, Isl-1, Mec-3
LIMK1	LIM kinase 1
LRR	leucin-rich repeat
MAG	myelin-associated glycoprotein
MAI	myelin-associated inhibitor
MPSS	methylprednisolone sodium succinate
mRNA	messenger ribonucleic acid
NFκ-B	nuclear factor κ-B
NGF	nerve growth factor
NgR	Nogo66 receptor
NGS	normal goat serum
NOD/SCID	non-obese diabetic/severe combined immunodeficient
NT-3	neurotrophin-3
OMgp	oligodendrocyte-myelin glycoprotein
$p75^{NTR}$	p75 neurotrophin receptor
PAK	p21 activated kinase
PAM	pan axonal marker
PBLs	peripheral blood leukocytes
PBS	phosphate buffered saline
PBSF	pre-B-cell growth stimulating factor
Pen-Strep	penicilline-streptomycine
PI3K	phosphatidylinositol 3-kinase
PKA	protein kinase A
PKC	protein kinase C
PLC-γ	phospholipase C-γ
PNS	peripheral nervous system
PTX	pertussis toxin (*Bordetella pertussis*)

Pyk2	proline-rich tyrosine kinase-2
Q-PCR	quantitative polymerase chain reaction
RHD	reticulon-homology domain
RIP	regulated intramembrane proteolysis
ROCK	Rho-associated kinase
RTK	receptor tyrosine kinase
RTN	reticulon
RT-PCR	reverse transcriptase polymerase chain reaction
SCI	spinal cord injury
scy	*small secretred cytokines*
SDF-1	stromal cell-derived factor-1
SDS-PAGE	sodium dodecylsulfate polyacrylamide gel electrophoresis
sema 3C	semaphorin 3C
sema3A	semaphorin 3A
SHH	sonic hedgehog
SIV	simian immunodeficiency virus
STAT	signal transduction and activation of transcription
TNFα	tumor necrosis factor α
VIP	vasoactive intestinal peptide

8. Acknowledgements

I am indebted to Prof. Dr. Hans Werner Müller for providing me with the opportunity to work on this subject. Especially with regard to neurite outgrowth, his long experience as to CNS regeneration mechanisms essentially advantaged my project.

I also want to thank Prof. Dr. Heinz Mehlhorn for critical reading and evaluation of this manuscript.

I am grateful to both Dr. Patrick Küry and Dr. Frank Bosse for kindly supporting my work and providing me with expert advice whenever necessary.

I certainly owe many thanks to the members of the Laboratory of Molecular Neurobiology, Heinrich-Heine-Universität, Düsseldorf, for a cooperative and helpful working atmosphere.

I want to especially thank Brigida Ziegler not only for expert advice on cell culture matters, but also for perpetual encouragement and friendship. Latter is also true for both Dr. Frauke Otto and Dr. Thorsten Nolting to whom I owe thanks for their assistance as well as constant support and friendship.

All my love and thanks go out to my family, my mom and dad, my sister and Sally, for providing me with lots of support and encouragement – and for their readiness to take sides when needed. Sally, I can not tell how much I miss you.

Thanks to all my friends for their support – and for distraction whenever it was necessary.

Hiermit erkläre ich, die vorliegende Arbeit selbständig und unter ausschließlicher Verwendung der angegebenen Hilfsmittel und Quellen angefertigt zu haben. Alle Stellen, die aus veröffentlichten und nicht veröffentlichten Schriften entnommen sind, wurden als solche kenntlich gemacht. Diese Arbeit hat in gleicher oder ähnlicher Form noch keiner anderen Prüfungsbehörde vorgelegen.

Düsseldorf, den 24. Mai 2007